The incorporation of poorly soluble drugs into nanofibres by electrospinning from carboxylic acid polymer solutions

by

Dumisani Shabangu

Thesis presented in fulfilment of the requirements for the degree of Master of Science in the Faculty of Science (Polymer Science) at Stellenbosch University

Supervisor: Professor P.E. Mallon

December 2017

Declaration

By submitting this thesis/dissertation electronically, I declare that the entirety of the work contained therein is my own, original work, that I am the sole author thereof (save to the extent explicitly otherwise stated), that reproduction and publication thereof by Stellenbosch University will not infringe any third party rights and that I have not previously in its entirety or in part submitted it for obtaining any qualification.

December 2017

Abstract

Carboxylic acids were used to generate electrospun fibres of polycaprolactone (PCL) via a free surface electrospinning methodology for the first time. The electrospinnability of the polymer solutions was dependent on the conductivity of the polymer solutions, which is related to the carboxylic acid's pKa. The pKa influenced the dissolution ability of the carboxylic acid. Furthermore, the carboxylic acid type influences the solution properties. Carboxylic acids with a lower value of the pKa lead to lower observed solution viscosity. Needle electrospinning results show that carboxylic acid type influences the occurrence of critical chain entanglements. Additionally, salt additives can be used to enable needle electrospinning in low conductivity carboxylic acid polymer solutions. Carboxylic acid type influences the average fibre diameter of electrospun PCL. Polymer solutions with a comparatively higher value of conductivity lead to thicker fibres. PCL polymer solution properties evolve with time, more specifically viscosity. The viscosity decreases with an increase in solution age. The decrease in polymer solution viscosity is accompanied by a decrease in average fibre diameter. Furthermore, the decrease in viscosity and average fibre diameter is accompanied by a decrease in polymer molecular weight. The polymer processing type influences the crystallinity of the polymer. More specifically, fibres show a larger crystallinity compared to films generated from the same solvent system. Free surface electrospinning leads to an inconsistent crystal size distribution. Stable oil-in-acid emulsions were successfully formed. The dispersed phase type influences the emulsion stability. The continuous phase type influences the emulsion electrospinning as it makes up the bulk of the solution. The surfactant type influences emulsion electrospinning, with cationic surfactants leading to thinner fibres when positive potential is applied. Emulsion electrospinning leads to the encapsulation of the dispersed phase components. This led to the successful incorporation of a hydrophobic, poorly soluble drug in electrospun fibres. The internal fibre morphology is an islands-at-sea type morphology. Sustained release of curcumin in a phosphate buffer proved unsuccessful. Burst release was obtained by solution modification which was obtained by surfactant addition. The difficulty in obtaining sustained release of curcumin may be related in the difficulty of wetting the electrospun fibres.

Opsomming

Karboksielsure was gebruik om elektrospin vesels van polikaprolaktoon (PKL) te produseer deur, vir die eerste keer, gebruik tee maak van ‘n vrye oppervlak elektrospin metode. Die elektrospin van die polimeeroplossings is afhanklik van die geleiding daarvan wat verwant is aan die karboksielsure se pKa waarde aangesien die pKa die ontbindingsvermoë van die karboksielsuur beïnvloed. Die tipe karboksielsuur speel ‘n rol in die eienskappe van die oplossing. Karboksielsure met ‘n lae pKa waarde lei tot oplossings met waarneembare laer viskositeit. Naald elektrospin resultate wys dat die tipe karboksielsuur die voorkoms van kettingverstrengelings beïnvloed. In die geval van oplossings met swak geleidingsvermoëns kan sout bygevoeg word om die elektrospin daarvan moontlik te maak. Die tipe karboksielsuur het ook ‘n invloed op die deursnee van die PKL vesels. Polimeeroplossings met goeie geleidingsvermoëns het gelei tot dikker vesels. Daar is ook waargeneem dat die eienskappe van die PKL oplossings verander het oor tyd. Meer spesifiek, die viskositeit het gedaal het met die verloop van tyd. Die afname in die viskositeit van die oplossings het gepaard gegaan met ‘n afname in die deursnee van die vesels en die molekulêre gewig van die polimeer. Die verwerkingsmetode van ‘n polimeer bepaal ondermeer die kristalliniteit daarvan. Polimeervesels byvoorbeeld, het ‘n hoër kristalliniteit as films wat geprodusser is van dieselfde oplosmiddelsisteem. Vrye oppervlak elektrospin lei tot ‘n strydige verspreiding van kristal grootte. Stabiele olie-in-suur emulsies was susksesvol voorberei. Die tipe verspreide fase beïnvloed die stabiliteit van die emulsie. Die deurlopende fase beïnvloed op sy beurt die elektrospin proses van die emulsie, aangesien dit die meerderheid van die oplossing opmaak. Die tipe benattingsmiddel het ook ‘n invloed op die elektrospin proses van ‘n emulsie deurdat ‘n kationiese benattingsmiddel lei tot dunner vesels met die toepassing van positiewe potensiaal. Die elektrospin van ‘n emulsie lei to die inkapseling van die komponente van die dispersie fase wat nodig is vir die suksesvolle inkorporasie van die hidrofobiese dwelmmiddel in die polimeervesels. Die interne morfologie van hierdie vesels was die eiland-by-die-see tipe. Die volgehoue vrylating van die curcumin in ‘n fosfaatbuffer was onsuksesvol. Bars vrylating was waargeneem na die aanpassing van die oplossing deur die byvoeging van ‘n benattingsmiddel. Die moeilikheid om die volgehoue vrylating van die curcurim te verkry kan moontlik verwant wees aan die moeilikhied om die vesels te benat.

Acknowledgements

I would like to thank the following people and organizations for their assistance during this project:

The Stellenbosch Nanofiber Company, for their support and encouragement.

Colleagues in the Polymer Science department for their assistance and insight with various instruments and techniques.

Professor P.E. Mallon for his mentorship, guidance and patience.

Table of contents

Declaration i

Abstract ii

Opsomming iii

Acknowledgements iv

Chapter 1: Introduction and objectives 14

1.1 Introduction 14

1.2 Objectives 15

1.3 References 16

Chapter 2: Literature survey 17

2.1 Electrospinning 17

2.1.1 Background (Capillary electrospinning) 17

2.1.2 Free surface electrospinning 18

2.2 Emulsions 20

2.2.1 Background 20

2.2.2 Emulsion stability 21

2.2.3 Acidic emulsions 22

2.2.4 Drug encapsulation 22

2.2.5 Emulsion electrospinning 23

2.3 Techniques for complex nanofibre morphology 25

2.3.1 Phase separation spinning 25

2.3.2 Coaxial spinning 25

2.3.3 Graft copolymers 26

2.3.4 Potential issues with complex fibre morphology 26

2.4 Polycaprolactone 27

2.4.1 Background 27

2.4.2 Electrospinning 27

2.4.2.1 Solvent influence 27

2.4.2.1.1 Organic solvents 27

2.4.2.1.2 Carboxylic acids 28

2.4.3 Drug delivery applications 28

2.5 Curcumin 29
2.5.1 Background 29
2.5.2 Solubility and stability 30
2.5.3 Electrospinning 30
2.6 References 31
Chapter 3: Experimental 35
3.1 Preparation of polycaprolactone solutions 35
3.1.1 Polymer solutions 35
3.1.2 Emulsions 35
3.2 Electrospinning 36
3.2.1 Needle electrospinning 36
3.2.1.1 Apparatus 36
3.2.1.2 Electrospinning setup and procedure 36
3.2.1.3 Fibre collection 36
3.2.2 Free surface electrospinning 37
3.2.2.1 Apparatus 37
3.2.2.2 Electrospinning setup and procedure 37
3.2.2.3 Fibre collection 37
3.3 Characterization techniques 37
3.3.1 Solution properties 37
3.3.1.1 Surface tension 37
3.3.1.2 Viscosity 38
3.3.1.3 Conductivity 38
3.3.2 Fibre morphology 38
3.3.2.1 Scanning electron microscopy (SEM) 38
3.3.2.2 Scanning transmission electron microscopy (STEM) 38
3.3.3 Thermal Analysis 38
3.3.3.1 Differential scanning calorimetry (DSC) 38
3.3.4 Molecular weight determination 39
3.3.4.1 Size exclusion chromatography (SEC) 39
3.4 References 39

Table of contents

Chapter 4: Results and discussion 40

4.1 Introduction 40

4.2 Polymer dissolution 40

4.3 Influence of solvent type on solution properties 41

4.3.1 Surface tension 41

4.3.2 Viscosity 42

4.3.3 Conductivity 44

4.4 Electrospinning 46

4.4.1 Needle electrospinning 46

4.4.2 Free surface electrospinning 47

4.5 Solution aging study 51

4.5.1 Solution properties 52

4.5.2 Free surface electrospinning 54

4.5.3 Molecular weight 61

4.5.4 Differential scanning calorimetry (DSC) thermograms 66

4.6.1 Formation and stability 72

4.6.2 Electrospinning 73

4.6.2.1 Continuous phase (solvent) influence 73

4.6.2.2 Surfactant type 74

4.6.2.3 Encapsulation 75

4.6.3 Summary 79

4.7 Drug release study 80

4.7.1 In vitro drug release 80

4.9 References 88

Chapter 5: Conclusions and recommendations 91

5.1 Conclusion 91

5.2 Recommendations for future work prospects 92

List of figures

Chapter 2

Figure 2.1: Needle electrospinning 17

Figure 2.2: Free surface electrospinning schematic (SNC BEST™) 19

Figure 2.3: Free surface electrospinning (SNC BEST™) 20

Figure 2.4: Emulsion electrospinning 23

Figure 2.5: Possible internal fibre morphology as a result of electrospinning 25

Figure 2.6: Chemical structure of PCL 27

Figure 2.7: Chemical structure of CUR 29

Figure 2.8: Reaction depicting anti-oxidant properties of CUR 29

Figure 2.9: Reaction depicting the protonation of CUR 30

Chapter 4

Figure 4.1: Surface tension of 15 wt% PCL polymer solutions as influenced by solvent composition 42

Figure 4.2: The viscosity of 15 wt% PCL polymer solutions as influenced by solvent composition 43

Figure 4.3: Conductivity of various 15wt% PCL polymer solutions as influenced by solvent type 45

Figure 4.4: Surface tension as a function of the solution age of 15 wt% PCL polymer solutions derived from various solvent systems 52

Figure 4.5: Conductivity as a function of solution age of 15 wt% PCL polymer solutions derived from various solvent systems 53

Figure 4.6: Viscosity as a function of the solution age of 15 wt% PCL polymer solutions derived from various solvent systems 54

Figure 4.7: M_n of electrospun fibres generated from various 15 wt% PCL polymer solutions as a function of solution age 62

Figure 4.8: M_w of electrospun fibres generated from various 15 wt% PCL polymer solutions as a function of solution age 63

Figure 4.9: Molecular weight distribution of 15 wt% PCL solutions as function of solution age 64

Figure 4.10: Đ of electrospun fibres of various 15 wt% PCL solutions as a function of solution age .. 64

Figure 4.11: Molecular weight distribution of 15 wt% PCL solutions as function of solution age 65

Figure 4.12: DSC thermograms (first heating cycle) of electrospun fibres and film generated from 15 wt% PCL polymer solutions 66

Figure 4.13: DSC thermograms (first heating cycle) of electrospun fibres generated from 15 wt% PCL polymer solutions as influenced by the nature of the solvent 67

Figure 4.14: DSC thermograms (second heating cycle) of electrospun fibres generated from 15 wt% PCL/FA polymer solutions 68

Figure 4.15: Crystallinity of electrospun fibres generated from various 15 wt% PCL solutions as a function of solution age 71

Figure 4.16: various stabiliser-free oil-in-acid emulsions with PCL as the continuous phase: (a) SO as the dispersed phase, (b) IPM as the dispersed phase 72

Figure 4.17: Light microscope image of oil-in-acid emulsions with (a) SO as the dispersed phase (stabilised with an anionic surfactant), (b) IPM as the dispersed phase 72

Figure 4.18: Emulsion derived electrospun fibres of encapsulated (a) curcumin and (b) oil red o (1-(2, 5-dimethyl-4-(2, 5-dimethylphenyl) phenyldiazenyl) azonapthalen-2-ol) 75

Figure 4.19: Electrospun PCL fibres generated from a PCL/SO emulsion with a surfactant, imaged with (a) STEM and (b) Fluorescence Microscopy 76

Figure 4.20: Fluorescence image of “washed” electrospun PCL fibres generated from a PCL/SO emulsion with a surfactant 77

Figure 4.21: STEM image of curcumin-encapsulated PCL fibres derived from PCL/SO emulsion with a surfactant 77

Figure 4.22: STEM image of curcumin-encapsulated PCL fibres derived from PCL/IPM emulsion, (a) unwashed, (b) washed with ethanol 78

Figure 4.23: Fluorescence image of “washed” electrospun PCL fibres generated from a PCL/IPM emulsion 79

Figure 4.24: The absorbance of curcumin in ethanol as influenced by curcumin concentration 81

Figure 4.25: The absorbance of curcumin in ethanol as influenced by curcumin concentration and UV-VIS spectra of curcumin in ethanol as influenced by curcumin concentration 81

Figure 4.26: UV-VIS spectra of curcumin in ethanol as influenced by curcumin concentration 82

Figure 4.27: Image of curcumin-encapsulated PCL fibres generated from an emulsion with IPM as the dispersed phase 83

Figure 4.28: Curcumin peaks obtained electrospun PCL fibres generated from (a) conventional, (b) emulsion 86

List of tables

Chapter 4

Table 4.1: Physical properties and dissolution observations of PCL in various carboxylic acids (the polymer (PCL) concentration evaluated was 15 wt %) 40

Table 4.2: Needle electrospinning observations for various PCL polymer solutions..... 46

Table 4.3: SEM images and fibre diameter distribution for various electrospun PCL fibres and PCL films 49

Table 4.4: SEM images of electrospun fibres generated from FA polymer solutions as a function of solution age 55

Table 4.5: SEM images of electrospun fibres generated from AA polymer solutions as a function of solution age 56

Table 4.6: SEM images of electrospun fibres generated from PA/FA polymer solutions as a function of solution age 57

Table 4.7: SEM images of electrospun fibres generated from BA/FA polymer solutions as a function of solution age 59

Table 4.8: DSC data of various PCL films and electrospun fibres in the first DSC cycle 69

Table 4.9: DSC data of various PCL films and electrospun fibres in the second DSC cycle 70

Table 4.10: Solvent influence on emulsion electrospinning results of various PCL polymer solutions..... 73

Table 4.11: Surfactant influence on emulsion electrospinning results of various PCL polymer solutions..... 74

Table 4.12: SEM image of electrospun PCL fibres generated from PCL/SO emulsion..... 76

Table 4.13: SEM image of electrospun PCL fibres and fibre diameter distribution as influenced by the presence of a dispersed phase..... 78

Table 4.14: SEM image of electrospun PCL fibres and fibre diameter distribution as influenced by the presence of a dispersed phase..... 83

Table 4.15: shows the relationship between solution composition and average fibre diameter..... 85

Table 4.16: Electrospun PCL fibres generated from a conventional solution and an emulsion solution as influenced by the presence of a surfactant 86

Appendix A

Table A1: Surface tension of PCL (15 wt %) polymer solutions. 93

Table A2: Viscosity of PCL (15 wt %) polymer solutions 93

Table A3: Conductivity of PCL (15 wt %) polymer solutions..... 94

Table A4: Needle electrospinning observations for various PCL polymer solutions 94

Glossary

List of Abbreviations

PCL	Polycaprolactone
CUR	Curcumin
IPM	Isopropyl Myristate
SO	Sunflower oil
EO	Ethyl oleate
FA	Formic acid
AA	Acetic acid
PA	Propionic acid
BA	Butyric acid
TEB	Benzyltriethylammonium chloride
$NaCH_3COO$ and SA	Sodium acetate
SEM	Scanning electron microscope
STEM	Scanning transmission electron microscopy
DSC	Differential scanning calorimetry
SEC	Size exclusion chromatography

Chapter 1: Introduction and objectives

1.1 Introduction

Nanofibres are fine fibres with diameters typically ranging from a few nanometres to a few micrometres[1,2]. They are typically generated from polymer solutions, although they can be generated from polymer melts, and non-polymeric systems such as native cyclodextrins[1–3]. Nanofibres can be formed by a variety of processes that include electrospinning, air-jet spinning, magneto-spinning and others[4,5]. Process parameters such as nozzle configuration, tip to collector distance, ambient conditions, viscosity, and surface tension and polymer concentration are influential in the morphology and average fibre diameter of the fibres[5,6]. Nanofibres can be post processed into a variety of structures such as yarns and composite materials[7,8].

The low diameter of nanofibres lead to intrinsic properties that are high specific surface area, high aspect ratio and bio-mimicking properties[2,9]. These properties have become interesting in the medical industry, more specifically tissue engineering and advanced wound care[10,11]. In tissue engineering polymer nanofibres are desirable because the electrospinning process parameters can be used to engineer scaffolds for specific tissue types, and in other cases provide specific features that are inherent to the polymer used. In advanced wound care, they have been used to deliver active compounds in either a sustained release or burst release. Furthermore, nanofibres can be post-processed to form multifunctional structrures[10]. This widespread use of nanofibres leads to more complex nanofibre morphologies and processing of complex multicomponent solutions to elicit specific properties.

The principal objective of this study is to utilize nanofibres to develop a method to deliver poorly soluble drugs that are of great benefit to specific target areas within the human body. The bio-mimicking nature of electrospun fibres makes desirable components of drug eluting implantable medical devices. Furthermore, the study focused on utilising the high throughput free surface electrospinning technology *SNC BEST*™. This technology enables the scaling up of novel nanofibre concepts, and is adaptable to process multicomponent polymer solutions.

Needle electrospinning has proven to be a versatile method in processing multicomponent solutions and obtaining complex nanofibre morphologies[12]. In this study, an attempt is made to mirror needle electrospinning results using the free surface electrospinning methods. The differences in the two electrospinning methods is the charge density experienced by a jet, the amount of polymer solution exposed at the spinneret surface and the path of the jet as it moves towards the collector. In free surface electrospinning, a larger amount of the solution is exposed to the atmosphere, which makes it vital to select low volatility solvents to avoid precipitation of the polymer before electrospinning occurs. Furthermore, the jet path in free surface electrospinning is narrower because of the presence of other jets, which may influence the electrospinning results.

In this study, we explore the use of alternative solvents to electrospin polymer nanofibres, this is important as it relates regulatory procedures that enable medical devices to reach the greater population. Carboxylic acids are classified as lower risk solvents compared to common organic solvents (dimethyl formamide, acetone and hexaisofluoropropanol). Polycaprolactone (PCL) is the model polymer because of its widespread use in research and biomedical applications.[13] It has been reported to electrospin from a variety of solvents, which may influence the electrospinning outcomes.[14] More specifically, it has been shown to degrade in acidic environments. Lastly, the incorporation and release of poorly soluble drugs is investigated with curcumin the model drug because of its therapeutic properties. It has been previously electrospun, shown to promote wound healing and is nontoxic.[15]

1.2 Objectives

The key objectives can be summarized below:

1) Investigate carboxylic acids as alternative electrospinning solvents
    - Electrospin with free surface electrospinning method
2) Investigate the influence of solution age on the electrospinning process
3) Form and electrospin oil-in-acid emulsions
    - Electrospin emulsions with free surface electrospinning method
4) Incorporated poorly soluble drugs into nanofibres
5) Establish a release study for poorly soluble drugs incorporated in nanofibres

1.3 References

(1) Greiner, A.; Wendorff, J. H. *Angew. Chem. Int. Ed. Engl.* **2007**, *46*, 5670–5703.

(2) Bhardwaj, N.; Kundu, S. C. *Biotechnol. Adv.* **2010**, *28*, 325–347.

(3) Celebioglu, A.; Uyar, T. *J. Colloid Interface Sci.* **2013**, *404*, 1–7.

(4) Abdal-hay, A.; Hamdy, A. S.; Lim, J. H. *Ceram. Int.* **2014**, *40*, 15403–15409.

(5) Benavides, R. E.; Jana, S. C.; Reneker, D. H. *ACS Macro Lett.* **2012**, *1*, 1032–1036.

(6) Neo, Y. P.; Ray, S.; Easteal, A. J.; Nikolaidis, M. G.; Quek, S. Y. *J. Food Eng.* **2012**, *109*, 645–651.

(7) Tian, L.; Yan, T.; Pan, Z. *J. Mater. Sci.* **2015**, *50*, 7137–7148.

(8) Feng, L.; Ning, X.; Zhong, J. *Materials (Basel).* **2014**, *7*, 3919–3945.

(9) Lee, S.; Kim, J.-S.; Chu, H. S.; Kim, G.-W.; Won, J.-I.; Jang, J.-H. *Acta Biomater.* **2011**, *7*, 3868–3876.

(10) Rieger, K. A.; Birch, N. P.; Schiffman, J. D. *J. Mater. Chem. B* **2013**, *1*, 4531.

(11) Leung, V.; Ko, F. *Polym. Adv. Technol.* **2011**, *22*, 350–365.

(12) Zhao, X.; Lui, Y.; Toh, P.; Loo, S. *Materials (Basel).* **2014**, *7*, 7398–7408.

(13) Woodruff, M. A.; Hutmacher, D. W. **2010**, *35*, 1217–1256.

(14) Gholipour Kanani, A.; Bahrami, S. H. B. *J. Nanomater.* **2011**, *2011*, 1–10.

(15) Nguyen, T. T. T.; Ghosh, C.; Hwang, S. G.; Tran, L. D.; Park, J. S. *J. Mater. Sci.* **2013**, *48*, 7125–7133.

Chapter 2: Literature survey

This literature survey aims to give an overview of the current state of research related to the study of electrospun fibres using various solvent systems. More specifically, how the electrospinning modality influences fibre size, fibre morphology and fibre distribution. Aspects discussed in the literature survey include different electrospinning methods, emulsion formation and stability, complex fibre morphologies and drug encapsulation. Furthermore, emulsion electrospinning is discussed, along with electrospinning polycaprolactone as a carrier of curcumin.

2.1 Electrospinning

2.1.1 Background (Capillary electrospinning)

Electrospinning is a processing technique that is used to produce fibres with diameters in the nanometre to micrometre range from polymeric solutions.[1] Electrospun fibres can be used in a multitude of applications including tissue engineering. The simplest form of electrospinning, traditionally referred to as needle or capillary electrospinning, a polymer droplet is deformed by an applied electric field (using a high voltage power supply) in the direction of the fibre collector as shown in Figure 2.1. The deformation of the droplet results in a Taylor cone being formed on the droplet; if the electric field overcomes the surface tension of the solution then typically a single straight liquid jet is projected from the apex of the cone. As the charged jet moves towards the collector it undergoes multiple bending and whipping instabilities, causing stretching and thinning of the jet, which results in evaporation of the solvent and the precipitation of the polymer to form dry solid fibres. Electrospinning can only occur if the solution properties have the correct range of surface tension, viscosity and conductivity for that particular system.[2] The viscosity of the solution can be related to the extent at which the polymer chains entangle in solution. Polymer chains occupy a certain hydrodynamic volume (the hydrodynamic volume is a theoretical volume a single polymer coil would occupy in a very dilute solution), the overlap of a number of polymer coils leads to entanglement and increased viscosity.[3] The chain entanglements promote mass flow into the liquid jet, this fact enables electrospinning to occur for a system.

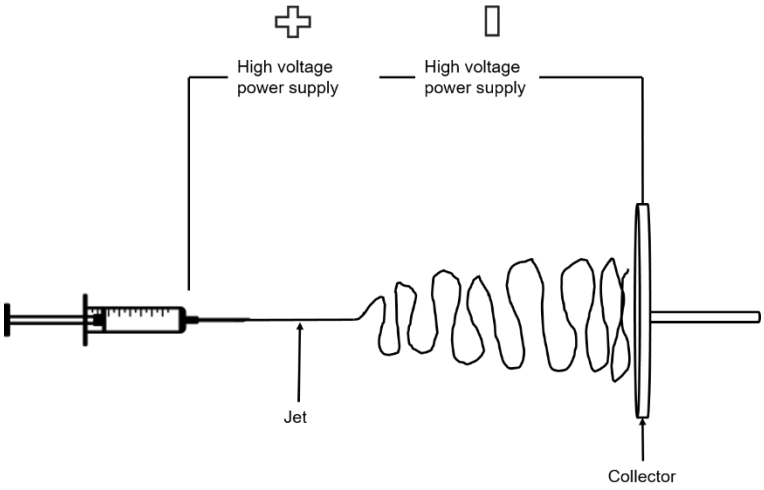

Figure 2.1: Needle electrospinning

2.1.2 Free surface electrospinning

Free surface electrospinning is a high throughput electrospinning process.[4] It differs from needle electrospinning in that multiple jets are produced during the electrospinning process that results in increased fibre production rates. Lukas *et al.*[5] showed that in free surface electrospinning multiple jets self-organize on spinneret surfaces to obtain the most favourable jet configuration when producing polyvinyl alcohol (PVA) fibres from aqueous solutions. This differs from needle electrospinning where, for higher throughput, multiple needles are used in a patterned array.[4] The high charge per unit area on these needles and jets results in repulsion of the charged jets between adjacent needles. The needles are fixed; therefore, the jets cannot move which results in them supressing or cancelling each other out to the point where spinning ceases.[4] Additionally, a large number of needles are required in the patterned arrays because of the low production rates associated with needle electrospinning (0.072 g per hour per needle). Because of charge interference between the needles they must be spaced far apart which results in larger machine footprints.[4] Problems like gelling at the capillary tip and the electrical interference from closely packed needles that accompanies multiple needle set-ups render scaling up problematic and undesirable.[6,7]

Free surface electrospinning can be differentiated in terms of rotating spinnerets and non-rotating spinnerets.[8] In the case of rotating spinnerets, the solution is stored in a reservoir and the spinneret rotates through the solution. This leads to a continuous coating of a thin polymer solution layer on the spinneret; when an electric field is applied to this layer it leads to instabilities. The instabilities are multiple waves that continue growing at different rates. A critical point is reached with each individual wave whereby the electric field applied overcomes the surface tension to initiate jetting on the crest of the wave and subsequent electrospinning occurs (if there are enough chain entanglements in the polymer solution and the solution has the minimum viscosity and conductivity for that system to enable electrospinning). Huang *et al.*[9] showed that the production of polystyrene (PS) fibres increased 60 times when using a rotating spinneret compared to needle electrospinning. They also showed that alignment of fibres was possible when the collector is rotating at high speeds. Additionally, they hypothesised that the high collector speeds lead to smaller fibre diameters as the fibres experience larger stretching forces. Forward *et al.*[10] showed that void-free core-shell fibres could be formed with needleless electrospinning when using a rotation wire electrode. The system used two immiscible polymeric solutions in a single bath with a co-solvent that allows the core solvent to travel to the jet surface and evaporate and thus producing void-free core-shell fibres composed of polyethylene glycol (PEG) and PS.

In the case of non-rotating spinnerets, they are designed to have a unique method that concentrates the charge on surfaces that are coated with the polymeric solutions. This can be in the form of protrusions such as e.g. spikes, rods, and edges. Yarin and Zussman[11] showed that a ferromagnetic fluid can be used to enable free surface electrospinning. An electrospinnable solution is coated onto a ferromagnetic fluid, so that when subjected to a high magnetic force creates spikes.[9] The spikes act as

the electric field concentrators that enable electrospinning. Similarly Lukas *et al.*[5] used serrated plates to initiate free surface electrospinning of PVA solutions

An additional example of non-rotating spinnerets is bubble electrospinning where gas flow forms bubbles at the surface of the polymeric solution in a reservoir. The bubbles deform when an electric field is applied, that deformation resulting in multiple jets being formed.[12] Liu *et al.*[13] showed that the number of jets produced during bubble electrospinning is dependent on the size of the bubble and the strength of the applied electric field when using polyvinyl pyrrolidone (PVP). Jiang *et al.*[14] then further investigated the use of micro-bubbles. They showed that bubble-electrospinning produces fibres of similar quality to non-aerated free surface electrospinning in polyvinyl alcohol (PVA) solutions. They further showed that using micro-bubbles leads increased productivity and they attribute this to an ease in jet formation when using microbubbles.

The SNC BEST™, or Ball Electrospinning Technology which is used later in the study, is a high throughput technology based on free surface electrospinning.[13] The technology uses partially submerged spheres in a reservoir that contains a polymeric solution, the spheres are moved through the solution such that a thin solution layer is always coated on the surface of the spheres. The solution is charged with a high voltage power supply through a primary electrode with the oppositely charged counter electrode positioned directly above it as seen in Figure 2.2. When critical electric field strength is applied between the electrodes, the normal electrospinning process occurs. Figure 2.3 shows the SNC BEST™ in operation.

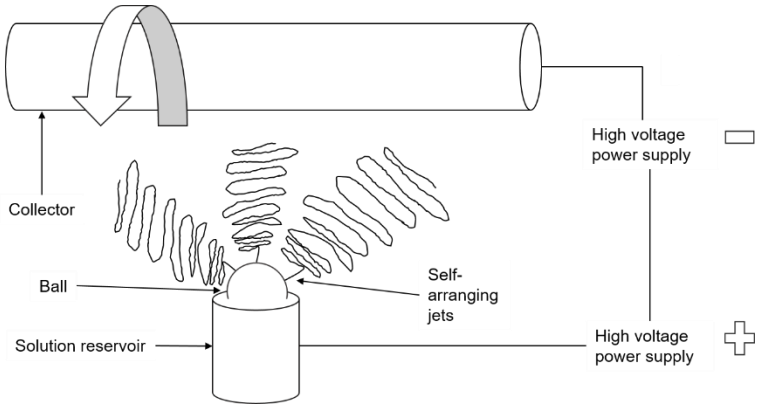

Figure 2.2: Free surface electrospinning schematic (SNC BEST™)

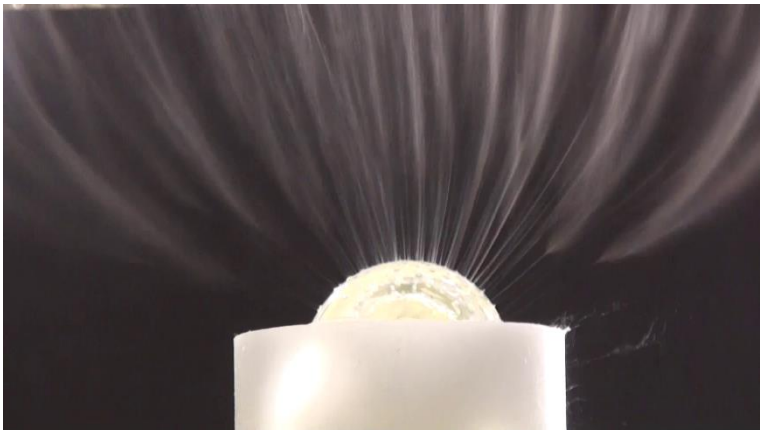

Figure 2.3: Free surface electrospinning (SNC BEST™)

A notable difference in the two electrospinning modalities (needle vs free surface), is the difference in the fibre diameter distribution, with free surface spinnerets (disc, ball and cylinder) typically resulting in fibres with a broad distribution.[8] Bhardwaj and Kundu[15] stated in a review that broad fibre diameter distributions are caused by the instability of the polymer solutions when exposed to an electric field, furthermore, this instability can be related to the solution conductivity. Liu *et al.*[16] stated that the jetting process in free surface electrospinning methods is a passive one, with no control on jet location which subsequently leads to inconsistency in fibre diameter. They showed that fibres of high quality and narrow distribution could be produced by controlling the jetting locations of the polymer layer on a free surface electrospinning apparatus, when electrospinning various polymers (PVDF, PMMA and PVA) using a needle-disk spinneret. Huang *et al.*[9] showed that, a narrower fibre distribution when using free surface electrospinning compared to needle electrospinning can be obtained when electrospinning polystyrene dissolved in DMF. They attributed the change in fibre diameter distribution to stretching forces that are caused by the applied voltage. In the review by Niu and Lin[8], it was stated that the spinneret morphology determines the distribution of the electric field. Spinnerets with smaller surface areas lead to a narrow electric field distribution, which leads to a narrow fibre diameter distribution.[8]

2.2 Emulsions

2.2.1 Background

Emulsions are colloidal systems that are a mixture of two or more immiscible phases that may be stable or unstable. They are encountered daily; Milk is an example of a natural emulsion while vinaigrettes are man-made examples. Emulsions have received attention in drug delivery applications where they have been used to produce nanofibres from dilute polymer solutions, and the encapsulation of active pharmaceutical ingredients (API) into nanofibres.[16,17] Xu *et al.*[17] used SDS stabilised water-in-oil to encapsulate the water-soluble drug doxorubicin hydrochloride in a poly (ethylene glycol)-poly (L-lactic acid) (PEG-PLLA) matrix. They showed that the drug retained its anticancer properties in the nanofibres, and that it was released via diffusion and enzymatic degradation of the PEG.

The components of an emulsion are a dispersed phase, a continuous phase and/or a stabiliser (also referred to as an emulsifier or surfactant). Systems that are more complex consist of an emulsion as the dispersed phase. An example configuration would be a water-in-oil-in-water (W/O/W). The amount of dispersed phase in these systems is expressed by the volume fraction, and this factor has a major effect on the stability and emulsion characteristics.

2.2.2 Emulsion stability

Emulsions can be formed by simple mechanical agitation of the immiscible phases. In the case where specific droplet size of the dispersed phase is desired more complex methods (ultra-sonication/high-speed blenders) can be used to produce nano-emulsions and micro-emulsions.[18] The interfacial tension between the dispersed phase and the continuous phase is a major contributing factor in the emulsification process. If the interfacial tension is too high, emulsions cannot be formed without the addition of a stabiliser. If the interfacial tension is not too high, manual agitation is the only requirement to prevent phase separation.[19] The stabiliser aids the emulsification process by lowering the interfacial tension and enabling the flow of the continuous phase at the interface.[20] For example, Dehghan *et al.*[21] used a novel anionic surfactant to decrease the surface tension between oil and water in the water flooding process in the oil industry.

Surfactants are amphiphilic compounds that consist of a polar head and hydrophobic chain that are used as stabilisers. The maximum decrease in interfacial tension only occurs once a critical micelle concentration is reached in solution. Micelles are surfactant structures that are a result of surfactant molecules rearranging to form geometric structures to find energetically favourable contact with the continuous phase for the hydrophile and lipophile. Surfactants decrease the surface tension through the presence of micelles at the fluid surface or interface. The micelles interrupt the cohesive intermolecular forces at the surface of the continuous phase which leads to the reduced surface tension.[22] The reduction of surface tension has a profound effect on the electrospinning process.[23] The relationship between the hydrophile and the lipophile is expressed by the HLB balance, a dimensionless scale, which denotes surfactants as “water-loving” or fat-loving”. The scale can be used to predict the best surfactant candidates for a desired emulsion (oil-in-water versus water-in-oil).[20]

The stability of emulsions refers to the system’s ability to maintain the initial droplet size of the dispersed phase. In the case of emulsions containing stabilisers, this ability to remain stable is influenced by an interfacial layer of stabilisers that surrounds the dispersed phase. This layer of micelles “protects” the dispersed phase by electrostatic repulsion if the surfactants used are anionic or cationic. When non-ionic surfactants are used, a similar phenomenon to charged surfactants occurs where the droplets are covered with multilayers of micelles.[24] The multilayer structures in non-ionic surfactants arise from intermolecular bonding (e.g. hydrogen bonding) of the micelles. Electrostatic interactions in the micelles can also be used to form secondary structures with co-surfactants that increase the stability of the emulsion by providing a more robust layer on the dispersed phase surface.[25]

2.2.3 Acidic emulsions

Protonation or deprotonation of the polar head of the surfactant is a common problem that is encountered when the continuous phase of the emulsion is acidic or alkaline in nature.[26,27] The protonation/deprotonation can often lead to creaming of the emulsion (the surfactant undergoes flocculation) rendering the emulsion unstable. Liu *et al.*[28] investigated the interactions between sodium caseinate/carboxymethylcellulose at the oil-water interface while varying the pH of the continuous phase from 4.0-7.0. They observed that the formation of multilayer structures between the sodium caseinate/carboxymethylcellulose helped stabilise the emulsion, these multilayer structures are formed via electrostatic interaction between sodium caseinate and carboxymethylcellulose. When the pH was lowered to 4 and 5, emulsions could not be formed using sodium caseinate as the lone stabiliser. The sodium caseinate would undergo creaming and the two phases would immediately separate. This issue was overcome by the addition of carboxymethylcellulose into the system. The emulsions were formed at pH 5 with the emulsion stability increasing with increasing amounts of carboxymethylcellulose. To further investigate the importance of electrostatic interactions between the two stabilisers, sodium chloride (NaCl) was added to these emulsions.[28] The presence of NaCl in the emulsion led to an increase in flocculation, which suggests that the presence of electrolytes in the emulsion might hinder the electrostatic interactions between sodium caseinate and carboxymethylcellulose.

Alba *et al.*[27] investigated the use of okra pods rich in pectin as emulsifiers for acidic aqueous emulsions at pH 3 using hexadecane as the dispersed phase with a volume fraction of 0.2. The okra pods were extracted at two different pH (4 and 6) with the aim of determining the influence of co-extracted proteins on emulsifying capability of the okra pods. It was suggested that the co-extracted proteins form multilayer structures via intermolecular forces with the pectin in the emulsion that leads to a stronger interfacial layer which enhances the stability of the emulsions. The okra pods extracted at pH 6 showed greater emulsion stability than the ones obtained at pH 4 and this was attributed to the extraction pH of the okra pods. The extraction pH influences the extent at which the co-extracted protein can unfold, it is proposed that proteins extracted at pH 6 unfold and form more robust multilayer structures that increase the strength of the interfacial layer and thereby enhances the emulsion stability.

2.2.4 Drug encapsulation

Micro-emulsions and nano-emulsions have been used in the food and pharmaceutical industries to achieve different outcomes. Stable emulsions lead to encapsulation of drugs or food ingredients dissolved in the dispersed phase component of the emulsion.[27] Yang *et al.*[29] used nano-emulsions to “protect” the aldehyde citral from an acidic continuous phase. They observed that a significant loss in citral was only observed after 28 days. Lin *et al.*[22] investigated the use of emulsions as a drug delivery vehicle for the water insoluble polyphenolic compound curcumin (CUR). Different oils were used as the dispersed phase, they observed that the stability of the emulsions was related to the type of oil used with ethyl oleate showing the greatest stability (14 days). Calligaris *et al.*[18] investigated nano-emulsions as a way to increase the in *vitro* bioaccessibility of the flavolignan silybin. They discovered that the

dispersed phase type slightly influenced the *in vitro* bioaccessibility. The overall increase in *in vitro* bioaccessibility was owed to the use of nano-emulsions to deliver silybin.

2.2.5 Emulsion electrospinning

Emulsion electrospinning differs from conventional single component solution electrospinning in that the accompanying components of the emulsion (dispersed phase and/or surfactant) may have a profound effect on the electrospinning and the resulting fibres because of their presence on the Taylor cone (Figure 2.4).[19,30] Carmelo *et al.*[19] used stabiliser-free emulsions to encapsulate the volatile compound (R)-(+)- limonene in PVA fibres. They determined that the presence of the dispersed phase led to bead formation in the fibres. Additionally, an increase in the dispersed phase amount led to an increase in the emulsion viscosity and emulsion age influenced the encapsulation efficiency.

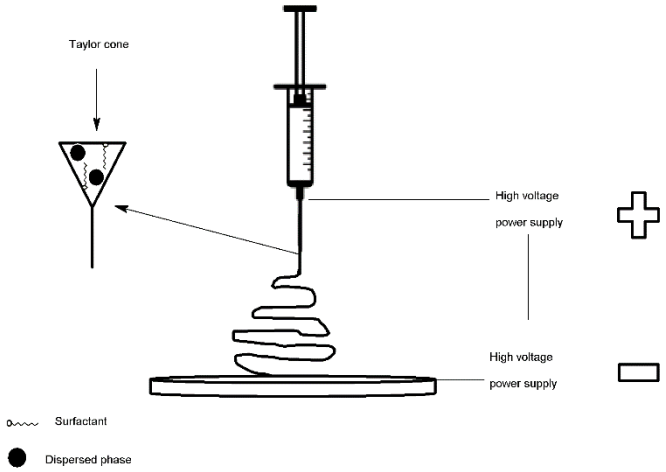

Figure 2.4: Emulsion electrospinning

In the case where surfactants are used to stabilise the emulsion, it is worth noting that micelles are responsible for the emulsion stability.[24] Yazgan *et al.*[31] showed that the addition of the non-ionic surfactant Sorbitan monooealete to water-in-oil emulsions (with PS dissolved in the continuous phase and PVP dissolved in the dispersed phase) reduced the size of the emulsion droplets. They further showed that the presence of the surfactant increased the wettability of the fibres and delayed the release of fluorescein sodium salt. Kong *et al.*[24] determined that the surfactant micelles form stratified layers that separate emulsion droplets. The stratified layers led to greater emulsion stability and restricted the emulsion destabilisation to Ostwald ripening when using the non-ionic surfactant Sorbitan monooleate (commonly referred to as Neodol 45-13) in an oil-in-water emulsion with *n*-hexadecane as the dispersed phase.

Micelles can increase the viscosity of the solution and lower the surface tension.[21,32] The increased viscosity of the solution increases the stability of the emulsion by decreasing the speed at which the dispersed phase globules travel under; this leads to a decrease in coalescence.[20] The increased viscosity can also influence the electrospinning process in a number of other ways.[16] A highly viscous

solution requires a stronger electric field for electrospinning to occur, and an increase in viscosity can lead to thicker fibres and increase fibre diameter variation (bimodality in fibre diameter distribution).[32]

The effect of an increase in viscosity in electrospinning may be counteracted or lessened by the fact that the surface tension is lowered by the presence of micelles. A lower surface tension usually means a lower electric field strength is required to initiate and sustain electrospinning. Nie *et al.*[33] showed that incorporation of glycerol in aqueous sodium alginate solutions decreased the surface tension and led to improved electrospinning.

An additional factor that influences electrospinning is the number of charged species (conductivity) in the polymeric solution.[1] The presence of surfactants can influence the solution's conductivity depending on whether the surfactants are anionic, cationic or non-ionic. In the case where conductivity is increased, the jet length is reduced, the jet undergoes more vigorous and rapid bending and stretching on the way to the collector which may lead to thinner fibres.[34] Hu *et al.*[34] determined that surfactant charge had a significant influence in emulsion conductivity. They found that when an anionic surfactant was used it led to increased conductivity which in turn led to lower fibre diameters and greater uniformity when sodium dodecyl sulphate was used to electrospin water-in-oil emulsion with PCL dissolved in the continuous phase.

It is presumed that in needle electrospinning of emulsions the globules of the dispersed phase are constricted by the walls of the needle and, therefore, cannot easily phase separate.[35,36] These globules are fed to the Taylor cone by a constant solution flow that results in relatively easy encapsulation of the dispersed phase. In free surface electrospinning, the ability to successfully electrospin emulsions is related to the strength of the interaction between the dispersed phase, the continuous phase and surfactant. The presence of a surfactant at the phase boundary enables the dispersed phase to travel with the continuous phase as electrospinning occurs. The dispersed phase undergoes a constant shearing action caused by the solution flow as the continuous phase is drawn into the electrospinning jets. The shearing action is the result of the surfactant bridging the two immiscible phases via an interaction with each individual phase. This interaction is most likely van der Waals forces or hydrogen bonding depending on the emulsion type (water-in-oil versus oil-in-water). A strong enough interaction promotes the flow of the dispersed phase droplets into the spinning jet and enables the droplets to undergo a shearing force as they are incorporated into the nanofibres. An insufficient interaction may result in "pooling" of the dispersed phase at the top of the solution reservoir because of phase separation as electrospinning of the continuous phase occurs. The identity of applied potential on the spinneret (positive or negative) can be influential in the electrospinning if the polymer dissolved is anionic/cationic or charged species are present in solution (surfactants/salts).[38,39] This can lead to enhanced bending whipping which could lead to thinner fibres and fibres with a broad fibre diameter distribution.

The initial globule shape might determine whether the final morphology of the nanofibres will have an "islands-in-the-sea" or "core-shell" morphology shown in Figure 2.5. Additionally, it is pre-assumed that another factor could be the size of encapsulated compounds and the ability of these to "stretch" in the fibre formation process. There is no literature on free surface electrospinning of emulsions of any type,

that fact leaves open an interesting research pathway that could prove beneficial to the food and pharmaceutical industry.

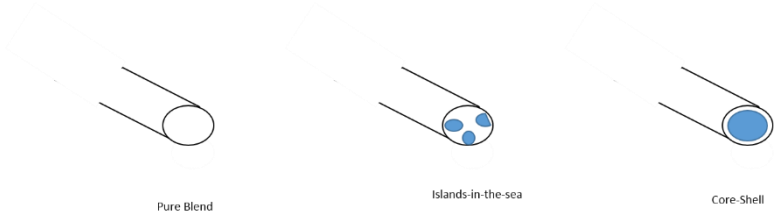

Figure 2.5: Possible internal fibre morphology as a result of electrospinning

2.3 Techniques for complex nanofibre morphology

2.3.1 Phase separation spinning

Porous fibres can be obtained in electrospinning in a single step by using phase separation. Phase separation in this context refers to the use of more than one solvent in polymeric solution, whereby one of the solvent is highly volatile. This combination leads to a formation of polymer rich and polymer poor regions in the polymer jet during electrospinning. As electrospinning occurs the solvent with high volatility leaves evaporates first, leaving voids in the fibres. Katsogiannis *et al.*[37] used a combination of chloroform and dimethyl sulfoxide (DMSO) to form porous PCL fibres. They showed that increasing the amount of non-solvent increased the average fibre diameter. Furthermore, porosity in fibres can be obtained by electrospinning a multi-polymer solution and selectively removing one of the polymers at a later stage with a washing step. Wei *et al.*[38] showed that porous Polyethersulfone (PES) can be obtained by initially electrospinning PES/polyethylene glycol (PEG) using DMSO as a solvent. The porous PES fibres were obtained by removing the PEG with a water washing step.

2.3.2 Coaxial spinning

Core-shell fibre morphology can be obtained by coaxial electrospinning. Coaxial electrospinning refers to electrospinning of two or more solution components that may be miscible or immiscible, this technique is used to encapsulate materials in a single step.[39] The simplest coaxial electrospinning configuration uses needle electrospinning. The configuration uses two needles whereby a small needle is inserted into a large needle.[40] This configuration allows the two different solutions to flow independently to the needle tip. It is important that the needles are of equal length such that both polymeric solutions are present at the needle tip. The polymeric solution flowing from the inner needle forms the core solution, and the shell solution is formed by the solution from the larger outer needle. Once a solution droplet arrives at the needle tip, normal electrospinning occurs.

The concept of core and shell solutions can be extended further to other forms of electrospinning. Benavides *et al.*[41] showed that core-shell fibres could be obtained by air jet spinning. They used two syringes that were configured perpendicularly, the syringes pumped polymeric solutions to a flat plate.

High speed gas flow was used to stretch polymer jet to fibres into the nanometer range. Additionally, they showed that fibres with a side-by-side morphology could be obtained by utilising two syringes side-by-side. This configuration allows solution A to flow on top of solution B. When the air-jet spinning process is applied, it leads to the formation of side-by-side fibres.

Jiang and Qin[42] showed that core-shell fibres can be obtained through free-surface electrospinning. They utilised core and sheath solutions pumped onto a stepped pyramid spinneret. Once the core and sheath were present on top of the spinneret, high voltage was applied, and the normal electrospinning process occurred. Forward *et al.*[10] used a bath to electrospin two immiscible polymeric solutions. A wire electrode rotates through the solution such that a core and sheath solution form onto the wire electrode. Once the solution is present on top of the wire electrode, normal electrospinning occurs.

2.3.3 Graft copolymers

Porous fibres can also be obtained by electrospinning amphiphilic polymers. Bayley and Mallon *et al.*[43] investigated the electrospinning of a polyacrylonitrile-graft-poly (dimethyl siloxane) (PAN-g-PDMS). using dimethylformamide (DMF) as a solvent. They showed that the PDMS potion of the polymer remained insoluble in the solvent (DMF); inducing phase segregation of the polymer components. This leads to the formation of network structures in the polymer solution, which when electrospun these network structures lead to porous fibres. They also showed that increasing the PDMS to a critical amount led to the formation of fully porous fibres using only electrospinning as the processing method.

2.3.4 Potential issues with complex fibre morphology

Complex fibre morphologies are used extensively in the food, medical and pharmaceutical industries. The complex morphologies allow for design control in drug delivery, and promote cell infiltration in tissue engineering applications. However, there are drawbacks associated with these complex morphologies.

Blend electrospinning refers to electrospinning an active pharmaceutical ingredient (API) or when a desired material is blended into the polymeric solution. The API is in incorporated into the nanofibres, this incorporation allows design into the type of release desired for the application. In some cases, the interaction between the encapsulated active and the polymer matrix determines the delivery profile. Wu *et al.*[44] showed that blend spinning of polyacrylonitrile (PAN) with magnesium L-ascorbic acid 2-phosphae (MAAP) and α-tocopherol acetate (α-Tac) led to a burst release of the two actives. Zhao *et al.*[45] attributed the burst release from the incompatibility of the polymer matrix and the active. Furthermore, Wu *et al.*[44] showed that fibres with a core-shell morphology obtained from coaxial electrospinning displayed a diminished burst release.

Zhao *et al.*[45] and Yoon and Kim[46] showed that even core-shell fibres can be problematic in drug delivery. They showed that a burst release of the active compound occurs at the edge of the fabricated fibres. They attributed the burst release to the fact that the core of the fibres is exposed at the edge of each mat (Zhao *et al.*[45] formed the edge by cutting the fibres). This exposure allows release media to permeate the cure and cause a burst release.

2.4 Polycaprolactone

2.4.1 Background

Poly (ε-caprolactone) (PCL) is a synthetic semi-crystalline aliphatic polyester in the same class of compounds (α-hydroxy esters) such as poly (lactic acid) (PLA) and poly (glycolic acid) (PGA).[47] It has a relatively low melting point (60 ^{0}C) with a glass transition temperature of -60 ^{0}C. It is biodegradable, biocompatible and is FDA approved for use in advanced wound care, tissue engineering applications[48] and medical devices.[51,52,53] PCL (shown in Figure 2.6) is popular in the research community because it is commercially available in different molecular weights ranges, is soluble in polar organic solvents (dimethylformamide, hexafluoroisopropanol, chloroform) and it is cheaper compared to PLA and PGA. It is commonly synthesised with ring opening polymerisation which yields the common homopolymer but copolymerisation with PLA, PGA and other polymers is often done to obtain polymer compositions with specific properties.[53,49,50]

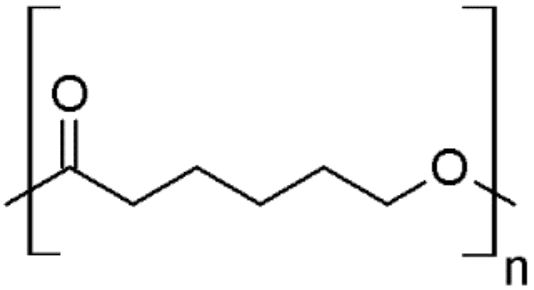

Figure 2.6: Chemical structure of PCL

2.4.2 Electrospinning

Poly (caprolactone) can easily be processed into nanofibres via electrospinning. Kołbuk *et al.*[51] showed that PCL in the nanometre range can be produced from HFIP solutions. They further showed that the average fibre diameter and fibre crystallinity were dependent on the collector type and speed.

2.4.2.1 Solvent influence

2.4.2.1.1 Organic solvents

Gholipour and Bahrami.[32] showed that PCL polymeric solutions made using methylene chloride as a single solvent could not generate nanofibres; this fact underlines a few considerations with regards to electrospinning. Firstly, a good solvent for a polymer does not necessarily mean the resulting polymer solution can be electrospun. This is further proven by Shen *et al.*[52] where they showed that even though dimethylacetamide (DMAc) is a good solvent for methacrylic acid-co-ethyl acrylate the solution could not be processed into nanofibres. They showed that the addition of ethanol or methanol led to fibre formation. It is hypothesized that addition of these solvents increases the conductivity of the solution

that enables electrospinning. Secondly, the number of charged species in the solution can be related to the solvent's dielectric constant, and solvents with low dielectric constants tend to yield polymer solutions that lack the threshold conductivity for that system to enable electrospinning. Luo *et al.*[53] showed that organic solvents cyclohexanone, acetophenone and benzene can dissolve PCL but cannot spin because of low dielectric values. Use of methylene chloride/dimethylformamide mixture led to successful electrospinning. The success might be owed to the addition of a solvent with a higher dielectric constant and lowering of the boiling point of the initial solvent. The vapour pressure is also lowered by the addition of dimethylformamide which improves the electrospinning by preventing gelling at the needle tip

2.4.2.1.2 Carboxylic acids

Common electrospinning solvents such as methylene chloride and dimethylformamide have been shown to cause cancer in humans which limits their use in medical applications of nanofibres.[59] Alternatively carboxylic acids have been investigated as potential replacements for their more harmful counterparts.[54] Van der Schueren *et al.*[54] showed that formic acid and acetic acid can be used as an alternative solvent system to produce PCL nanofibres. They showed that acidic media leads to an evolution of solution viscosity over time. Lavielle *et al.* further expanded the used of the above mentioned binary solvent and they showed that it is possible to tune the molecular weight of electrospun nanofibres by manipulating the solution age with needle electrospinning.

Gholipour and Bahrami.[32] showed that the addition of a non-solvent (such as water) to acetic acid-derived polymeric solutions improved the electrospinning and fibre quality. They hypothesize that the water acts as a non-solvent for PCL whose addition into the system enhances chain entanglements by increasing the hydrodynamic volume of the single polymer coils, this proposed phenomenon may result in enhanced electrospinning and average fibre diameter distribution.[34] Water may further influence the electrospinning process by changing the chemical nature of the acetic acid, the presence of water may lead to enhance the ionisation of acetic acid leading to an increased conductivity. Gholipour and Bahrami.[32]. further showed that incorporation of water into the acetic acid PCL solution led to the conductivity increasing by 1.6 times.

2.4.3 Drug delivery applications

PCL has been used in drug delivery applications owing to relatively slow degradation rate of the polymer and its high permeability.[55] PCL has a glass transition temperature of -60^{o}C, which renders the material being soft and pliable at room temperature, this make the material compatible in wound dressings where it may increase comfort in patients.[56]

Sinha *et al.*[57] stated that PCL microspheres can be produced into microspheres by utilizing techniques such as spray drying, emulsion and solution-enhanced dispersion method. These microspheres were used to deliver the hydrophilic and lipophilic drugs; nifedipine and propranolol HCl. In an additional review, Woodruff and Hutmacher[55] indicated that PCL nanofibres promoted the growth and attachment of osteoblastic cells. The PCL nanofibres were surface modified, to possess bone-like apatite layer. Alhusein *et al.*[58] showed that the incorporation of PCL into zein electrospinning solutions increased the

stability of zein fibres in an aqueous environment. The electrospun fibres were successfully used to control the release of the antibiotic tetracycline. Lastly, Lee *et al.*[59] showed that electrospun PCL fibres can be useful in gene therapy. The fibres were used to control the release of the gene carrier adeno-associated virus, that the adeno-associated virus can be used in cellular transduction.

2.5 Curcumin

2.5.1 Background

CUR is a hydrophobic polyphenolic compound (shown in Figure 2.7) which has proven to possess anti-cancer, anti-oxidant, anti-HIV and anti-inflammatory properties.[60] Its anti-oxidant properties arise from its ability to act as a scavenger for radicals. This occurs by hydrogen donation from any of the phenol groups leading to a phenoxyl radical that is easily stabilised by resonance as shown in Figure 2.8.

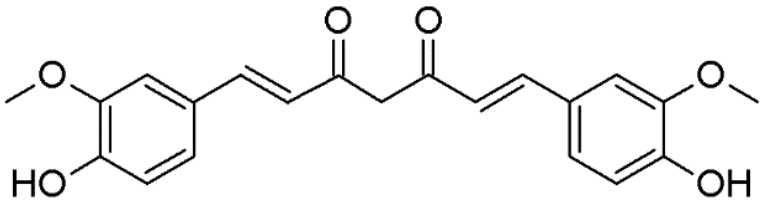

Figure 2.7: Chemical structure of CUR

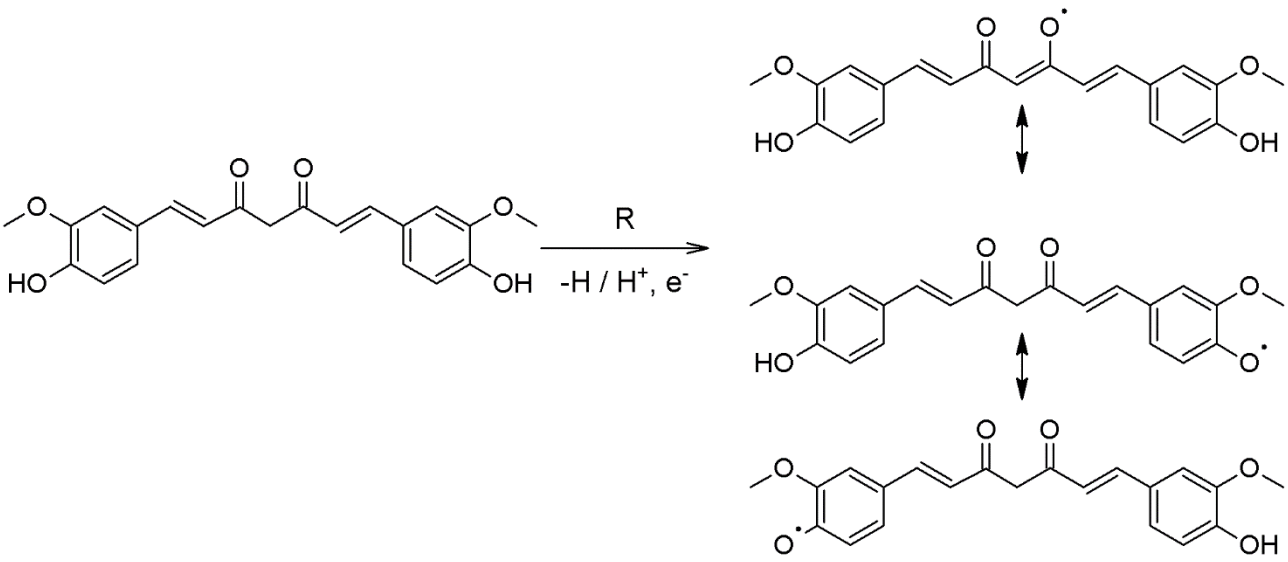

Figure 2.8: Reaction depicting anti-oxidant properties of CUR[60]

It has historically been used to treat colds, inflammation and as a dye in paintings. It is readily available as it is one curcuminoids of the household spice turmeric.[22] It is commonly extracted from the spice via

alcohol (ethanol) based solvent extraction although polar and non-polar organic solvents can be used coupled with soxhlet, microwave or ultrasonic extraction amongst others.[61]

2.5.2 Solubility and stability

Curcumin has limited solubility in aqueous media although it is soluble in a number of FDA approved oils for topical emulsions.[22] This poor solubility has led to the drug's limited pharmaceutical use; however, attempts have been made to increase its solubility via encapsulation and nano-emulsions. [22] Additionally, hydrotropes have been used to increase the solubility of CUR without the need for emulsification.[62] CUR degrades relatively quickly in different environments. It quickly degrades in the presence of light which has led to the common method of removing turmeric stains by exposing stained materials to the sun's rays. It degrades in organic phases; however, the instability increases with increasing pH. Erez *et al.*[63] investigated the effect of different acids on the UV-VIS and emission properties of CUR. A trend was observed with the different acids where the CUR absorption and emission wavelengths shifted to new values (shorter wavelength for emission, and longer wavelength for the absorption). It was suggested that the shifts can be attributed to a protonated CUR ion (ROH_2^+) as shown in Figure 2.9 which absorbs and has an emission at different wavelengths. Further inquiry was done with CUR exposed to alkaline conditions. Another set of shifts was observed, this time a deprotonated form (RO^-) was believed to be the reason for the shifts.

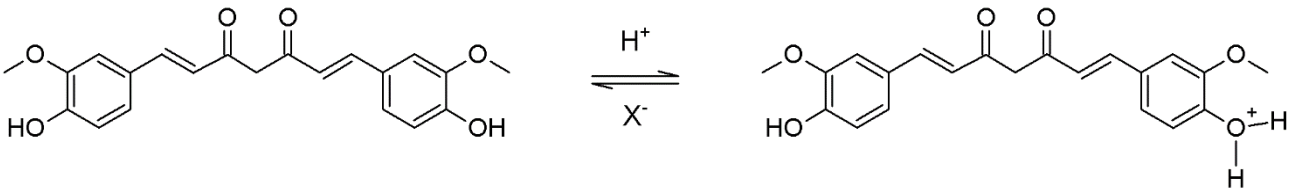

Figure 2.9: Reaction depicting the protonation of CUR

2.5.3 Electrospinning

The physical properties of CUR have led to its limited use in medical applications.[64] It is hydrophobic in nature and has low bioavailability, this had led to attempts at creating delivery vehicles. CUR has been successfully incorporated into nanofibres in a variety of methods. Merrell *et al.*[65] investigated CUR-loaded PCL nanofibres for their wound healing capabilities. In the study a mixture of chloroform/methanol was used as the solvent for both the polymer and CUR, it is reported that the inclusion of CUR in the electrospinning solution increased the average fibre diameter and yielded a larger variation in fibre diameter. A reason or hypothesis for the increase in variation was not provided. It was also found that the system had a ceiling of how much CUR can be added to the electrospinning solution. If more was added, then the CUR precipitated out of solution and nanoparticles of CUR were visible on scanning electron microscopy (SEM) images.

2.6 References

(1) Greiner, A.; Wendorff, J. H. *Angew. Chem. Int. Ed. Engl.* **2007**, *46*, 5670–5703.

(2) Liu, Y.; Ma, G.; Fang, D.; Xu, J.; Zhang, H.; Nie, J. *Carbohydr. Polym.* **2011**, *83*, 1011–1015.

(3) McKee, M. G.; Wilkes, G. L.; Colby, R. H.; Long, T. E. *Macromolecules* **2004**, *37*, 1760–1767.

(4) Zhou, F. L.; Gong, R. H.; Porat, I. *Polym. Int.* **2009**, *58*, 331–342.

(5) Lukas, D.; Sarkar, A.; Pokorny, P. *J. Appl. Phys.* **2008**, *103*, 1–8.

(6) Augustine, R.; Kalarikkal, N.; Thomas, S. *Polym. - Plast. Technol. Eng.* **2016**, *55*, 518–529.

(7) Yang, E.; Shi, J.; Yuan, X. *J. Appl. Polym. Sci.* **2010**, *116*, 3688–3692.

(8) Niu, H.; Lin, T. *J. Nanomater.* **2012**, *2012*, 1–13.

(9) Huang, C.; Niu, H.; Wu, J.; Ke, Q.; Mo, X.; Lin, T. *J. Nanomater.* **2012**, *2012*.

(10) Forward, K. M.; Flores, A.; Rutledge, G. C. *Chem. Eng. Sci.* **2013**, *104*, 250–259.

(11) Yarin, A. L.; Zussman, E. *Polymer.* **2004**, *45*, 2977–2980.

(12) He, J. X.; Qi, K.; Zhou, Y. M.; Cui, S. Z. *Fibers Polym.* **2014**, *15*, 2061–2065.

(13) Liu, Y.; He, J.-H.; Yu, J.-Y. *J. Phys. Conf. Ser.* **2008**, *96*.

(14) Jiang, G.; Zhang, S.; Wang, Y.; Qin, X. *Mater. Lett.* **2015**, *144*, 22–25.

(15) Bhardwaj, N.; Kundu, S. C. *Biotechnol. Adv.* **2010**, *28*, 325–347.

(16) Liu, Z.; Chen, R.; He, J. *Mater. Des.* **2016**, *94*, 496–501.

(17) Xu, X.; Yang, L.; Xu, X.; Wang, X.; Chen, X.; Liang, Q.; Zeng, J.; Jing, X. *J. Control. Release* **2005**, *108*, 33–42.

(18) Calligaris, S.; Comuzzo, P.; Bot, F.; Lippe, G.; Zironi, R.; Anese, M.; Nicoli, M. C. *LWT - Food Sci. Technol.* **2015**, *63* (1), 77–84.

(19) Camerlo, A.; Vebert-Nardin, C.; Rossi, R. M.; Popa, A. M. *Eur. Polym. J.* **2013**, *49*, 3806–3813.

(20) Schramm, L. L.; Stasiuk, E. N.; Marangoni, D. G. *Annu. Reports Sect. "C" (Physical Chem.* **2003**, *99*, 3–48.

(21) Dehghan, a. a.; Masihi, M.; Ayatollahi, S. *Fluid Phase Equilib.* **2015**, *396*, 20–27.

(22) Lin, C. C.; Lin, H. Y.; Chen, H. C.; Yu, M. W.; Lee, M. H. *Food Chem.* **2009**, *116*, 923–928.

(23) Leung, V.; Hartwell, R.; Elizei, S. S.; Yang, H.; Ghahary, A.; Ko, F. *J. Biomed. Mater. Res. B. Appl. Biomater.* **2014**, *102*, 508–515.

(24) Kong, Y.; Nikolov, A.; Wasan, D. *Ind. Eng. Chem. Res.* **2010**, *49*, 5299–5303.

(25) Kute, S. B.; Saudagar, R. B. *J. Adv. Pharm. Educ. Res.* **2013**, *3*, 368–376.

(26) Papagianni, M.; Anastasiadou, S. *Enzyme Microb. Technol.* **2009**, *45*, 514–522.

(27) Alba, K.; Ritzoulis, C.; Georgiadis, N.; Kontogiorgos, V. *Food Res. Int.* **2013**, *54* (2), 1730–1737.

(28) Liu, L.; Zhao, Q.; Liu, T.; Kong, J.; Long, Z.; Zhao, M. *Food Chem.* **2012**, *132*, 1822–1829.

(29) Yang, X.; Tian, H.; Ho, C. T.; Huang, Q. *J. Agric. Food Chem.* **2011**, *59*, 6113–6119.

(30) Arecchi, A.; Mannino, S.; Weiss, J. *J. Food Sci.* **2010**, *75* (6), 80–88.

(31) Yazgan, G.; Popa, A. M.; Rossi, R. M.; Maniura-Weber, K.; Puigmarti-Luis, J.; Crespy, D.; Fortunato, G. *Polymer.* **2015**, *66*, 268–276.

(32) Gholipour Kanani, A.; Bahrami, S. H. B. *J. Nanomater.* **2011**, *2011*, 1–10.

(33) Nie, H.; He, A.; Zheng, J.; Xu, S.; Li, J.; Han, C. C. *Biomacromolecules* **2008**, *9*, 1362–1365.

(34) Hu, J.; Prabhakaran, M. P.; Ding, X.; Ramakrishna, S. *J. Biomater. Sci. Polym. Ed.* **2015**, *26*, 57–75.

(35) Shastri, V. P.; Sy, J. C.; Klemm, A. S. *Adv. Mater.* **2009**, *21* (18), 1814–1819.

(36) Wang, C.; Tong, S. N.; Tse, Y. H.; Wang, M. *Adv. Mater. Res.* **2012**, *410*, 118–121.

(37) Katsogiannis, K. A. G.; Vladisavljević, G. T.; Georgiadou, S. *Eur. Polym. J.* **2015**, *69*, 284–295.

(38) Wei, Z.; Zhang, Q.; Wang, L.; Peng, M.; Wang, X.; Long, S.; Yang, J. *Sep. Sci. Technol.* **2013**, *48*, 2287–2292.

(39) Li, J.; Feng, H.; He, J.; Li, C.; Mao, X.; Xie, D.; Ao, N.; Chu, B. *J. Biomater. Sci. Polym. Ed.* **2013**, *24* (17), 1923–1934.

(40) Jiang, H.; Zhao, P.; Zhu, K. *Macromol. Biosci.* **2007**, *7*, 517–525.

(41) Benavides, R. E.; Jana, S. C.; Reneker, D. H. *ACS Macro Lett.* **2012**, *1*, 1032–1036.

(42) Jiang, G.; Qin, X. *Mater. Lett.* **2014**, *128*, 259–262.

(43) Bayley, G. M.; Mallon, P. E. *Polymer.* **2012**, *53* (24), 5523–5539.

(44) Wu, X. M.; Branford-White, C. J.; Yu, D. G.; Chatterton, N. P.; Zhu, L. M. *Colloids Surfaces B Biointerfaces* **2011**, *82*, 247–252.

(45) Zhao, X.; Lui, Y.; Toh, P.; Loo, S. *Materials (Basel).* **2014**, *7*, 7398–7408.

(46) Yoon, H.; Kim, G. H. *Macromol. Res.* **2012**, *20*, 402–406.

(47) Abdelrazek, E. M.; Hezma, A. M.; El-khodary, A.; Elzayat, A. M. *Egypt. J. Basic Appl. Sci.* **2015**, *3* (1), 10–15.

(48) Park, K. E.; Kim, B. S.; Kim, M. H.; You, H. K.; Lee, J.; Park, W. H. *Polymer.* **2015**, *76*, 8–16.

(49) Bui, H. T.; Chung, O. H.; Dela Cruz, J.; Park, J. S. *Macromol. Res.* **2014**, *22*, 1288–1296.

(50) Schindler, C.; Williams, B. L.; Patel, H. N.; Thomas, V.; Dean, D. R. *Polymer.* **2013**, *54*, 6824–6833.

(51) Kołbuk, D.; Sajkiewicz, P.; Maniura-Weber, K.; Fortunato, G. *Eur. Polym. J.* **2013**, *49*, 2052–2061.

(52) Shen, X.; Yu, D.; Zhu, L.; Branford-White, C.; White, K.; Chatterton, N. P. *Int. J. Pharm.* **2011**, *408*, 200–207.

(53) Luo, C. J.; Stride, E.; Edirisinghe, M. *Macromolecules* **2012**, *45*, 4669–4680.

(54) Van der Schueren, L.; De Schoenmaker, B.; Kalaoglu, Ö. I.; De Clerck, K. *Eur. Polym. J.* **2011**, *47*, 1256–1263.

(55) Woodruff, M. A.; Hutmacher, D. W. *Prog. Polym. Sci.* **2010**, *35*, 1217–1256.

(56) Luo, C. J.; Stoyanov, S. D.; Stride, E.; Pelan, E.; Edirisinghe, M. *Chem. Soc. Rev.* **2012**, *41*, 4708–4735.

(57) Sinha, V. R.; Bansal, K.; Kaushik, R.; Kumria, R.; Trehan, A. *Int. J. Pharm.* **2004**, *278* (1), 1–23.

(58) Alhusein, N.; Blagbrough, I. S.; de Bank, P. a. *Drug Deliv. Transl. Res.* **2013**, *3* (6), 542–550.

(59) Lee, S.; Jin, G.; Jang, J.-H. *J. Biol. Eng.* **2014**, *8*, 30.

(60) Mahmood, K.; Zia, K. M.; Zuber, M.; Salman, M.; Anjum, M. N. *Int. J. Biol. Macromol.* **2015**, *81*,

877–890.

(61) Priyadarsini, K. *Molecules* **2014**, *19*, 20091–20112.

(62) Shafi, M.; Saudagar, R. **2015**, *4*, 324–332.

(63) Erez, Y.; Simkovitch, R.; Shomer, S.; Gepshtein, R.; Huppert, D. *J. Phys. Chem. A* **2014**, *118*, 872–884.

(64) Mayol, L.; Serri, C.; Menale, C.; Crispi, S.; Piccolo, M. T.; Mita, L.; Giarra, S.; Forte, M.; Saija, A.; Biondi, M.; Mita, D. G. *Eur. J. Pharm. Biopharm.* **2015**, *93*, 37–45.

(65) Merrell, J. G.; McLaughlin, S. W.; Tie, L.; Laurencin, C. T.; Chen, A. F.; Nair, L. S. *Clin. Exp. Pharmacol. Physiol.* **2009**, *36*, 1149–1156.

Chapter 3: Experimental

3.1 Preparation of polycaprolactone solutions

Various carboxylic acids were investigated as alternative solvents for biodegradable polyesters.[1,2] Biodegradable esters are widely used in the drug delivery and tissue engineering industries owing to their biocompatibility.[3] Polycaprolactone (PCL) was chosen as the model polymer because of its widespread use in research and in industry applications. Both needle and free surface electrospinning were chosen as the method of processing the polymer into nanofibre/microfibre form. The carboxylic acids investigated in this work are formic acid, acetic acid, propionic acid and butyric acid.

3.1.1 Polymer solutions

PCL pellets were weighed, then added to each solvent to achieve the desired polymer concentration. The solution was stirred with a magnetic stirrer at room temperature for 3-12 hours. Heat was used to complete the dissolution where necessary.

Sodium acetate (SA), curcumin (CUR) and benzyltriethylammonium chloride (TEB) were added to certain polymeric solutions. The salts were added with an aim to increase the conductivity of the polymeric solutions where necessary.[4,5] The salts were added once the PCL was completely dissolved. Once added, the solution was allowed to stir for a further 30 minutes. Additionally, the non-ionic surfactant Polysorbate 80 was added to some solutions with the aim of altering the surface properties of the electrospun fibres.[6,7] The Polysorbate 80 was added to the polymeric solution once the polymer had dissolved and 30 minutes prior to electrospinning.

The PCL, SA, CUR, isopropyl myristate (IPM), propionic acid, butyric acid, Polysorbate 80 and benzyltriethylammonium chloride were supplied by Sigma Aldrich. The acetic acid and formic acid were supplied by Kimix Chemicals. All chemicals and raw materials were used as received.

3.1.2 Emulsions

Emulsions were prepared by dropwise addition of the dispersed phase to the continuous phase. In the cases where a stabilizer was used, it was dissolved in the continuous phase beforehand. The emulsions were formed by manual agitation with an overhead stirrer at 2000 rpm using a paddle stirrer. The emulsions were allowed to stir for 30 minutes. The CUR was dissolved in the dispersed phase prior to addition.

3.2 Electrospinning

3.2.1 Needle electrospinning

3.2.1.1 Apparatus

A high voltage power supply was used to apply positive potential on a blunt tip needle while a second high voltage power supply simultaneously applied negative potential on a collector to complete an electric field of a desired strength. The collector was a flat piece of aluminium foil. The aluminium foil was wrapped over a 15 cm cardboard square. A syringe pump was used to drive the polymeric solution to the needle capillary. The needle had a diameter of 0.8 mm while the syringe used had a volume capacity of 1 millilitre (ml).

The high voltage power supplies are manufactured by Spellman® High Voltage Electronics. The model used to apply positive potential is the SL80P150/220, it is capable of producing up to 80 kilovolts (kV) of positive potential and 1.7 milliamperes (mA) of current. The model used to apply negative potential is the SL80N150220, it also produces up to 80 kV and 1.7 mA. The syringe pump is supplied by New Era Pump Systems and the model is the Master Dual Pump.

3.2.1.2 Electrospinning setup and procedure

The polymeric solution was placed in the syringe with the needle attached at the end of the syringe barrel (refer to Figure 2.1). The syringe was connected to a hydraulic setup that transferred the force from the syringe pump to the syringe containing the solution. The reason a hydraulic setup was added to the electrospinning setup was to distance the syringe pump in case there is electric discharge from the electrospinning that might cause damage to the pump. The syringe of the hydraulic setup was placed on the syringe pump with the plunger flange resting against the pusher block of the syringe pump. The needle tip was placed 15 cm away from the collector, it was connected to the positive power supply by a stripped wire cable. The collector was connected to the negative power supply by stripped wire as well to complete the electric field. A flow rate of 0.1 ml/hr was sufficient to form a consistent droplet on the needle tip. The positive potential was applied to the droplet, it ranged from 8-12 kV. The negative potential was applied to complete the electric between the droplet and the collector, it ranged from 0-2 kV. The applied potentials resulted in electrospinning of the polymeric solution. The resulting fibres were collected on the aluminium foil.

3.2.1.3 Fibre collection

The fibres were collected onto aluminium foil. The resulting mats were carefully removed and placed between wax paper then stored in a freezer until they were required for analysis. Storing the materials in the freezer prevents/lessens the extent to which the materials are being exposed to moisture. Additionally, the low temperatures prevents/slows the hydrolysis of the polymer, prior to analysis.

3.2.2 Free surface electrospinning

The free surface electrospinning methodology used in this study is the patented SNC BEST™ methodology. Electrospinning occurs on the surface of a ball that is rotated during the electrospinning process as discussed in the literature review section.

3.2.2.1 Apparatus

The electrospinning was conducted on custom made equipment that housed the power supplies, collector, and solvent extraction system. A high voltage power supply was used to supply positive potential to the solution reservoir (cup). The connection to the power supply to the cup was made via a banana connector (a single wire connector). A ball (13 mm in diameter) was rotated through the solution at a constant speed to obtain the desired coating of fibres on the collector. A counter electrode was connected to a drum wrapped in aluminium foil by stripped wire cable. The drum was rotated to a desired speed with a stepper motor.

3.2.2.2 Electrospinning setup and procedure

The cup with a ball was placed on a flat surface on the custom-made equipment with the drum collector positioned directly above it (refer to Figure 2.2). The spinning distance was determined by the desired electric field strength. Additionally, the spinning distance was set such that there was adequate time for the solvent to evaporate as the jets moves towards the collector. The ball in the cup was rotated in a clockwise direction, the ball speed (2-3 rpm) was determined by the stability of jets on the ball surface. The solution was charged by the positive potential high voltage power supply inserted at the base of the cup. The ball motion led to a thin coating of polymeric solution on the ball surface. The solution layer feeds the jets as determined by the jet stability. The drum collector was connected to a negative high voltage power supply by a stripped wire cable. Once the ball was rotating both high voltage power supplies were switched on creating an electric field in the range of 50-70 kV. Electrospinning occurred with the fibres depositing directly onto the drum collector.

3.2.2.3 Fibre collection

The fibres were collected with a cardboard drum wrapped in aluminium foil. The drum was connected to the negative high voltage power supply by a stripped wire cable. The collection speed was 300 rpm. This yielded randomly aligned fibres on the drum. The drum had a length of 40 cm and an internal diameter of 16 cm. The resulting mats were stored in a freezer prior to analysis.

3.3 Characterization techniques

3.3.1 Solution properties

3.3.1.1 Surface tension

The surface tension measurements were done on a Krüss K6 Tensiometer at 25 ^{0}C. Readings were done in triplicate. A 20 ml volume polymeric solution was placed in a 25 ^{0}C water bath for 30 minutes

prior to the analysis. The values were adjusted against the reported value of distilled water that was measured prior to the analysis of the polymeric solutions.

3.3.1.2 Viscosity

The viscosity of each polymeric solution was measured in order to determine the influence of molecule size on solution viscosity. The solution viscosity is an important parameter in electrospinning.[4] The viscosity was measured by a Brookfield Digital Viscometer. The readings were done in triplicates at 24-25 ^{0}C. A 7 ml volume sample was measured with an s21 spindle. A common stirring speed was selected to compare the different polymeric solutions. The value of the common speed was determined by the maximum stirring speed that could be attained in the most viscous solution. 12 rpm was the speed selected, the readings on the instrument were stable after 10 minutes.

3.3.1.3 Conductivity

Electrical conductivity of the spinning solutions was measured by a multi-range conductivity bench meter (the model used is the EC215-02) supplied by Hanna instruments. The instrument was calibrated with a calibrated standard and temperature. The calibration standard was supplied by Hanna instruments. The solutions were place in a 25 ^{0}C water bath for 30 minutes prior to the analysis. Readings were done in triplicate.

3.3.2 Fibre morphology

3.3.2.1 Scanning electron microscopy (SEM)

SEM analysis was done to obtain the morphology of the electrospun fibres. The instrument used was a Zeiss Merlin Field Emission Scanning Electron Microscope (FE-SEM) with the Zeiss SmartSEM software. The electrospun fibre mats were mounted onto stubs with carbon tape and coated using an Edwards S150A Gold Sputter Coater that yielded 10 nm of coating onto the samples. The beam had an accelerating voltage of 5.0 kV with 250 pA beam current and a working distance of 3.8-4.0 mm, the column was in high resolution mode.

3.3.2.2 Scanning transmission electron microscopy (STEM)

The STEM analysis was done with an aim of obtain an internal fibre morphology. A Merlin FE-SEM was used for STEM analysis with a Zeiss five-diode Scanning Transmission Electron Detector (Zeiss aSTEMA Detector). The electrospun fibres were placed onto carbon-coated copper TEM grids. The beam had an accelerating voltage of 20 kV with a 250 pA probe current and a working distance of 4 mm. The images were acquired in bright field's mode.

3.3.3 Thermal Analysis

3.3.3.1 Differential scanning calorimetry (DSC)

Thermal analysis was done on the electrospun fibres and films to determine the effect of processing on the thermal behaviour of PCL. The instrument used was a Q100 DSC manufactured by TA instruments.

The samples were not annealed prior to analysis as the aim of the study was to determine whether the rapid nature of electrospinning had an influence on the observed crystallinity. In other words, the first heating cycle was recorded and used for the analysis, unless otherwise stated. The sample weight used was 5.0 mg (±0.2) place into aluminium pans. There were two heating cycles and a cooling cycle performed at a rate 10 kelvin per minute (K/m). The temperature range used was 0-100 ^{o}C, under nitrogen at a flow rate of 50 ml/min.

3.3.4 Molar mass determination

3.3.4.1 Size exclusion chromatography (SEC)

Films made from polymeric solutions and electrospun fibres were submitted for SEC analysis. The instrument used was manufactured by Waters, the detectors used were a Waters 2487 dual wavelength absorbance detector with a Waters 2414 refractive index detector and Waters 717 $_{plus}$ Autosampler. The operating parameters were a column injection of 100 µL with the column oven temperature of 30 ^{0}C. Tetrahydrofuran (THF) was used as the eluent with polystyrene used as standards. The molecular weight range of the standards was 580-3.42 x 10 ^{6} g/mol. The columns used were two PL gel 5 µm Mixed-C columns and a PL gel 5 µm guard column.

The full details of the protocol used in the model drug release are given in the relevant section.

3.4 References

(1) Van der Schueren, L.; De Schoenmaker, B.; Kalaoglu, Ö. I.; De Clerck, K. *Eur. Polym. J.* **2011**, *47*, 1256–1263.

(2) Lavielle, N.; Popa, A. M.; De Geus, M.; Hébraud, A.; Schlatter, G.; Thöny-Meyer, L.; Rossi, R. M. *Eur. Polym. J.* **2013**, *49*, 1331–1336.

(3) Marin, E.; Briceño, M. I.; Caballero-George, C. *Int. J. Nanomedicine* **2013**, *8*, 3071–3091.

(4) Kim, S. J.; Lee, C. K.; Kim, S. I. *J. Appl. Polym. Sci.* **2005**, *96*, 1388–1393.

(5) Ding, W.; Wei, S.; Zhu, J.; Chen, X.; Rutman, D.; Guo, Z. *Macromol. Mater. Eng.* **2010**, *295*, 958–965.

(6) Rieger, J.; Dubois, P.; Jerome, R.; Jerome, C. *Langmuir* **2006**, *22*, 7471–7479.

(7) Ferreira, J. L.; Gomes, S.; Henriques, C.; Borges, J. P.; Silva, J. C. *J. Appl. Polym. Sci.* **2014**, *41068*, 37–39.

(8) McKee, M. G.; Wilkes, G. L.; Colby, R. H.; Long, T. E. *Macromolecules* **2004**, *37*, 1760–1767.

Chapter 4: Results and discussion

4.1 Introduction

This chapter describes the dissolution of polycaprolactone (PCL) in different carboxylic acid solvent systems with an aim to process these solutions via electrospinning. The solution properties associated with each polymer solution are also investigated. The electrospinnability of each polymer solution is determined via needle and free surface electrospinning methods. Electrospinnability refers to the ability of a polymer solution, of a certain composition, to produce smooth bead-free fibres when exposed to an electric field.

4.2 Polymer dissolution

The aim of this study is to investigate the influences that effect the dissolution ability of carboxylic acids with regards to (α-hydroxy) polyesters. The carboxylic acids used include formic acid (FA), acetic acid (AA), propionic acid (PA) and butyric acid (BA). The PCL pellets and solvents were stirred (at 200 rpm) using a magnetic stirrer. This is a continuation of the work done by Van der Schueren *et al.*[1], where they showed that PCL is soluble in carboxylic acid derived solvent systems.

Table 4.1 shows the relationship between the nature of the solvent, pKa, dielectric constant and dissolution rate of 15 wt% polymer solutions. In some cases, heat was used to facilitate the dissolution.

Table 4.1 Physical properties and dissolution observations of PCL in various carboxylic acids (the polymer (PCL) concentration evaluated was 15 wt %)[2,3]

Solvent	Dielectric constant	pKa	Polymer dissolution rate
FA	57.9	3.75	Complete polymer dissolution in 3-4 hours
AA	6.2	4.75	Partial dissolution in 12 hours, requires heating for 10-15 minutes at 40 ^{o}C
PA	3.2	4.87	Partial dissolution in 12 hours, requires heating for 30 minutes at 40 ^{o}C
BA	3.0	4.91	Partial dissolution in 12 hours, requires heating for 30-45 minutes at 40 ^{o}C

The results suggest that the dissolution rate is highly dependent on the type of carboxylic acid used. The trend indicates that the dissolution ability decreases with an increase in carboxylic acid molecular size. It is well known that an increase in the molecular size in carboxylic acids is accompanied by an increase in the pKa.[3] Large pKa values are associated with poorly dissociating acids.

The dissociation ability of carboxylic acids is determined by the degree of stabilisation of the resulting carboxylate ion. Molecules in which the carboxylate ion is resonance stabilised possess a higher degree of stability, which increases the dissociation ability. The resonance stabilisation is influenced by whether the adjacent group on the carboxylate ion is electron-withdrawing or electron-donating. Electron-withdrawing groups (or atoms) render the carbon atom more electron deficient. This deficiency enables electron distribution across the carboxylate ion and thus increases the stability of the ion. Electron-donating groups (or atoms) hinder the stability of the carboxylate ion by performing the reverse function.[3]

FA displays a lower pKa than the other carboxylic acids. This is due to FA possessing an electron-neutral adjacent group. The other carboxylic acids possess a carbon atom that donates electrons via induction, and thus decreases the stability of the carboxylate ion. The results in Table 4.1 suggest that dissolution ability increases with a decrease in pKa. This may be due to the tendency of PCL to degrade in acidic media.[4] The more acidic the media, the more the polymer can degrade and hence the ease of dissolution. The degradation behaviour of PCL in acidic media is discussed in more detail later in the chapter.

4.3 Influence of solvent type on solution properties

4.3.1 Surface tension

Niu and Lin[5] stated that the surface tension of polymer solutions, significantly affects the electrospinning process when utilising a needleless apparatus. The surface tension of the polymer solutions can be related to the bulk properties of the solvent system and polymer-solvent interactions. Since an equal amount of polymer is present in all the solvent systems evaluated, polymer concentration can be minimized as a contributing factor to the solution properties. Given the low values of the dielectric constant, and larger pKa values for PA and BA shown in Table 4.1 additional solutions were made with each solvent system with additives that might promote electrospinning. Yalcinkaya *et al.*[6] showed that adding lithium chloride led to improved electrospinning when processing polyurethane polymer solutions with DMF as the solvent. They attributed the improved electrospinning to the salt-polymer interactions that lead to an increase in entanglements, thus leading to better electrospinning. The additives used in the current study were sodium acetate ($NaCH_3COO$) and benzyltriethylammonium chloride (TEB). Figure 4.1 (and Table A1 in the Appendix A) show the relationship between surface tension and the nature of the solvent.

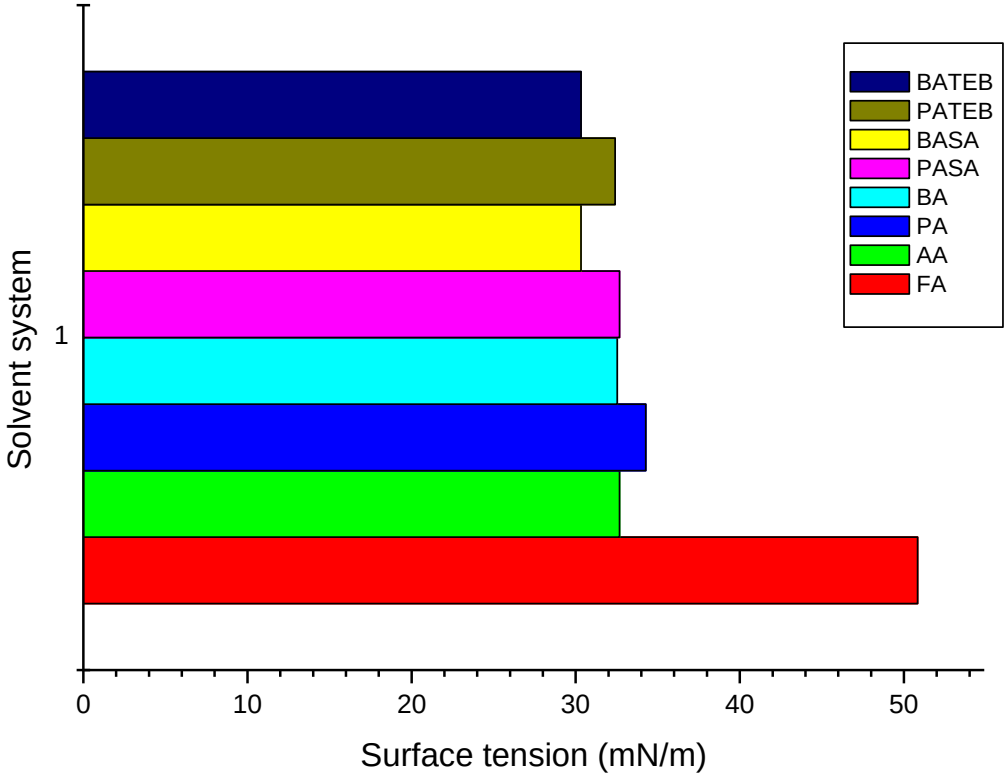

Figure 4.1: Surface tension of 15 wt% PCL polymer solutions as influenced by solvent composition

Only the FA solution displayed results which significantly differed from the other solvent systems evaluated (AA, PA and BA). The higher value obtained can be related to a higher polarity of FA compared to the other carboxylic acids. The increased polarity means that the intermolecular forces (hydrogen bonding) are stronger when compared to the other carboxylic acids, and leads to larger surface tension values.

The results obtained for AA are comparable to the values determined by Ferreira *et al.*[7]. When compared to the original solutions, polymer solutions containing the salts $NaCH_3COO$ (SA) and TEB salts showed a slight decrease in surface tension, which is in agreement with the observations of Yalcinkaya *et al.*[6], where the presence of the salt did not influence the surface tension significantly.

4.3.2 Viscosity

Solvent-polymer interactions are essential to electrospinning.[8] These interactions lead to the inherent solution viscosity. The inherent viscosity may be related to the dissolution ability of different solvent systems. Furthermore, the viscosity can be related to ambient conditions. Yang *et al.*[9] and De Vrieze *et al.*[10] showed that the viscosity of polymer solutions decreases with an increase in ambient temperature when processing cellulose acetate, PVP and PAN with electrospinning. Additionally, Zhou *et al.*[11] state that the polymer molecular weight is related to the viscosity, and this factor is important in determining whether the process will undergo electrospinning or electrospray. Figure 4.2 (and Table A2 in Appendix

A) show the relationship between the viscosity and the nature of the solvent for the systems in this study. (Note that these measurements were all done at fixed times after solution preparation due to potential polymer degradation discussed in more detail in section 4.5.1).

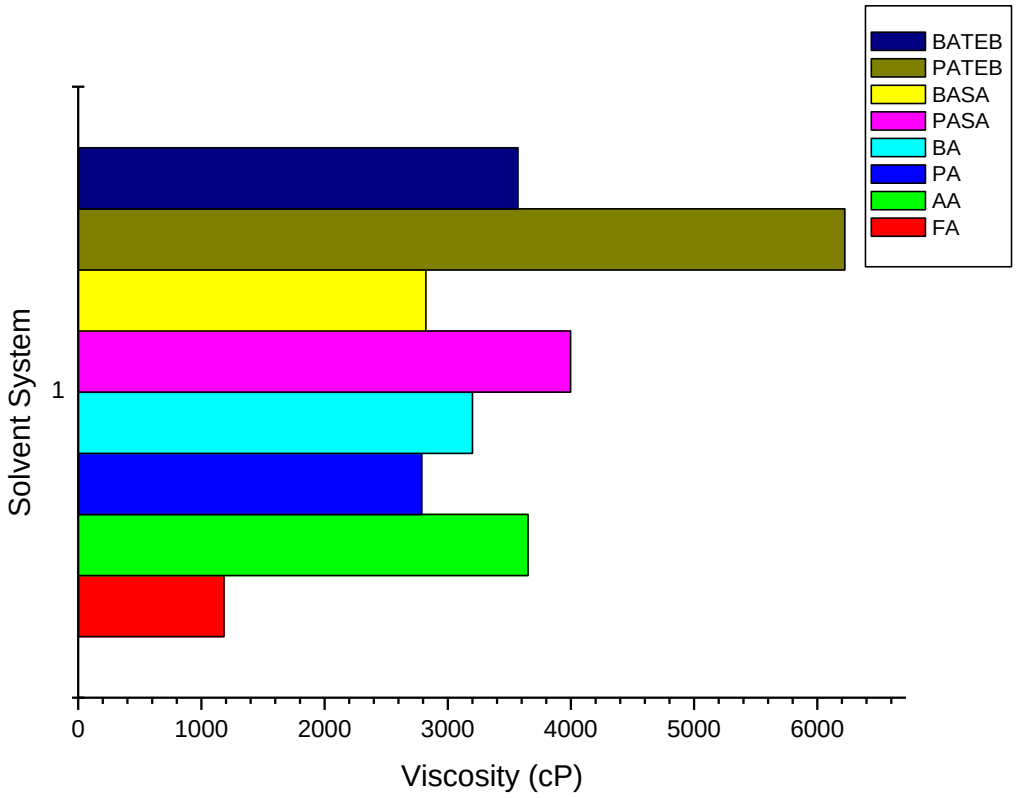

Figure 4.2: The viscosity of 15 wt% PCL polymer solutions as influenced by solvent composition

Interestingly, Van der Shueren *et al.*[1] and Lavielle *et al.* [12] reported that the solution viscosity of PCL in acetic acid/formic acid decreases with time. It can, therefore, be assumed that, when looking at the viscosity results obtained for the various polymer solution compositions (refer to Table A2) in conjunction with the dissolution results in Table 4.1 that at a given time the viscosity results shown in Figure 4.2 are a combination of solvent dependant factors and solution age. The effect of the solution aging in the electrospinning process is discussed in detail in a later section. This means that FA is expected to display the lowest viscosity as it only requires 3 hours to dissolve the polymer. All viscosity measurements were taken at a solution age of 20 hours after preparation. The relatively low viscosity obtained for the FA solution are expected due to the short dissolution time required (refer to Table 4.1), this effective increase in the solution age may explain the observed viscosity.

Figure 4.2 clearly shows that the carboxylic acid type significantly influences the polymer solution viscosity. It appears that AA, PA and BA are in the same range with FA the only exception. This may be related to the pKa of the carboxylic acid. Table 4.1 shows that there is a significant difference in pKa

values between FA and the other carboxylic acids. It appears that a lower pKa value may be associated with a low viscosity value. This trend was shown by Gholipour and Bahrami[13] in PCL polymer solutions, where they reported a viscosity increase of 2.5 times when FA was used versus AA.

It is possible for the solvent-polymer interactions to influence solution viscosity. Yalcinkaya et al.[6] postulated that salts dissolved in the solution can form complexes with the polymer, which leads to an increase in viscosity. PA and BA polymer solutions where $NaCH_3COO$ (SA) was used to enable electrospinning were investigated. The viscosity data presented in Figure 4.2 shows polymer solutions containing SA possessed higher observed viscosities compared to the additive-free solutions. These results support the hypothesis that the solvent-polymer interactions between PCL and the acetate ion most likely led to a complex forming in the solution which may increase the solution viscosity. A similar phenomenon is observed with TEB as an additive, which suggests that a wide range of ions have a possibility to complex with PCL in carboxylic acids.

4.3.3 Conductivity

The conductivity of polymer solutions has an influence on the process of electrospinning and the fibre morphology. Bhardwaj and Kundu[2] stated, in a review article that polymer solutions with high values of conductivity form thinner fibres the high conductivity aids jet formation by increasing the tension applied by the electric field on the solution. Furthermore, an increase in conductivity is accompanied by a decrease in jet radius, which may lead to fibres with smaller diameters.[2]Figure 4.3 (and Table A3 in Appendix A) show the relationship between conductivity of the polymer solutions and the nature of the solvent.

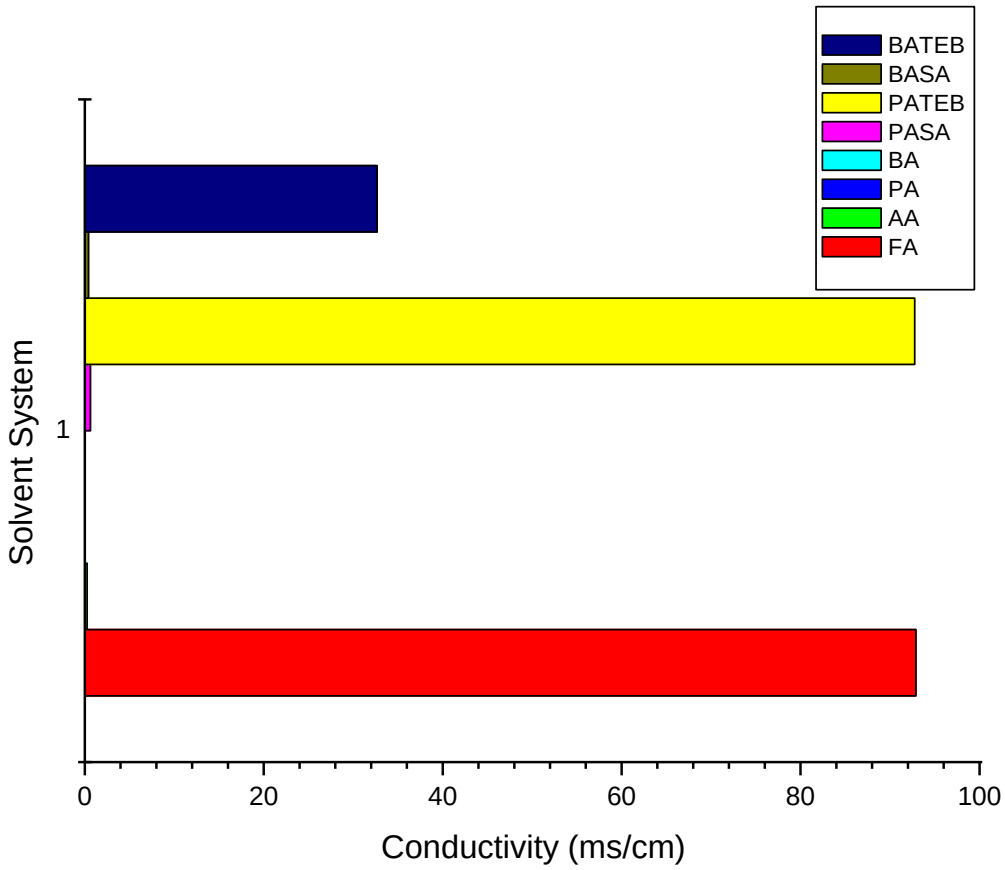

Figure 4.3: Conductivity of various 15wt% PCL polymer solutions as influenced by solvent type

The conductivity of the solvents without any polymer dissolved was determined. Only the FA showed a conductivity value of 175 ms/cm. These results support the hypothesis (as stated in the literature review section) that the carboxylic acids can act as organic solvents. It is believed that the poor dissociation of these carboxylic acids contributes to their organic nature, and this hypothesis is supported by the low values of dielectric constants and high values of pKa obtained for the carboxylic acids shown in Table A3.

The polymer solutions showed a similar trend when compared to the pure solvents as shown in Table A3. The AA conductivity values are similar to the values obtained by Ferreira *et al.*[7]. The addition of salts to PA and BA led to an increase in conductivity as expected, where the benzyltriethylammonium chloride (TEB) in PA displayed a conductivity value similar to the FA polymer solution (shown in Table A3 and Figure 4.3).

4.4 Electrospinning

4.4.1 Needle electrospinning

A study was conducted to determine the concentration at which polymer chain entanglements become significant enough for single needle electrospinning to occur. All the initial tests contained only the solvent and the polymer. Table 4.2 (and Table A4 in Appendix) show the relationship between electrospinnability and the nature of the solvent. The electrospinning tests of the various polymer solutions were done at a set time after preparation (an hour after complete polymer dissolution). SEM images of FA and AA derived samples were obtained at a magnification of 10 000 times, while images of PA and BA derived samples were obtained at 1000 times magnification.

Table 4.2: SEM images and fibre diameter distribution for various electrospun PCL fibres

Sample	SEM (1000X MAG)	Fibre diameter distribution
10 wt% PCL in FA (avg diameter : 99 ± 17 nm)	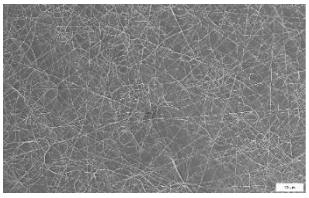	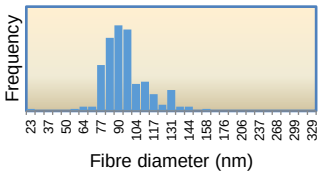
10 wt% PCL in AA (Avg diameter: 110 ± 57 nm)	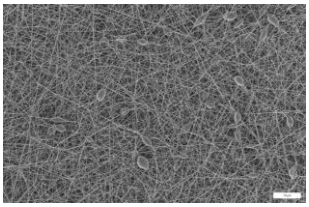	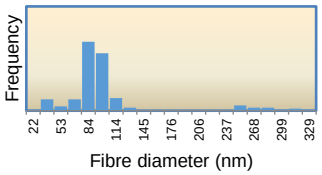
10 wt% PCL in PA	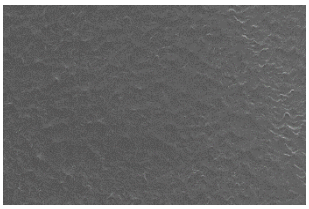	
10 wt% PCL in BA	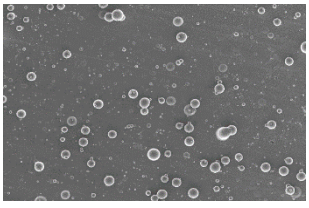	

Only polymer solutions derived from AA and FA resulted in electrospinning occurring at 10 wt% polymer concentration. Table 4.2 shows that FA solutions produced smooth bead-free fibres while the AA

solution led to fibres with a few beads. These results confirmed what was observed by Van der Shueren *et al.*[1] whereby solutions derived from FA display electrospinning at lower polymer concentrations than in AA. It should be noted that not all parameters were investigated in the current study and it is possible that fibres will be obtained at the lower polymer concentrations

Electrospinning was not observed in the case of PA and BA polymer solutions, the solutions formed stable jets but only film and electro-spray respectively were deposited on the collector. The initial assumption was that the polymer solutions were too dilute to electrospin, as observed by Ferreira *et al.*[7] when trying to generate nanofibres from AA/PCL solutions. It was assumed that an increase in the polymer concentration might lead to fibre formation from these solutions. This is due to the increase in polymer concentration leading to an increase in the solution viscosity which might result in an increase in the concentration and the amount of chain entanglements, which would enable fibre formation.

In some cases, however, an increase in viscosity does not necessarily mean an increase in the amount of chain entanglement concentration. Brenner *et al.*[14] showed that hyaluronic acid dissolved in aqueous media exhibits very strong polymer-polymer interactions that lead to high solution viscosities at low polymer concentrations. This means that an increase in viscosity does not necessarily result in an increase in the amount of chain entanglements present. They further showed that, to achieve electrospinning, they had to employ an additive that diminishes the polymer-polymer interactions to allow the chain entanglement concentration to rise with an increase in polymer concentration. In this specific case, the authors stated an increase in chain entanglement was achieved by changing the structure of the hyaluronic acid to a more flexible one that can entangle in solution.

What was observed in the current study disproved the initial assumption where a more concentrated solution failed to electrospin. Given the low conductivity observed in the solutions section (section 4.3.3), the next attempt in electrospinning from these solutions was to increase the conductivity. This was done by the addition of SA and TEB salts. The conductivity increased after the salts were added, with polymer solutions containing TEB being more conductive. The increase in conductivity resulted in electrospinning. It is fair to assume that these solutions were lacking the adequate conductivity to enable electrospinning to occur in these systems.

4.4.2 Free surface electrospinning

A study was conducted to determine whether polymer solutions that resulted in electrospinning through needle electrospinning could be electrospun using the free surface electrospinning method. This is of interest since single needle electrospinning could be a useful pre-screening method for the upscaling of the nanofibre production using the free surface electrospinning technique. Table 4.3, shows the relationship between free surface electrospinnability, the nature of the solvent and fibre diameter distribution (it should be noted that the fibre diameter distribution is not plotted on the same x-axis).

Electrospinning could not occur when using PA and BA as solvent systems without any additives as determined in section 4.4.1. The salts sodium acetate (SA) and benzyltriethylammonium chloride (TEB) added to the PA and BA polymer solution led to fibres in the micron-range with relatively high fibre

diameter variation. A potential issue is that the salts remains in the fibres after electrospinning.[15] FA was added to PA and BA solutions to perform a similar role as SA and TEB, with the added benefit that the resulting fibres will be free of additives as FA would evaporate. The optimal ratios that led to consistent electrospinning were 60:40 PA/FA and 50:50 BA/FA.

Table 4.3: SEM images and fibre diameter distribution of free surface electrospun PCL fibres, as influenced by the nature of the solvent and additives.

Sample	SEM 1	SEM 2	Fibre diameter distribution
FA (Avg fibre diameter: 611 ± 324 nm)	250X MAG 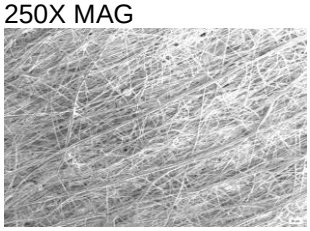	5000X MAG 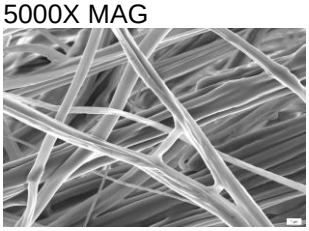	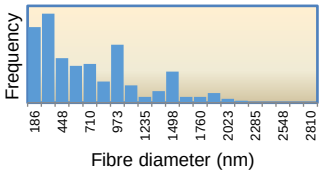
AA (Avg fibre diameter: 329 ± 148 nm)	250X MAG 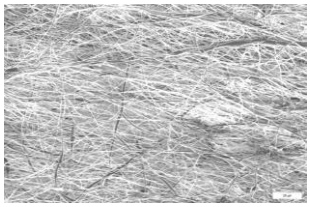	5000X MAG 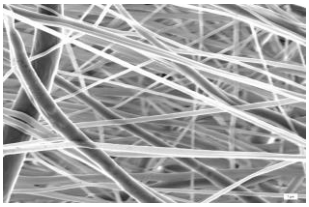	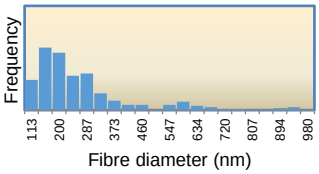
PA, 4 wt% $NaCH_3COO$ (Avg fibre diameter: 1156 ± 994 nm)	250X MAG 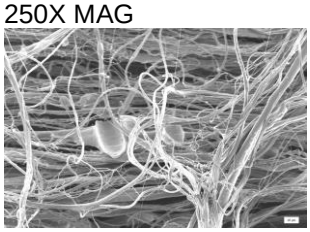	2000X MAG 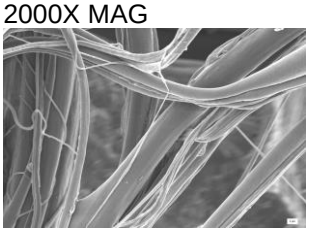	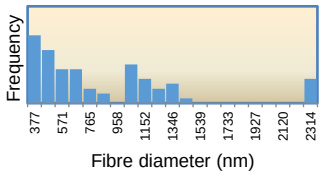
PA/FA (Avg fibre diameter: 145 ± 84 nm)	500X MAG 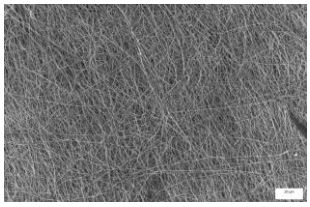	5000X MAG 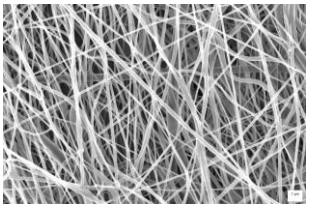	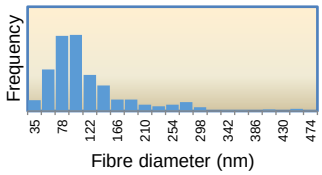
BA, 6 wt% $NaCH_3COO$ (Avg fibre diameter: 1412 ± 1299 nm)	250X MAG 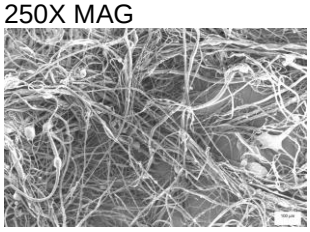	2000X MAG 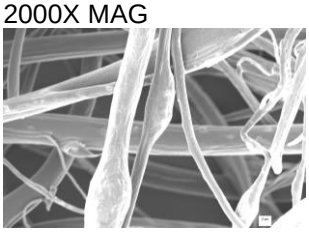	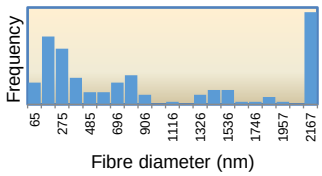
BA/FA (Avg fibre diameter: 96 ± 62 nm)	500X MAG 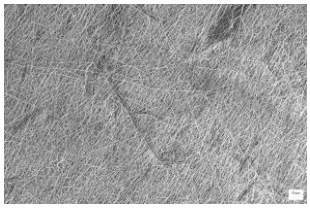	5000X MAG 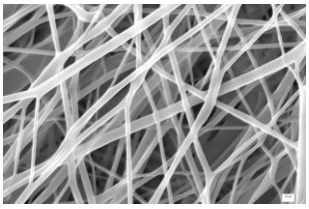	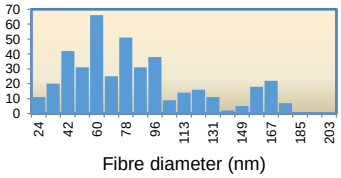

Table 4.3 shows that all the solutions tested resulted in successful electrospinning. The notable difference between the two types of electrospinning (free surface versus needle) is the increase in average fibre diameters and fibre diameter distribution observed for free surface electrospinning. Table 4.2 and Table 4.3 show that the average fibre diameter of FA derived solutions is 6 times larger when free surface electrospinning is utilized as opposed to needle electrospinning. Furthermore, the fibre diameter distribution evolves from a unimodal distribution to a more bimodal distribution. The increased average fibre diameter in free surface electrospinning was previously noticed by Huang *et al.*[16] when electrospinning polystyrene (PS) dissolved in N,N'-dimethylformamide using a rotating disk spinneret. Additionally, they showed that fibres obtained from free surface electrospinning had narrower fibre diameter distribution, which they attributed to the larger stretching forces caused by the high speed of the collector.

This difference in average fibre diameter can be explained by the hypothesis that the jets in free surface electrospinning do not experience the same level of instabilities as in needle electrospinning. This is because in free surface electrospinning, the solution is charged via a connection to the solution reservoir, as opposed to needle electrospinning where the needle itself is charged. This might lead to a higher charge per unit area in needle electrospinning, leading to enhanced jet instabilities that results in thinner fibres. This enhancement is as a result of a single jet which is charged in the needle electrospinning process, while in the free surface electrospinning multiple jets "share" or distribute the charge and have the ability to self-organize[17,18], which might decrease the charge per jet. This above hypothesis is similar to the one presented by Jiang *et al.*[19] when they investigated the merit of utilizing micro-bubbles in free surface electrospinning of polyvinyl alcohol (PVA) derived from aqueous solutions. They suggested that the micro-bubbles led to a single jet being formed on each bubble which led to a decrease in the overall average fibre diameter.

It is evident from the results (refer to Table 4.3) that the average fibre diameter is highly dependent on the solvent system when processing solutions via the free surface electrospinning process. This is not the case when it comes to the needle electrospinning where the difference in the average fibre diameter between AA and FA was only 10% as shown by Table 4.2. A similar result was reported by Van Der Schueren *et al.*[1] which showed that varying the amount of AA in the FA solvent system from 10-80% led to only a slight increase in the fibre diameter in the needle electrospinning process.

The FA and AA polymer solutions used without additives can provide insight into the differences in the electrospinning of nanofibres from carboxylic acid based polymer solutions. It was shown that in the needle electrospinning section, that using FA as a solvent produces nanofibres at a lower polymer concentration than that of AA. A similar result is found in the free surface electrospinning process, where the FA solutions resulted in an average fibre diameter that is 50% higher than that of the AA solution. This increase in the average fibre diameter cannot be explained simply as these solutions do not follow the trend shown by Oğulata and İčoğlu[20] where it was shown that an increase in the viscosity results in an increased average fibre diameter. Additionally, the higher conductivity of the FA solution did not lead to thinner fibres as reported by Hu *et al.*[21].

This implies that it is the polymer-solvent interactions which is the main contributing factor that determine the different fibre diameters as well as the other processing parameters (applied voltage, spinning distance and environmental conditions) were the same between the two polymer solutions. Since FA dissolves PCL much faster than all the carboxylic acids, it is fair to assume that it is a better solvent for PCL than AA. It is hypothesized that this difference in dissolution between the solvents leads to PCL occupying a larger hydrodynamic volume in FA than in AA. This larger hydrodynamic volume in FA leads to an enhanced polymer coil overlap, which increases the overall chain entanglements of the solution. This leads to FA possessing a lower chain entanglement concentration than AA, which results in FA solutions producing fibres at lower concentrations. The tendency of FA to possess a higher chain entanglement concentration than AA at the same polymer concentration may lead to the FA solution producing thicker fibres than is the case for the AA solution.

4.5 Solution aging study

Carboxylic acids have been previously proven to be good electrospinning solvents.[13,1,12] They can dissolve aliphatic polymers as well as hygroscopic salts with ease as shown earlier in this section. They are of relatively low volatility which renders them suitable for free surface electrospinning, and certain of them are FDA approved for use in human implantable devices. This chapter focuses on different processing pathways of carboxylic acid derived polymer solutions with an aim to gain insight into the multitude of processing options for these systems.

Lavielle *et al.*[12] showed that PCL undergoes hydrolytic degradation in acidic media. They further determined that the degradation is accompanied by a decrease in solution viscosity. Polymer solution viscosity can be related to the molecular weight and molecular chain entanglements in the solution.[22] Electrospinning can only occur if a critical chain entanglement concentration is reached in the solution.[14] An observed loss in the polymer solution viscosity, might result in a decrease in chain entanglement concentration. Lavielle *et al.*[12] showed that a decrease in the solution viscosity resulted in a decrease in average fibre diameter and subsequent bead formation as the solution age increased. Additionally, further decreases in the viscosity forced the process to transition from electrospinning to electrospraying.

Changes in the solution viscosity might also affect additional solution properties such as conductivity and the surface tension. These changes in solution properties could be enhanced by the solution age. It is presumed that as the solution age increases, the solution properties will vary significantly as the above-mentioned degradation is dependent on the length of exposure of PCL to acidic media.[1]

Various solvent systems composed of carboxylic acids and salts were evaluated to determine the effect of solution age on solution properties, electrospinnability and physical properties of resulting nanofibres. The experiment was performed over a 5-day period with measurements and electrospinning done at 24-hour intervals. In some solvent systems, measurements were stopped once electrospinning no longer occurred.

4.5.1 Solution properties

Section 4.3 showed that the polymer solution properties are related to the nature of the solvent, the presence of additives in the solution and the solvent-polymer interaction. This section aims to determine the effect of solution age on the initial solution properties. The solution measurements were performed on two separate occasions, to validate the data. Figure 4.4 shows the relationship between surface tension and solution age for the various polymer solutions.

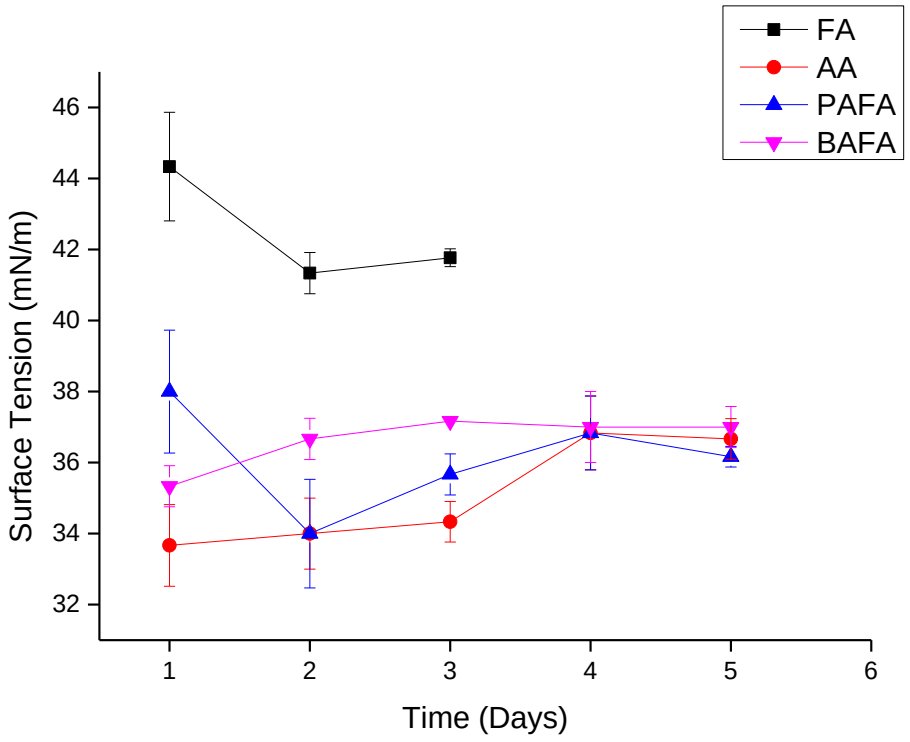

Figure 4.4: Surface tension as a function of the solution age of 15 wt% PCL polymer solutions derived from various solvent systems

The figure shows that as the solution age increases, the surface tension of the solution fluctuates. This type of fluctuation is further seen in Figure 4.5 where the figure shows the relationship between the conductivity, and the nature of the solvent and solution age. The surface tension remained relatively constant for all the solvents except for the FA solution. This agrees with the statement of Lavielle *et al.*[12], where it was stated that a decrease in molecular weight of polymer, does not affect the surface tension and conductivity of the solution significantly. This statement was based on empirical evidence, and no additional hypothesis was provided.

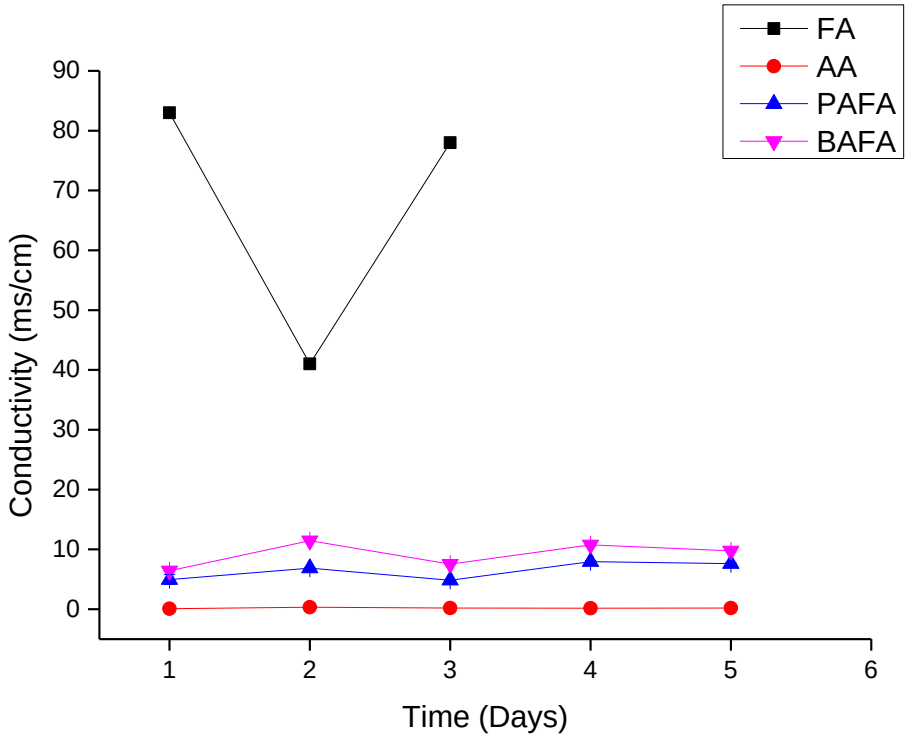

Figure 4.5: Conductivity as a function of solution age of 15 wt% PCL polymer solutions derived from various solvent systems

Figure 4.6 shows the relationship between the solution viscosity and solution age. It can be seen that the general trend is that there is a general decrease in the viscosity as the solution ages. These results are in agreement with those of Van Der Schueren *et al.*[1] where they showed that the viscosity remains stable only for 3 hours. The FA solution showed the largest decrease in viscosity with an approximately 50% decrease in viscosity in a 24 hour period while the viscosity of the AA solution only showed a slight decrease over the five-day period. This suggests that the hydrolytic degradation occurs at a higher rate in FA compared to AA. This is most likely related to lower pKa of FA which has more free protons available to catalyse the degradation. The PA/FA and BA/FA solutions followed a similar trend to the FA solution. The hydrolytic degradation of aliphatic polyesters responsible for the decrease in molecular weight which in turn leads to the lowering of the solution viscosity is known to be catalysed by an acidic environment.[4] It is expected that the degradation would occur faster in the FA solution as there would be more dissociated H^+ ions in solution owing to the lower pKa value of FA.

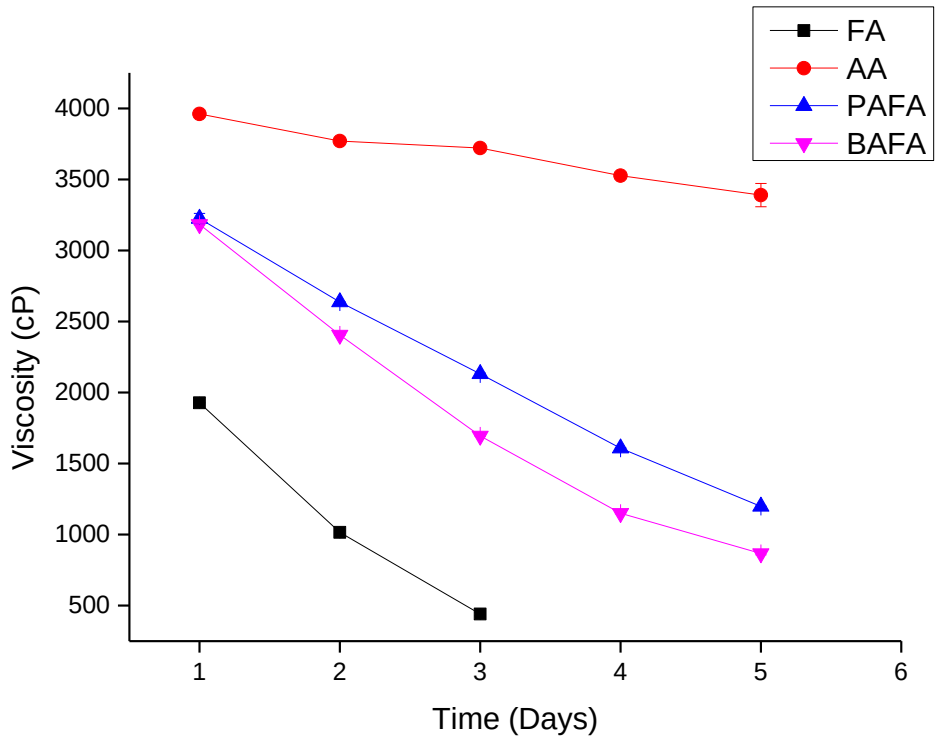

Figure 4.6: Viscosity as a function of the solution age of 15 wt% PCL polymer solutions derived from various solvent systems

4.5.2 Free surface electrospinning

Solution properties play a significant role in electrospinning and subsequent fibre morphology. The previous section has shown that the solution properties evolve with increasing solution aging. Lavielle *et al.*[12] showed that increasing the solution age leads to the process transitioning from electrospinning to electrospraying for needle electrospinning. Zhou *et al.*[11] postulated that the electrospraying is caused by insufficient chain entanglements.

The results of free surface electrospinning study are summarized in Tables 4.8, 4.9, 4.10 and 4.11. The tables show the relationship between electrospinnability, fibre morphology, average fibre diameter, fibre diameter distribution and solution age. The results are influenced by two factors namely: solvent-polymer interactions and solution age.

Table 4.4: SEM images of electrospun fibres generated from FA polymer solutions as a function of solution age

Sample	500X MAG	5000X MAG	Fibre diameter distribution
15 wt% PCL in FA, Day 1 (Avg fibre diameter: 919 ± 523 nm)	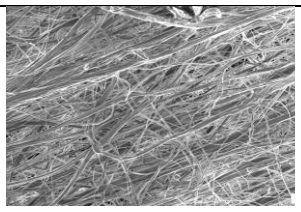	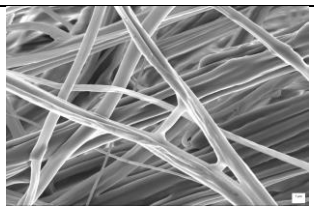	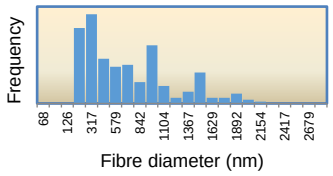
15 wt% PCL in FA, Day 2 (Avg fibre diameter: 447 ± 212 nm)	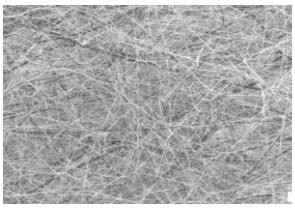	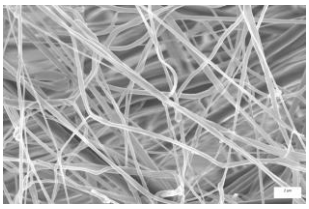	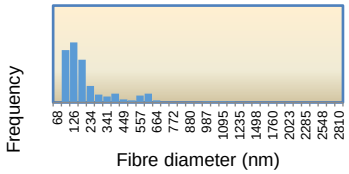
15 wt% PCL in FA, Day 3 (Avg fibre diameter: 209 ± 135 nm)	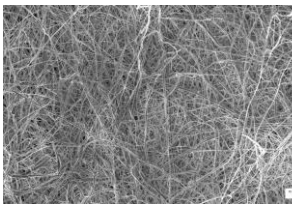	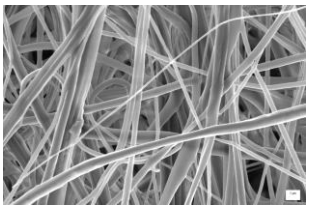	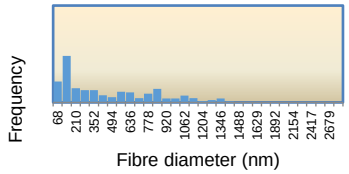

It is well known that for electrospinning to occur, the chain entanglements of the polymer in solution must reach a critical concentration value (C_{crit}). However, C_{crit} is not usually equal to the minimum chain entanglements (C_m). Wang *et al.* [23] showed that C_{crit} is equal to $2C_m$ when electrospinning poly(*N*-isopropylacrylamide) fibres from dimethylformamide solutions. These results bring into consideration what a good solvent is for a specific polymer with regards to fibre generation via electrospinning. Shenoy *et al.*[24] postulated that in a good solvent electrospinning occurs when C_m is equal or very close to $C_{crit.}$

Table 4.2 showed that electrospinning occurs at lower polymer concentration when FA was used as a solvent compared to AA. This result is in agreement with the observations of Van der Schueren *et al.*[1] who observed that fibre formation in FA polymer solutions occurs at lower polymer concentrations when compared to AA polymer solutions. This suggests that FA is a better solvent than AA with regards to electrospinning PCL. This implies that at equivalent polymer concentrations FA solutions possess a larger chain entanglement concentration. This presumed larger chain entanglement in FA polymer solutions is expected to form thicker fibres compared to AA polymer solutions.[22,24] Table 4.4 and Table 4.5 show that after 24 hours, fibres derived from FA polymer solutions possess an average fibre diameter almost twice as thick as fibres obtained from AA polymer solutions. This result confirms the hypothesis that FA polymer solutions possess larger chain entanglements compared to AA solutions.

Table 4.5: SEM images of electrospun fibres generated from AA polymer solutions as a function of solution age

Sample	500X MAG	5000X MAG	Fibre diameter distribution
15 wt% PCL in AA, Day 1 (Avg fibre diameter: 516 ± 350 nm)	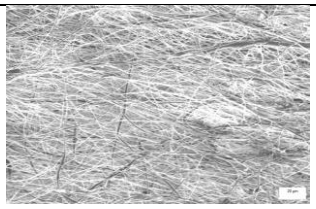	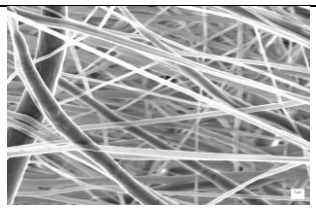	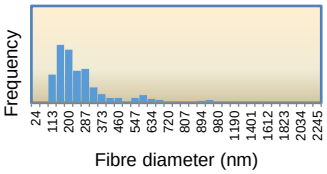
15 wt% PCL in AA, Day 2 (Avg fibre diameter: 307 ± 233 nm)	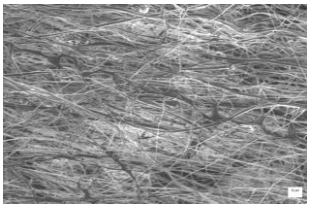	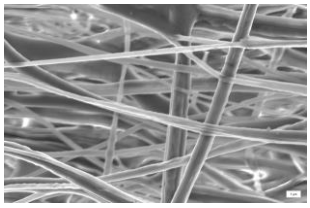	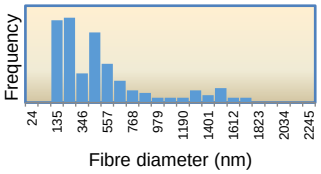
15 wt% PCL in AA, Day 3 (Avg fibre diameter: 432 ± 349 nm)	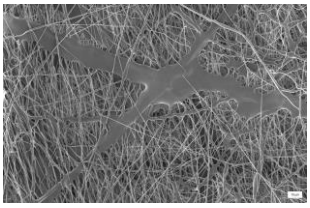	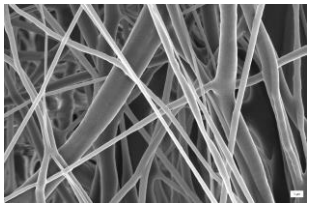	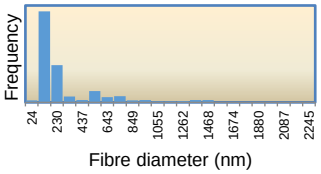
15 wt% PCL in AA, Day 4 (Avg fibre diameter: 659 ± 468 nm)	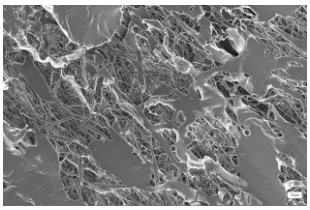	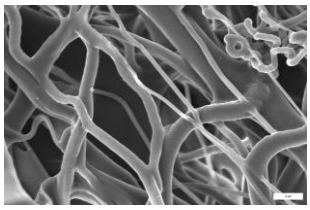	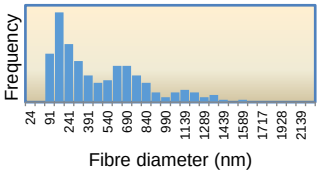
15 wt% PCL in AA, Day 5	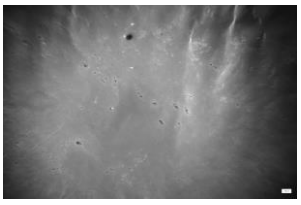		

PCL is less soluble in PA and BA as determined in section 4.2, as heat is required to complete the dissolution. This leads to the hypothesis that solvent suitability diminishes with an increase in pKa (which is related to the size of the aliphatic chain on the carboxylic acid) when processing PCL. Furthermore, polymer solutions derived from these solvent systems required additional components (salts TEB and SA) to promote electrospinning. Table 4.7 shows that even a 1:1 ratio of FA: BA leads to the smallest fibre diameters compared to the other solvent systems. This diminishing solvent

suitability leads to fibre diameters thinning with increasing carboxylic acid pKa. Table 4.7 further reinforces this hypothesis, as fibres derived from PA/FA polymer solutions are thicker compared to BA/FA polymer solutions, while being thinner than fibres derived from AA polymer solutions.

Table 4.6: SEM images of electrospun fibres generated from PA/FA polymer solutions as a function of solution age

Sample	500X MAG	5000X MAG	Fibre diameter distribution
15 wt% PCL in PA/FA, Day 1 (Avg fibre diameter: 145 ± 84 nm)	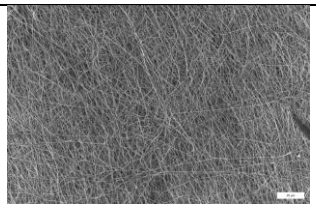	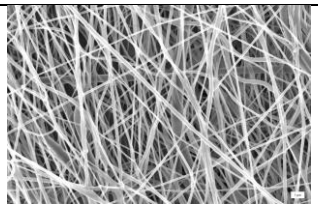	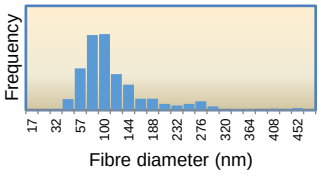
15 wt% PCL in PA/FA, Day 2 (Avg fibre diameter: 142 ± 96 nm)	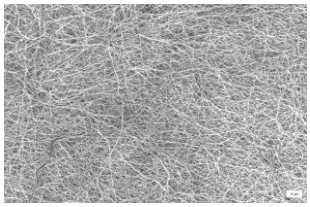	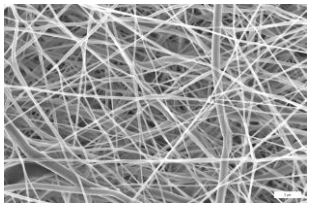	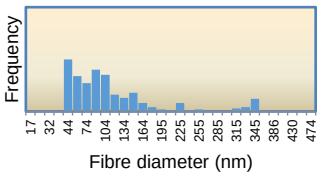
15 wt% PCL in PA/FA, Day 3 (Avg fibre diameter: 140 ± 78 nm)	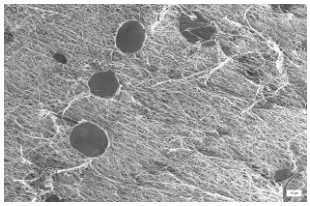	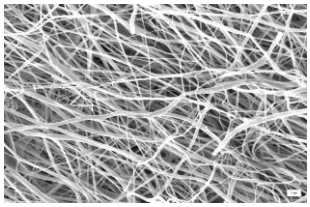	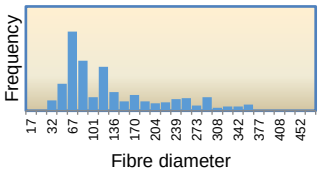
15 wt% PCL in PA/FA, Day 4 (Avg fibre diameter: 150 ± 95 nm)	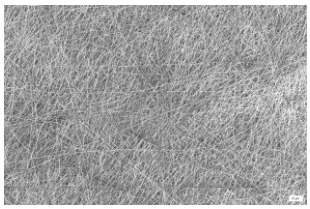	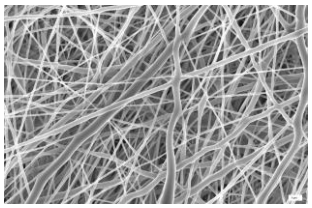	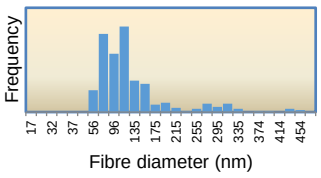
15 wt% PCL in PA/FA, Day 5 (Avg fibre diameter: 113 ± 55 nm)	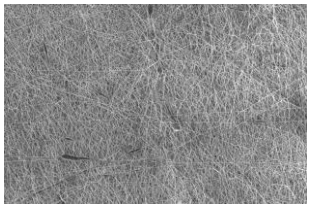	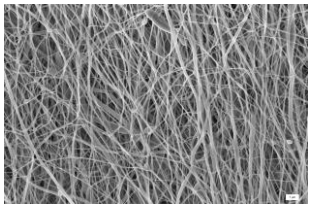	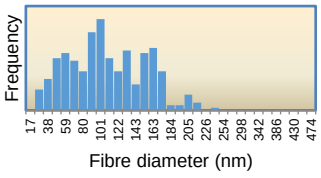

Sample	500X MAG	5000X MAG	Fibre diameter distribution
15 wt% PCL in PA + SA, Day 1 (Avg fibre diameter: 86 ± 40 nm)	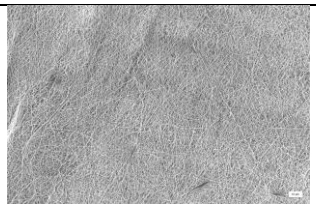	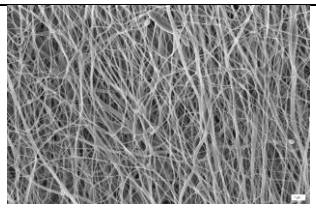	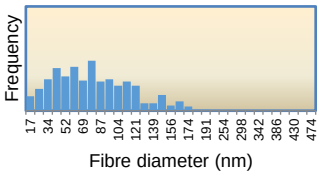
15 wt% PCL in PA + SA, Day 2 (Avg fibre diameter: 1156 ± 1108 nm)	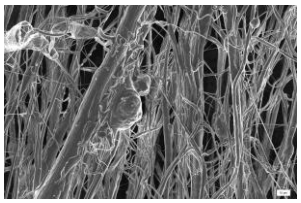	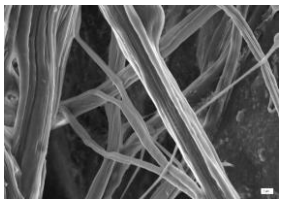	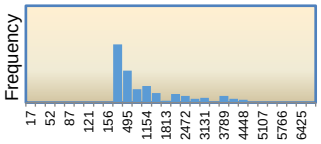

Table 4.7: SEM images of electrospun fibres generated from BA/FA polymer solutions as a function of solution age

Sample	500X MAG	5000X MAG	Fibre diameter distribution
BA/FA, Day 1 (Avg fibre diameter: 96 ± 62 nm)	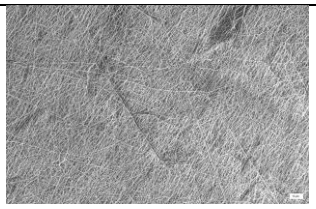	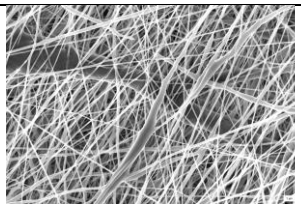	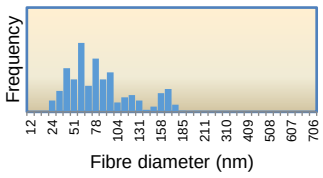
BA/FA, Day 2 (Avg fibre diameter: 77 ± 52 nm)	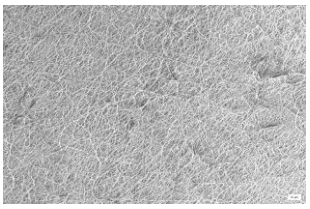	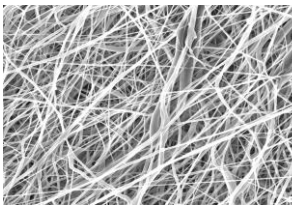	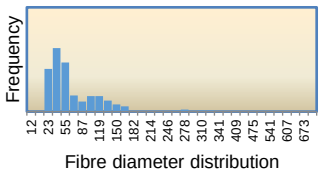
BA/FA, Day 3 (Avg fibre diameter: 88 ± 62 nm)	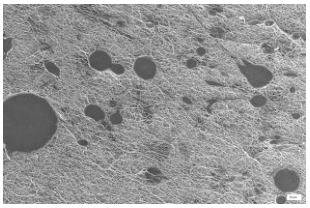	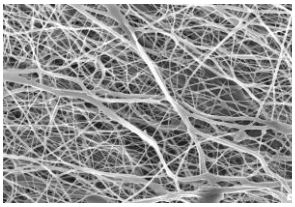	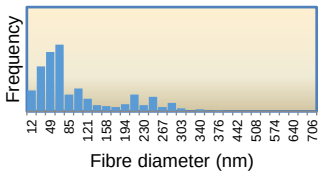
BA/FA, Day 4 (Avg fibre diameter: 181 ± 146 nm)	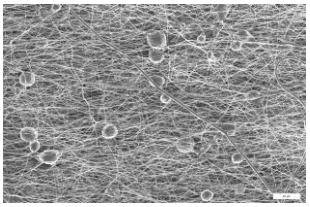	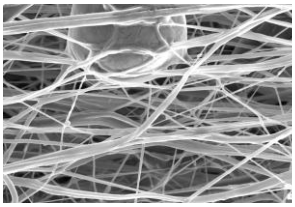	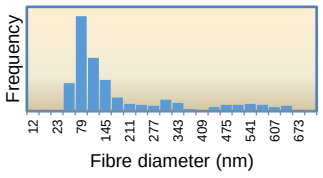
BA/FA, Day 5 (Avg fibre diameter: 75 ± 38 nm)	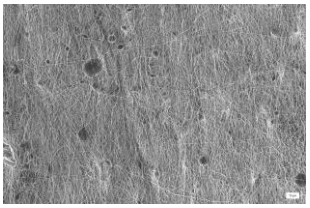	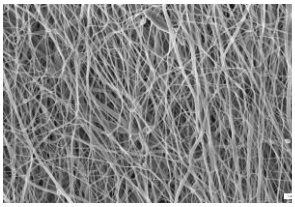	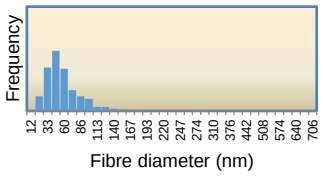

Van der Schueren *et al.*[1] was the first to show that the viscosity of carboxylic acid-derived solutions evolves with time. They showed that the viscosity remains stable for the first three hours after complete polymer dissolution. Lavielle *et al.*[12] further expanded by showing that as the viscosity decreases so does the average fibre diameter, and that ultimately the process transitions from electrospinning to

electrospraying when using needle electrospinning methods. What was observed is a similar trend to the earlier work but with a few notable differences. Including the fact that in the current study free surface electrospinning has been employed.

Table 4.4 shows that the FA polymer solutions displayed almost a 50% decrease in the average fibre diameter every 24 hours. Electrospinning ceased in that solvent system (FA solvent system) after 3 days. This decrease in fibre diameter is proportional to the decrease in solution viscosity. This suggests that as the solution age increased, the chain entanglement concentration decreased in the solution. The inability to electrospin after 3 days suggests that the chain entanglement concentration was below C_{crit}. The AA solution showed a related trend, however, electrospinning did not stop after 3 days but the morphology transitioned from pure fibres to a film-fibre mixture. After 5 days, a film formed even though sustained jetting was achieved during electrospinning with this solution.

The PA/FA and BA/FA polymer solutions showed an interesting trend, as electrospinning continued in these systems for the 5-day period. Table 4.6 and Table 4.7 shows that the average fibre diameter remained somewhat stable over the period while the viscosity decreased steadily. This result firstly suggests that during the 5-day period the chain entanglement concentration did not decrease below C_{crit}. Secondly, an increase in the viscosity (and subsequently an increase in chain entanglement concentration) does not lead to an increase in average fibre diameter in these solvent systems.

When polymers are dissolved in suitable solvents the individual chains entangle in solution. These entanglements are related to solvent-polymer interactions, viscosity and polymer concentration. The chain entanglement concentration can be related to fibre thickness in electrospinning.[1,12] A decrease in entanglement concentration will most likely be accompanied by a decrease in average fibre diameter. Table 4.4 and Table 4.5 shows that with increasing solution age in carboxylic acid derived polymer solutions, the average fibre diameter decreases. This fact suggests that the chain entanglement concentration decreases with an increase in solution age.

The FA polymer solution failed to spin after 3 days, additionally the AA polymer solution developed a mixture of film and fibres after 3 days as mentioned above. This phenomenon suggests that the chain entanglement of the FA polymer solutions is lower than the critical concentration for sustained electrospinning after 3 days. In the case of the AA polymer solution, the solution viscosity did not decrease as rapidly as in the FA polymer solutions. However, smooth fibres were not obtained after 3 days, which suggests that the AA solution's initial chain entanglement concentration was much closer to C_{crit} than all the other solutions, and a minimal decrease in solution viscosity led to a mixture of film and fibres.

The PA/FA and BA/FA continued electrospinning for the 5-day period without film formation and produced a near constant average fibre diameter while the viscosity continued to decrease daily. This fact suggests one of two possibilities contribute to the observed data. The first possibility is that the chain entanglement concentration of PA/FA and BA/FA is much higher than that of AA and FA, such that the continued degradation does not reduce it below the critical chain entanglement concentration. However, this does not explain the near constant average fibre diameter for the duration of the

experiment. The second possibility is that the presence of PA and BA slows the hydrolytic degradation of the polymer. The decreased rate of degradation allows spinning to occur over a longer period as the chain entanglement concentration is decreasing at a much slower rate compared to FA and AA polymer solutions.

SA was used effectively to produce smooth bead-free fibres in section 4.4. However, the presence of the salt may contribute to the precipitation of the polymer. The $NaCH_3COO$ may cause the precipitation by introducing excess water to the polymer solution when the salt is hydrated. This excess water may cause the hydrophobic PCL to precipitate. In the BA and PA solutions containing $NaCH_3COO$, a precipitate was observed after 0.5 and 2.5 days respectively. The average fibre diameter of the two different spin days of the PA polymer solutions with SA added in the solution were compared. Table 4.6 shows that after 24 hours, the average fibre diameter was 86 nm, but rose to over 1 µm after 48 hours. Additionally, the morphology was drastically different. These results suggest the presence of SA for prolonged periods lead to increased fibre diameter possibly caused by changes in viscosity associated with the acetate ion. The association may be between the polymer and SA which may lead to a complex being formed, and an increased entanglement.[6]

4.5.3 Molecular weight

Koski *et al*.[25] showed that an increase in average molecular weight (M_w) led to an increase in average fibre diameter when electrospinning polyvinyl alcohol (PVA) from aqueous solutions. Given that the solution viscosity and average fibre evolve with solution age from the previous sections, it is worth investigating whether the molecular weight of PCL changes with solution age.

It is presumed that the number average molecular weight of PCL would decrease as acidic media promotes hydrolytic degradation of aliphatic polyesters.[1,12] Figure 4.7 shows the relationship between the number average molecular weight (M_n) and solution age, with Figure 4.8 showing the relationship between weighted average molecular weight (M_w) and solution age.

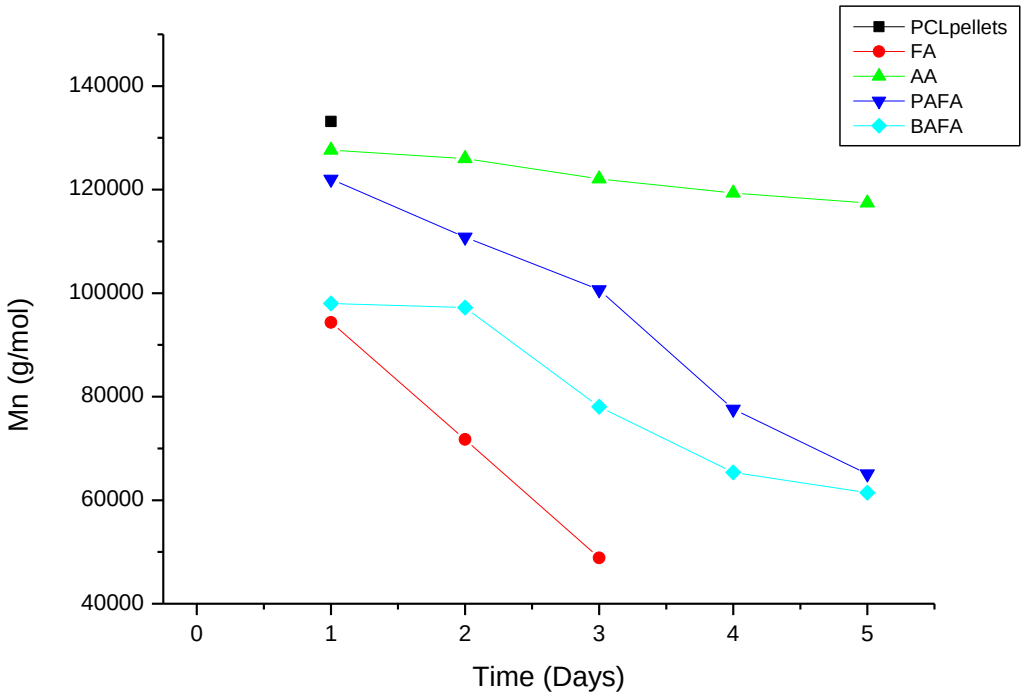

Figure 4.7: M_n of PCL electrospun fibres generated from various 15 wt% polymer solutions as a function of solution age

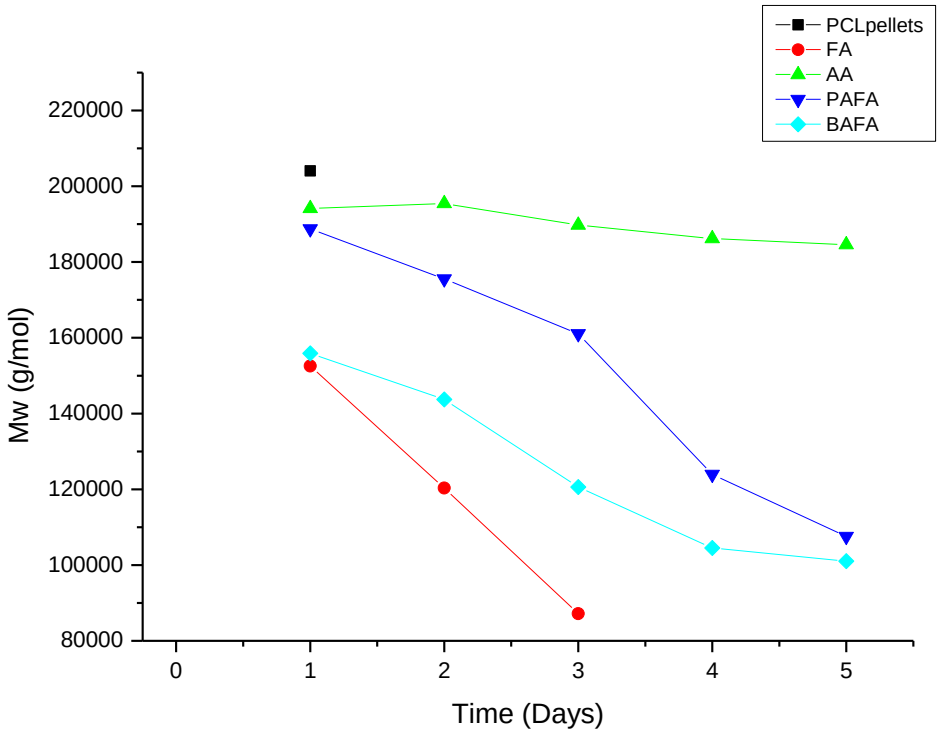

Figure 4.8: M_w of PCL electrospun fibres generated from various 15 wt% polymer solutions as a function of solution age

The number average molecular weight (M_n) and weight average molecular weight (M_w) mirror the results obtained in the solution viscosity tests. Both values decrease with increasing solution age. This suggests that the solution viscosity is directly linked to molecular weight in carboxylic acid derived PCL polymer solutions.

One aspect which was considered before the solution aging study, was how the hydrolytic degradation is achieved. The molecular weight distribution and dispersity index (Đ) could possibly lead to an idea of which degradation model is dominant. Figure 4.9 shows the relationship between molecular weight distribution and solution age for FA derived electrospun fibres, the numbers in the legend refer to the age of solution from which the fibres were electrospun. The numbers in the figure's legend refer to the solution age in number of days. Figure 4.10 shows the relationship between Đ, nature of the solvent and solution age.

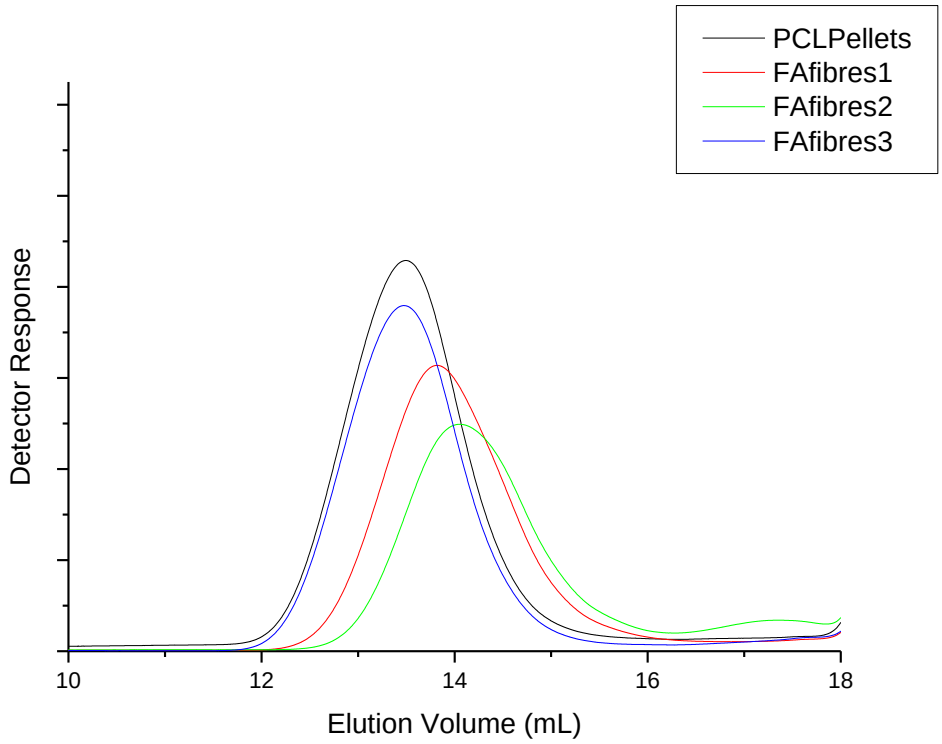

Figure 4.9: Molecular weight distribution of 15 wt% PCL solutions as function of solution age

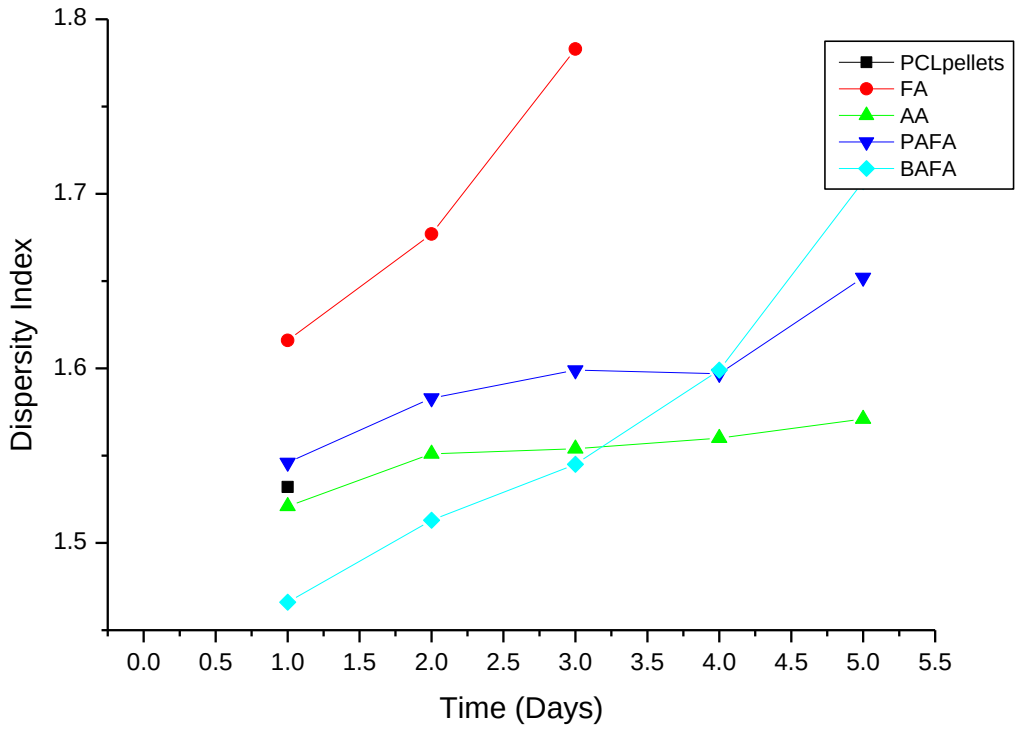

Figure 4.10: Đ of electrospun fibres of various 15 wt% PCL solutions as a function of solution age

In the case of degradation of the polymer chains, different types of degradation modes are possible: a single molecular chain can split into two shorter chains (random chain scission), a single molecular chain can shorten at the chain ends (end chain scission), and autocatalytic degradation.[26,4] Autocatalytic degradation refers to the degradation model whereby random chain scission occurs first with the degradation products render the local media acidic, this acidity of the media catalyses further degradation of the polymer matrix.[4,26,27]

It has been postulated in literature that autocatalysis may not be the degradation model followed by PCL when exposed to highly concentrated acidic media containing trace amounts of water.[12] Figure 4.9 shows that the distribution curves shorten and widen as the solution age increases when FA is used as the solvent to electrospin fibres, and that the molecular mass distribution never loses the unimodal shape that is also observed in the control samples (the raw PCL pellets). Figure 4.11 further shows that the unimodal shape is observed when utilising other carboxylic acid solvent systems.

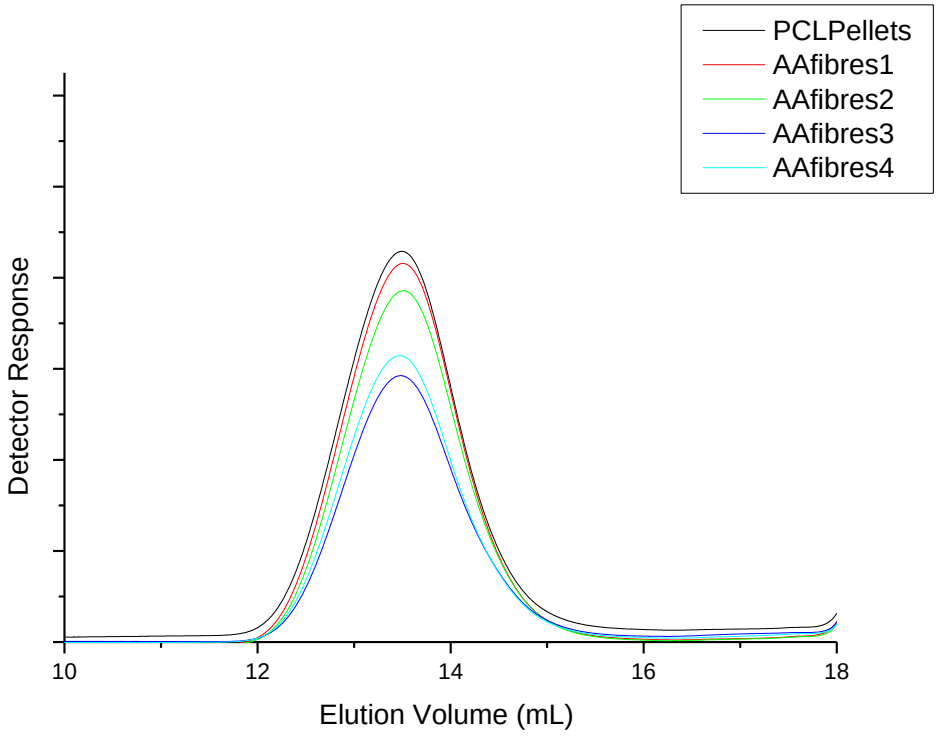

Figure 4.11: Molecular weight distribution of 15 wt% PCL solutions as function of solution age

Additionally, Figure 4.10 shows that the Đ increases with solution age. Yu *et al.*[28], postulated that a random chain scission degradation model is observed, if a polymer's initial Đ (is lower than the value 2) increases towards the value 2 when studying thermal degradation of poly (L-lactide). Figure 4.10 shows that the Đ of the FA polymer solution rapidly approaches the value 2, which suggests that the degradation model followed is random chain scission, this hypothesis is in agreement with the results observed by Lavielle *et al.*[12] when electrospinning PCL fibres from carboxylic acid derived solutions.

4.5.4 Differential scanning calorimetry (DSC) thermograms

Of particular interest is the change in crystallinity of the polymer when processed using different methods, or using different solvent systems to dissolve the polymer. DSC analysis was performed on films and fibres derived from carboxylic acid polymer solutions. The first heating cycle was recorded as this would reveal the effect of each processing pathway on crystallinity. Figure 4.12 shows the relationship between processing type and crystalline melt endotherm in the first DSC cycle of FA derived film and fibres (the crystallinity of each sample is given in Table 4.8, as the Day 1 samples).

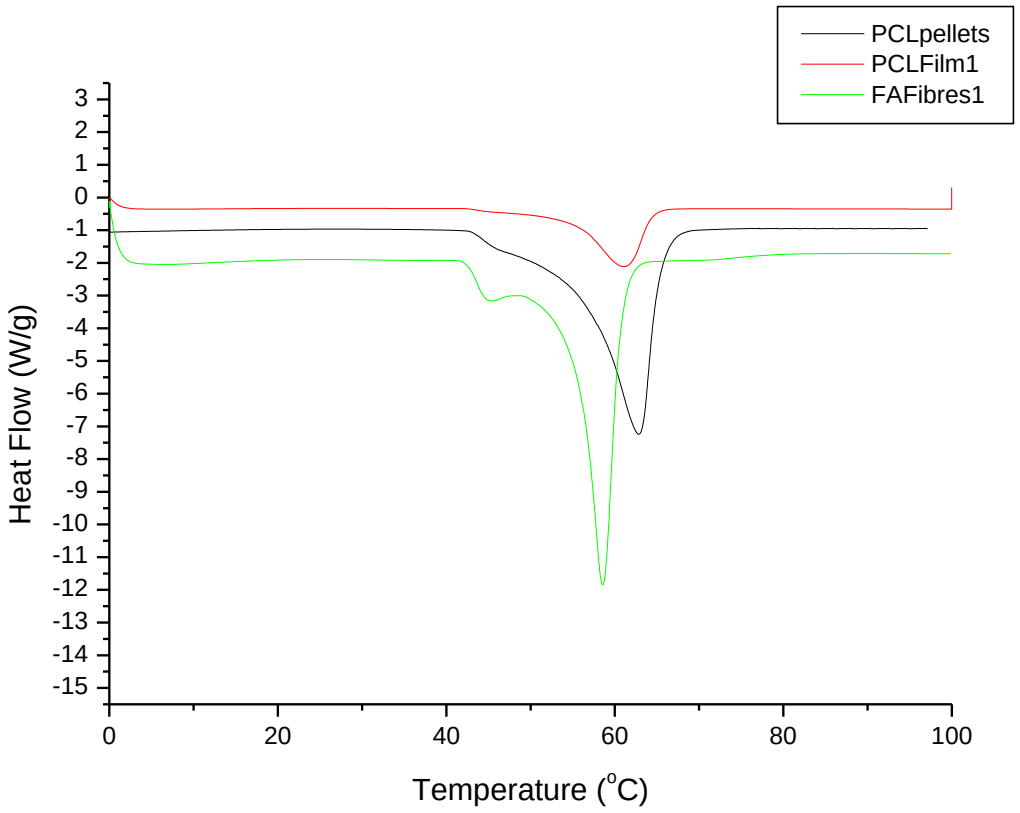

Figure 4.12: DSC thermograms (first heating cycle) of electrospun fibres and film generated from 15 wt% PCL polymer solutions

The electrospun fibres showed a shoulder on the left side of the curve, which suggest that the crystals/lamella have different sizes.[29] It is important to determine whether the shoulder on the DSC and subsequent difference in crystal size in the electrospun fibres is a result of the processing (electrospinning). The PCL pellets and film showed less pronounced shouldering compared to electrospun fibres, suggesting that electrospinning may lead to an enhanced heterogenous crystal size distribution when processing PCL from FA solutions. This result is similar to those of Jenkins and Harrison[30] when they were monitoring the degradation of PCL in phosphate buffer. They determined that these shoulders are result of thinner crystal lamellae that form as the polymer degrades. Furthermore, Figure 4.12 shows that the peak melting temperature of the electrospun fibres is

significantly reduced compared to the film and the PCL pellets. A similar result was obtained by Chang *et al.*[29] when analysing degraded PCL films, the authors attributed the reduction of the peak melting temperature to thinning of crystal lamella. This further supports that there is a heterogenous crystal size distribution as a result of electrospinning. It is of interest whether the inconsistency in crystal size is dependent on the nature of the carboxylic acid. Figure 4.13 shows the relationship between the nature of the solvent and crystallinity in first DSC cycle of various carboxylic acid solutions.

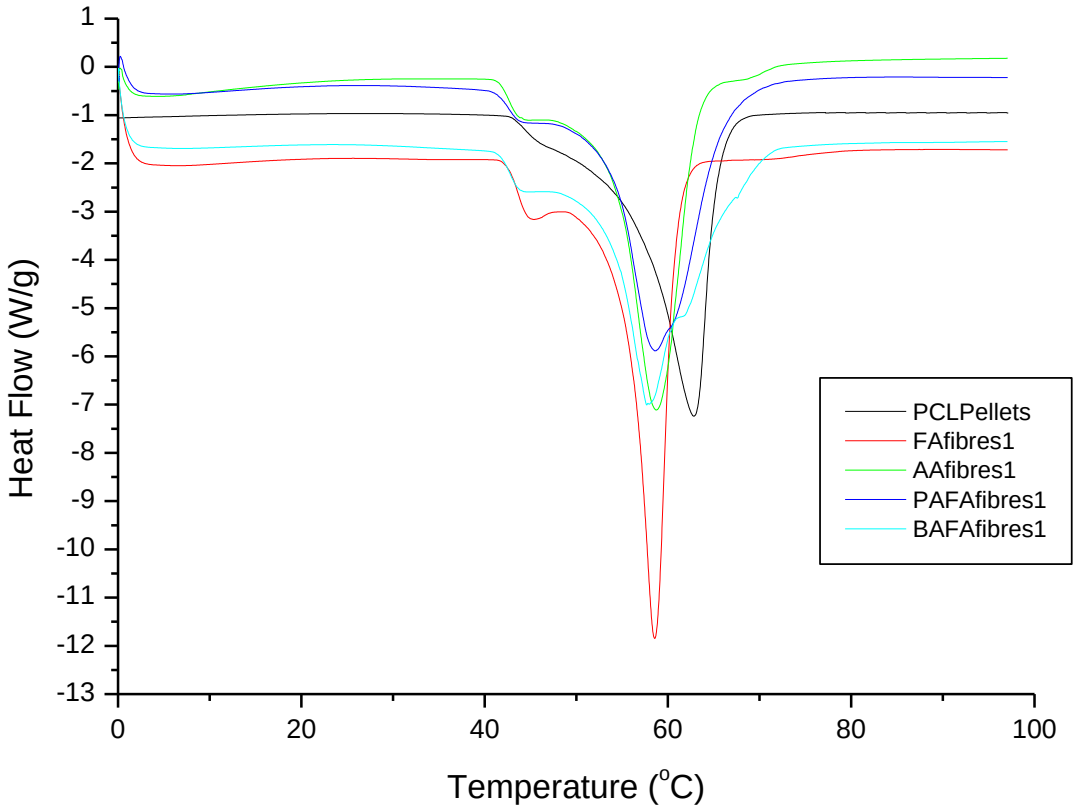

Figure 4.13: DSC thermograms (first heating cycle) of electrospun fibres generated from 15 wt% PCL polymer solutions as influenced by the nature of the solvent

The figure shows that the inconsistency in crystal size is not dependent on the nature of the carboxylic acid. The second heating cycle was recorded, which would effectively anneal the samples, and thus removing processing history. This is of interest because it would determine whether the inconsistency in crystal size is permanent. Figure 4.14 shows the relationship between processing type and crystallinity in the third DSC cycle.

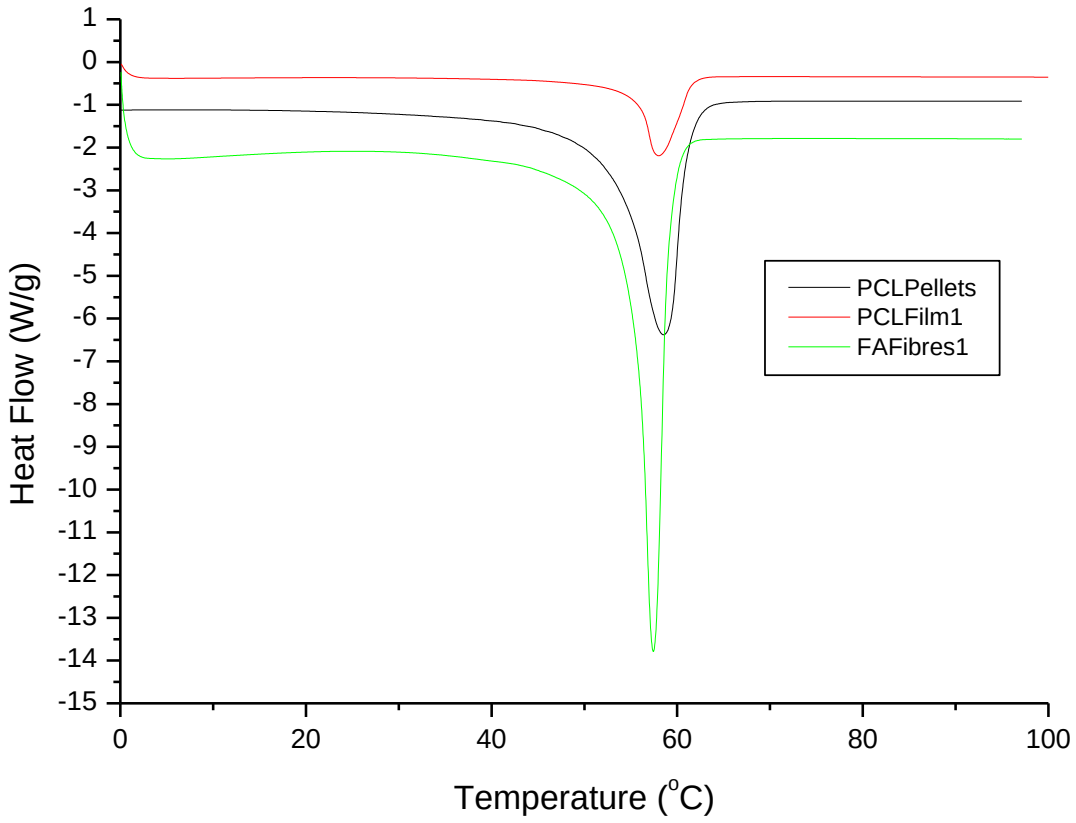

Figure 4.14: DSC thermograms (second heating cycle) of electrospun fibres generated from 15 wt% PCL/FA polymer solutions

Figure 4.14 shows that the shoulder disappeared on the second heating cycle, confirming that that it is a result of processing the polymer. Similarly, the shoulder disappeared for all the fibres on the second cycle. The nature of electrospinning leads to rapid precipitation of the polymer, which hinders optimal crystal formation, leading to differing crystal sizes.[31]

It is presumed that different processing methodologies will determine the nature of crystallinity of the films/fibres. Additionally, it is of interest whether solution age and solvent nature influences the crystallinity. Table 4.8, shows the relationship between processing pathway and physical properties in the first DSC cycle. The shouldering in the DSC analysis discussed above leads to multiple onset melting temperatures shown in the Table 4.8. Table 4.9 shows the relationship between processing pathway and crystallinity in the first DSC cycle. The percentage crystallinity was determined by calculating the ratio of the enthalpy of fusion of each individual sample with the theoretical enthalpy of fusion for 100% crystalline PCL (139.5 J/g).

Table 4.8: DSC data of various PCL films and electrospun fibres in the first DSC cycle

Sample	% Crystallinity	Onset Temperature 1 (Shoulder) (°C)	Onset Temperature 2 (°C)	Peak Temperature (T_m) (°C)
PCL pellets	45.5	42.1	55.5	62.9
FA film day 1	28.9	41.5	54.6	61.1
FA fibres day 1	47.0	41.0	55.2	58.6
FA fibres day 2	57.3	40.2	54.6	59.6
FA fibres day 3	46.2	40.4	55.8	58.6
AA film day 1	60.4	40.2	53.7	60.9
AA fibres day 1	48.7	40.9	53.5	58.7
AA fibres day 3	52.4	40.8	54.0	59.1
AA fibres day 4	47.9	41.0	54.7	58.9
PAFA film day 1	69.5	40.8	54.7	60.9
PAFA fibres day 1	49.8	40.4	52.9	58.6
BAFA film day 1	51.0	40.5	53.6	59.9
BAFA fibres day 1	50.8	40.8	52.9	57.7

Table 4.9: DSC data of various PCL films and electrospun fibres in the second DSC cycle

Sample	% Crystallinity	Onset Temperature (°C)	Peak Temperature (T_m) (°C)
PCL pellets	37.6	53.2	58.5
FA film day 1	21.6	55.7	58.0
FA fibres day 1	42.2	55.4	57.4
FA fibres day 2	47.2	55.0	57.8
FA fibres day 3	39.0	55.1	57.5
AA film day 1	31.3	53.3	57.4
AA fibres day 1	36.4	54.9	58.0
AA fibres day 3	40.4	54.2	58.7
AA fibres day 4	38.9	54.8	57.9
PAFA film day 1	36.0	54.6	57.8
PAFA fibres day 1	38.3	54.9	58.2
BAFA film day 1	36.6	54.2	57.9
BAFA fibres day 1	40.3	54.6	57.9

The change in the crystal size distribution manifests in changes in the onset temperature and crystallinity. Figure 4.15 shows that the crystallinity in the electrospun fibres increases from day 1 to day 2 for the FA and AA polymer solutions, and decreases from day 2 to day 3. It is hypothesized that the increase in crystallinity after the first day is related to how the polymer degrades in the solvents.

PCL has an upper limit in the degree of crystallinity it can obtain. It is hypothesized that initially as the polymer dissolves, the bulk of the amorphous regions are first degraded as it is expected that the initial diffusion of the solvent occur in these areas. Regardless, the degradation is evidenced by the decreased viscosity and average molecular weight

This apparent increase in crystallinity is most likely caused by the overall decrease in the molecular weight of the polymer. The effect of the decreased molecular weight is well known to generally lead to an increase in crystallinity due to factors such as an increase in chain mobility during the crystallisation process. In this case, given the relatively slow process of dissolution an additional factor could be the initial degradation of the amorphous regions during the very slow dissolution process (the parts of the

chain not in the crystal structure). However, it should be pointed out that this is most likely a secondary factor in influencing the recrystallized structure. Regardless of the mechanism, it is clear that the apparent crystallinity increases for all the electrospun samples after day 1. This increase in crystallinity occurs despite the rapid polymer solidification associated with electrospinning, the rapid nature of polymer solidification has been shown to decrease crystallinity in nanofibres as evidenced by Enayati *et al.*[32] when electrospinning poly (vinyl alcohol) nanofibres from an aqueous solution.

Alternatively, the change in crystallinity in the electrospun fibres could be related to molecular weight of the polymer. It was earlier shown that, an increase in solution age leads to a decrease in molecular weight. Jenkins and Harrison[33] showed that, the degree of crystallinity decreased with an increase in molecular weight when analysing PCL plaques. Figure 4.15 shows that the degree of crystallinity for FA and AA derived electrospun fibres increases from day 1 to day 2, which corresponds with a decrease in molecular weight (Figure 4.10 and Figure 4.11). This suggests that the change in crystallinity is related to the molecular weight. The crystallinity also decreases in day 3. It is not clear what may be responsible for this observation, but it may be related to the extent of the chain degradation after this time.

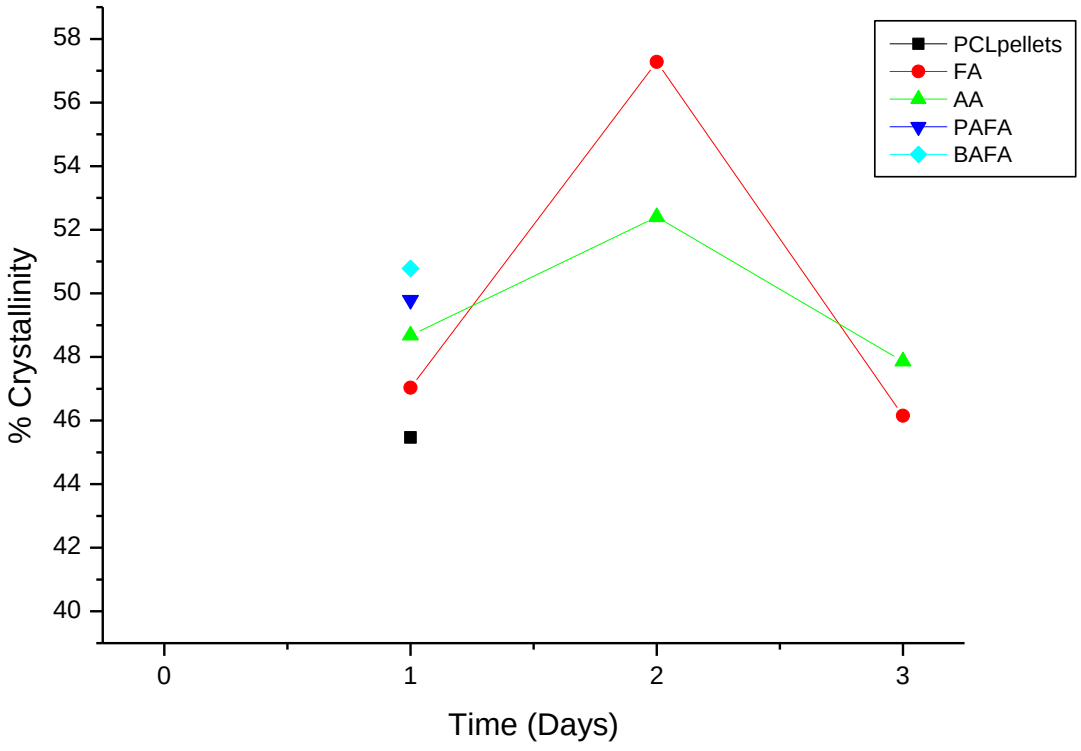

Figure 4.15: Crystallinity of electrospun fibres generated from various 15 wt% PCL solutions as a function of solution age

4.6 Emulsions

4.6.1 Formation and stability

As mentioned previously in the literature review, emulsion formation and stability are partly governed by the interfacial tension between the dispersed and continuous phases. Different dispersed phases may give varied amount of interfacial tension. Therefore, some emulsion compositions might require a stabilizer to form. Three oils were evaluated in the study as a potential to be used in emulsion formation, namely: ethyl oleate (EO), isopropyl myristate (IPM) and sunflower oil (SO), the oils were chosen because of they are FDA-approved for topical emulsions. Figure 4.16 and Figure 4.17 show the influence of the dispersed phase type on phase separation of the dispersed phase component of the emulsion.

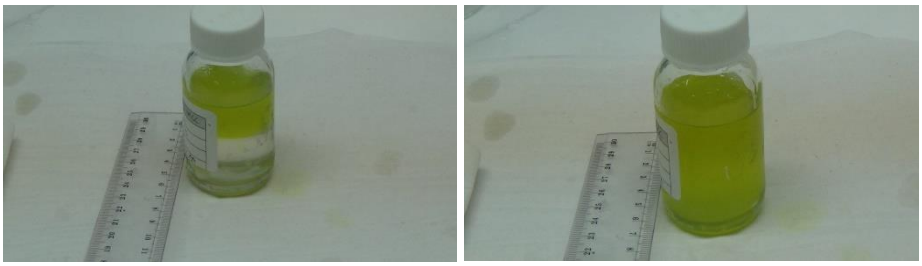

Figure 4.16: various stabiliser-free oil-in-acid emulsions with PCL as the continuous phase: (a) SO as the dispersed phase, (b) IPM as the dispersed phase

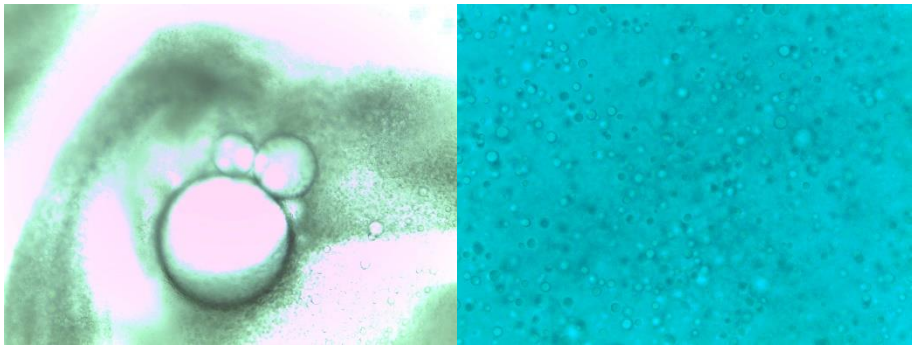

Figure 4.17: Light microscope image of oil-in-acid emulsions with (a) SO as the dispersed phase (stabilised with an anionic surfactant), (b) IPM as the dispersed phase

When SO is used as the dispersed phase, phase separation occurs with the oil (and curcumin) rising to the top of the vessel as is seen in Figure 4.16. The EO and IPM formed emulsions readily without the need of a stabilizer in the solvent systems used. Figure 4.16 shows that SO could not form stable emulsions without a stabiliser, the dispersed phase would immediately phase separate and accumulate at the top of the solution vessel. Figure 4.17 shows that the emulsion droplets are much bigger in size when SO is used as the dispersed phase. Furthermore, it was observed that the emulsion droplet size increased rapidly with time when SO was used as the dispersed phase. In addition, the number of droplets in the sample slide were observed to be constantly changing, suggesting that the emulsion

stability is governed by Ostwald ripening.[34] The results suggest that an addition of SO into the solvent systems results in high interfacial tension that leads to phase separation. The EO and IPM yield low interfacial tensions that lead to the dispersion of the oils in the acid phases and subsequent emulsion stability.[35]

4.6.2 Electrospinning

4.6.2.1 Continuous phase (solvent) influence

As determined in section 4.4, the properties of the solvent can contribute to the electrospinning process. This contribution typically arises in parameters, such as conductivity and/or inherent solution viscosity.[36] In emulsion spinning, there are several solution components that might influence the above-mentioned factors.[37–39]

In the current study, the nature of solvent and surfactant type were evaluated. Table 4.10 shows the relationship between nature of the solvent, fibre morphology and average fibre diameter in free surface emulsion electrospinning.

Table 4.10: Solvent influence on emulsion electrospinning results of various PCL polymer solutions

Sample	SEM 1	SEM 2	Fibre diameter distribution
15 wt% PCL polymer solution (FA),8.33% (v/v) SERVOXYL 20/100, 8.33% (v/v) Sunflower Oil	2500X MAG 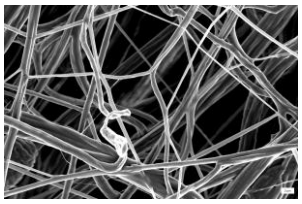	5000X MAG 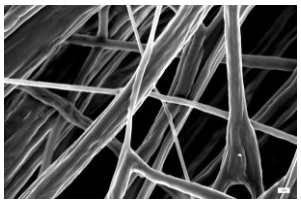	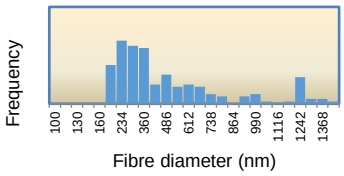
15 wt% PCL polymer solution (AA),8.33% (v/v) SERVOXYL 20/100, 8.33% (v/v) Sunflower Oil	500X MAG 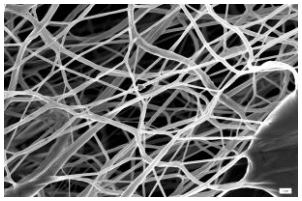	15000X MAG 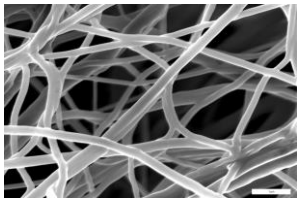	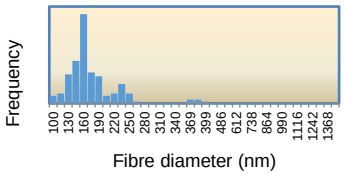

FA and AA emulsions were compared with SO as the dispersed phase and an anionic surfactant (SERVOXYL 20/100) as a stabiliser with a dispersed phase volume fraction of 8.3%. The maximum volume fraction of the dispersed phase that could be added, was 8.3%. Attempts at increasing this value led to destabilization of the emulsion and rapid phase separation. Table 4.10 shows that the FA emulsion derived fibres were thicker and have a higher fibre diameter distribution compared to the fibres derived from AA emulsion. This result is similar to the conventional electrospinning observations shown in Table 4.3 and Table 4.4, whereby fibres derived from FA polymer solutions were thicker compared

to fibres generated from AA polymer solutions. This observation suggests that the nature of the solvent (continuous phase type), does influence the fibre diameter (thickness).

4.6.2.2 Surfactant type

Additives, such as such surfactants, incorporated into the electrospinning solutions can aid electrospinning.[21] Hu *et al.*[21] showed that a surfactant that increases the emulsion conductivity leads to thinner fibres. In the above-mentioned reference, they showed that the surfactant sodium dodecyl sulphate (SDS) led to increased conductivity of the solution. It should be noted that while SDS has a negative net electrical charge it contains sodium as a counter-ion. It is hypothesized that the SDS molecules contributes to electrospinning in two ways. The dodecyl sulphate decreases the surface tension of the polymer solution. This reduction in surface tension allows electrospinning to occur with ease. The SDS molecule is electrically negative, however during electrospinning, positive potential is applied to the solution and the presence of a cation may result in charge repulsion that may enhance the bending and whipping of the polymer jets.

In the present study, the aim was to determine whether the presence of a surfactant in the emulsion influences electrospinning similarly to conventional electrospinning. Two stabilisers namely: SERVOXYL 9/100 (Ethoxylated (9 EO) i-C13 phosphate ester) and NJAD 19 (tallow amine surfactant) were tested with SO as the dispersed phase. SERVOXYL 9/100 is an anionic surfactant, while NJAD 19 exhibits cationic properties in acidic media. Table 4.11 shows the relationship between nature of surfactant, fibre morphology and average fibre diameter. No flocculation was observed with either surfactant. Phase separation was observed after 15 minutes with NJAD 19 while SERVOXLY 9/100 remained stable for an hour.

Table 4.11: Surfactant influence on emulsion electrospinning results of various PCL polymer solutions

Sample	SEM 1	SEM 2	Fibre diameter distribution
70/30 AA/FA, 8.33% v/v NJAD 19, 8.33% v/v Sunflower Oil	1000X MAG 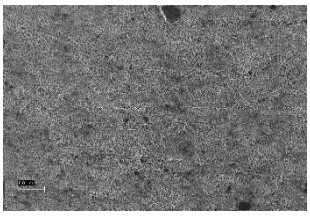	15000X MAG 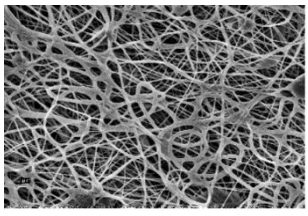	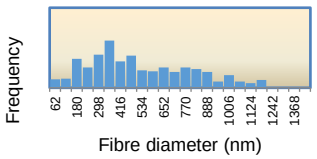
70/30 AA/FA, 8.33% v/v SERVOXYL VPDZ 9/100, 8.33% v/v Sunflower Oil	1000X MAG 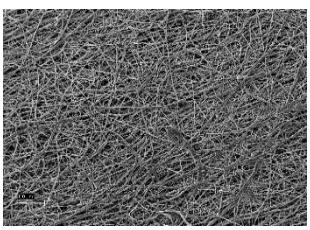	15000X MAG 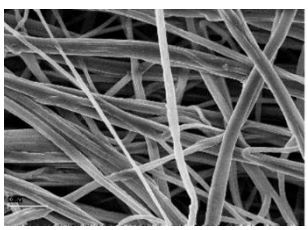	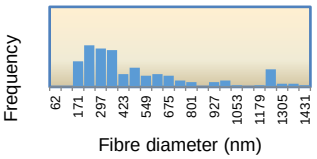

Table 4.11 shows that thinner fibres were observed when the cationic surfactant was, used as initially expected. The conventional electrospinning polymer solution (does not contain surfactant or dispersed phase) usually electrospins with a linear jetting region of 1.5-2 cm length. However, when the cationic surfactant was used the linear segment was not visible, whipping started from the ball surface. When the anionic surfactant was evaluated, it was observed that the linear jetting region increased to 4-5 cm. These results support the initial hypothesis that when positive potential is applied to polymer solutions that contain cationic additives, the presence of charged species influence the electrospinning process. The identity of the applied potential (negative or positive) may cause charge repulsion between the applied potential and the cations in the polymer solution. This charge repulsion is a result of electrostatic interactions. Table 4.11 suggests that the charge repulsion causes a decrease in average fibre diameter.

4.6.2.3 Encapsulation

Voids in electrospun fibres have been shown to occur when electrospinning multi-component polymer solutions where the components are immiscible.[40] It is understood that the voids form because of the inability of the core solution's solvent to diffuse into the shell solution. Forward *et al.*[40] solved the formation of voids by employing the use of a co-solvent in the multi-component polymer solution. The co-solvent enables the core solvent to diffuse fully into the shell solvent. Figure 4.18 and Table 4.12 show the images and SEM images of electrospun PCL fibres generated from a PCL/SO emulsion (with curcumin dissolved in the oil/dispersed phase).

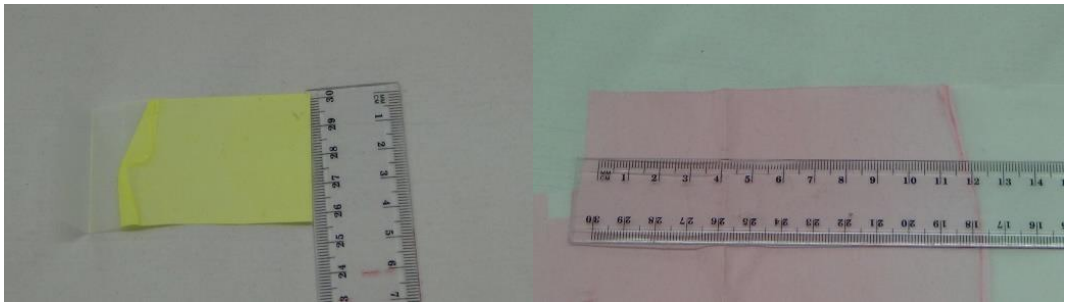

Figure 4.18: Emulsion derived electrospun fibres of encapsulated (a) curcumin and (b) oil red o (1-(2, 5-dimethyl-4-(2, 5-dimethylphenyl) phenyldiazenyl) azonapthalen-2-ol)

Table 4.12: SEM image of electrospun PCL fibres generated from PCL/SO emulsion

Sample	SEM 1 (1000X)	SEM 2 (5000X)	Fibre diameter distribution
15 wt% PCL/SO emulsion generated fibres	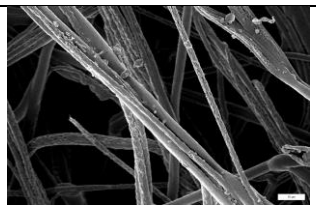	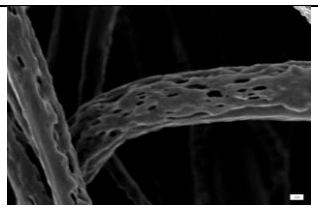	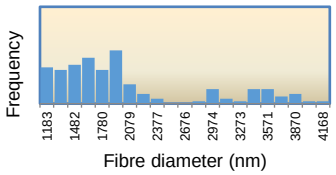

Oil red o (an oil soluble diazo dye) was dissolved similarly to the curcumin, with the aim to determine whether it is incorporated in the same manner as curcumin. Figure 4.18 shows that oil red o behaves similarly to curcumin when used in emulsion electrospinning, it stained the electrospun fibres a pink colour, while curcumin stains electrospun fibres a yellow colour. This suggests that emulsion electrospinning can be used to encapsulate a variety of compounds. Table 4.12 shows that voids in the fibres were observed when sunflower oil was used as the dispersed phase. This result suggests that SO does not fully diffuse into the continuous phase (15 wt% PCL solution). When IPM was used as the dispersed phase, the voids disappeared as seen in Table 4.13. This suggests that IPM is a more miscible oil with the continuous phase than SO, which is also evidenced by that IPM forms transparent emulsions while SO forms opaque emulsions.[41]

As mentioned in the literature review section, the outcome of electrospinning emulsions could be the encapsulation of the dispersed phase (the oil in this case). The morphology of the encapsulated phase could either be “core-shell” or “islands-in-the-sea.[40,42,43] Figure 4.19 shows a STEM and fluorescence image of electrospun fibres generated from the PCL/SO emulsion.

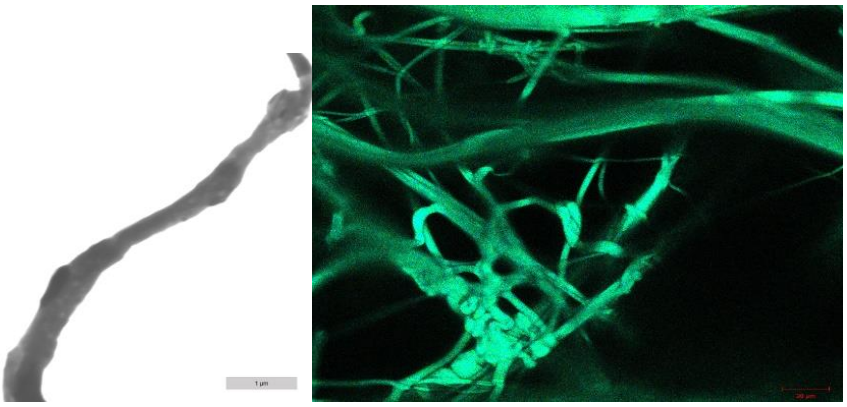

Figure 4.19: Electrospun PCL fibres generated from a PCL/SO emulsion with a surfactant, imaged with (a) STEM and (b) Fluorescence Microscopy

The fluorescence analysis was done on the electrospun fibres, in order, to determine whether the curcumin retains its activity after the processing (electrospinning) the emulsion and exposure to an acidic environment.[44] Figure 4.19 shows that the electrospun fibres containing curcumin fluoresce at an

excitation wavelength of 405 nm, which is the same wavelength that the raw curcumin powder exhibited fluorescence. Erez *et al.*[45], postulated that when exposed to an acidic environment, curcumin excites at a higher wavelength. The authors attributed the wavelength shift to a protonated form of curcumin, (this result was determined utilizing acetic acid and formic acid). Curcumin excited at a wavelength of 405 nm in the current study, the lack of a shift in wavelength suggests that the curcumin remains chemically active and unchanged after incorporation into polymer solutions and subsequent electrospinning. Furthermore, Figure 4.19 shows that the internal fibre morphology cannot be determined, as there is a lack of contrast between the surface of the fibre and the internal components, although there is some indication of lighter areas in the fibres. This could be caused by the oil and the curcumin being present at the surface of the fibres, thus hindering a view of the internal fibre morphology. The fibres were briefly (2-3 minutes) immersed in ethanol, in order to wash oil and curcumin on the fibre surface, the briefness of the washing step is to hinder the potential of the oil and curcumin seeping from the PCL fibres. Figure 4.20 and Figure 4.21 show the fluorescence and STEM analysis of the washed electrospun fibres.

Figure 4.20: Fluorescence image of “washed” electrospun PCL fibres generated from a PCL/SO emulsion with a surfactant

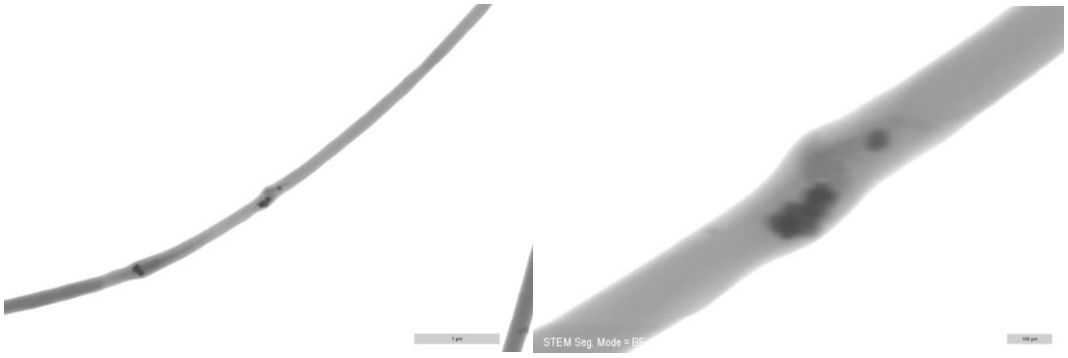

Figure 4.21: STEM image of curcumin-encapsulated PCL fibres derived from PCL/SO emulsion with a surfactant

Figure 4.20 shows that the fibres do not fluoresce, suggesting that the curcumin is no longer present on the surface of the fibres. It is possible that some curcumin maybe be present inside the fibres, but that the fluorescence of the curcumin may be shielded by the polymer.[46] An alternative analysis method

was used to confirm the presence of the curcumin inside the fibres. The results of the STEM analysis shown in Figure 4.21 indicates that the internal fibre morphology of electrospun emulsion fibres (15 wt% PCL/SO) is the “islands-in-the-sea” morphology and that the oil and curcumin were successfully encapsulated.

The ability to form the “core-shell” morphology could be related to whether the material dissolved in the dispersed phase has fibre forming capabilities. This is evidenced by the fact that studies that report core/shell morphology typically utilize polymers in the core solution that have been proven to possess fibre-forming capabilities.[40,47]

Of particular interest is, the influence the dispersed phase type has on the electrospun fibre internal morphology, and also the presence of a stabiliser. IPM was used as the dispersed phase without a stabiliser, curcumin was dissolved in the oil (IPM). Table 4.13 shows the relationship between solution composition and average fibre diameter.

Table 4.13: SEM image of electrospun PCL fibres and fibre diameter distribution as influenced by the presence of a dispersed phase

Sample	SEM	Fibre diameter distribution
15 wt% PCL/IPM emulsion (avg diameter: 333 ± 198 nm)	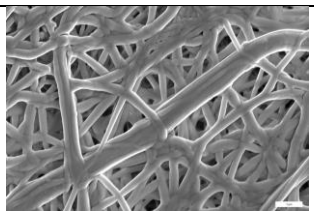	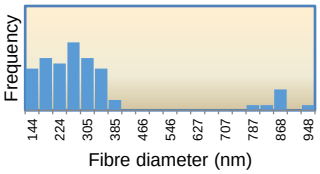

Table 4.13 shows that the presence of a dispersed phase leads to a larger average fibre diameter. The emulsion derived electrospun fibres were analysed with fluorescence and STEM under the same conditions as the PCL/SO emulsion (with a surfactant), some of the fibres were washed briefly with ethanol, as previously done with the PCL/SO generated fibres. Figure 4.22 shows a STEM image of PCL/IPM emulsion derived electrospun fibres.

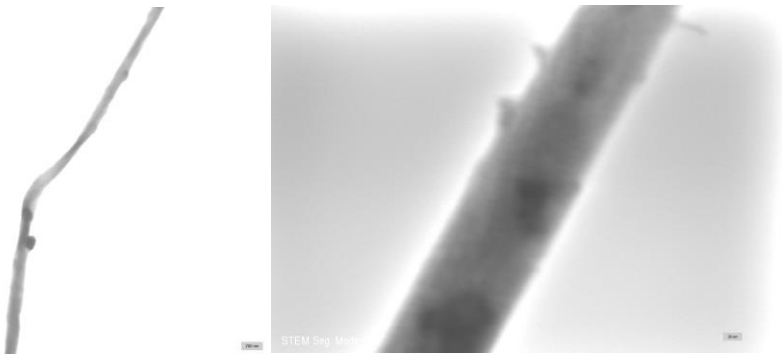

Figure 4.22: STEM image of curcumin-encapsulated PCL fibres derived from PCL/IPM emulsion, (a) unwashed, (b) washed with ethanol

Figure 4.22 shows that fibres generated from PCL/IPM emulsion have a similar morphology to fibres generated from PCL/SO emulsion with a surfactant. The oil and curcumin are present on the surface of the fibres, and when the fibres are briefly washed with ethanol, the internal fibre morphology is an islands-at-sea. Furthermore, Figure 4.23 below shows that curcumin fluoresce (at an excitation wavelength of nm).

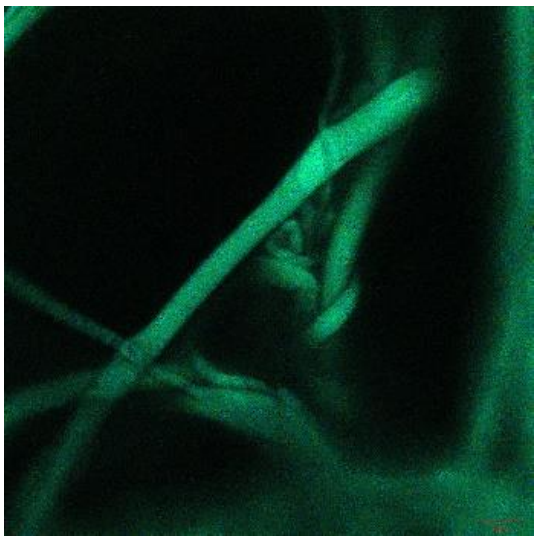

Figure 4.23: Fluorescence image of “unwashed” electrospun PCL fibres generated from a PCL/IPM emulsion

4.6.3 Summary

Kong *et al.*[34] stated emulsion stability can be characterised by the changes in droplet size and droplet size distribution as the emulsion ages, when investigating the role of micellar ordering and Ostwald ripening. Ostwald ripening occurs when the droplet size and distribution evolve with time. In the current study, it similarly observed that the droplet size and distribution evolve with time. This suggests that oil-in-carboxylic acid emulsions’ stability is governed by Ostwald ripening. Hu *et al.*[21] showed that physical properties of nanofibres can be influenced by the components of an emulsion when utilizing needle electrospinning. Solution conductivity was a significant factor in determining the average fibre diameter the study when utilising needle electrospinning. In the current study, it was shown that a similar result is obtained when using free surface electrospinning to electrospin emulsions. This fact suggests that spinneret configuration does not influence the emulsion electrospinning process. Needle electrospinning may be used to predict free surface electrospinning results. Furthermore, the identity of the charge applied to the solution may influence the average fibre diameter, with positive applied potential possibly leading to thinner fibres. The current study further explored the influence of the continuous phase on electrospinning. As expected, the highly conductive continuous phase led to thinner fibres. STEM imaging showed that the curcumin is present on the inside and outside of the electrospun fibres. The internal fibre morphology was an islands-at-sea morphology, which may be related to the electrospinnability of the components of the dispersed phase. Lastly, fluoresce imaging showed that electrospinning curcumin does not harm the compound or modify its chemical

characteristics. This fact suggests the emulsion electrospinning may be useful in encapsulating curcumin into fibres. Furthermore, the encapsulation of oil red o shows the versality of this emulsion electrospinning method.

4.7 Drug release study

The curcumin-loaded nanofibres can act as models for delivering poorly soluble drugs to a wound target site.[47] IPM was chosen as the dispersed phase, as emulsions made with IPM do not require a stabiliser. Stabilisers or surfactants have been shown to alter the surface properties of electrospun fibres, which may influence the drug release study.[47] The results obtained from the solution aging study suggest that polymer solutions derived from the PA/FA solvent system produce a relatively constant average fibre diameter over a 5-day period. This fact can be used to determine the effect of molecular weight of the polymer on the release profiles of the drug (curcumin). To present a more complete study, the release study was performed on curcumin-loaded fibres obtained from a conventional single component polymer solution spinning and emulsion spinning. The emulsion was stabiliser free.

4.7.1 In vitro drug release

Existing literature reports utilize a wavelength of 425 nm when determining curcumin in ultraviolet-visible spectroscopy with methanol/ethanol as solvents, furthermore it has been reported that curcumin absorbs in the wavelength range of 350-450 nm.[49,50] In the current study, curcumin was determined at 425 nm with ethanol as a solvent. A range of curcumin concentrations were prepared, in order to determine the maximal loading that could be achieved in the electrospun fibres. Figure 4.24 shows the relationship between curcumin concentration and absorbance.

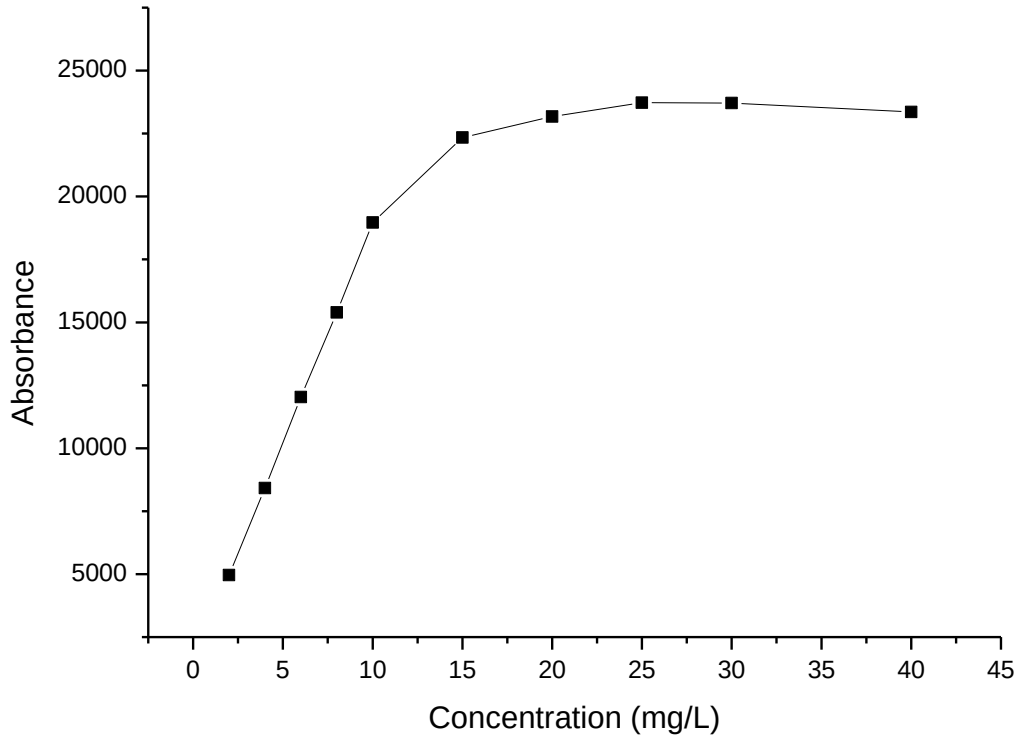

Figure 4.24: The absorbance of curcumin in ethanol as influenced by curcumin concentration

Figure 4.24 shows that a loss of linearity in the curve occurs when the curcumin concentration in ethanol exceeds 10 mg/L, this means that a maximum of 10 mg/L can be analysed per sample with confidence. A narrower concentration range was analysed to determine a calibration curve for the analysis of electrospun fibres. Figure 4.25 shows the relationship between curcumin concentration and absorbance.

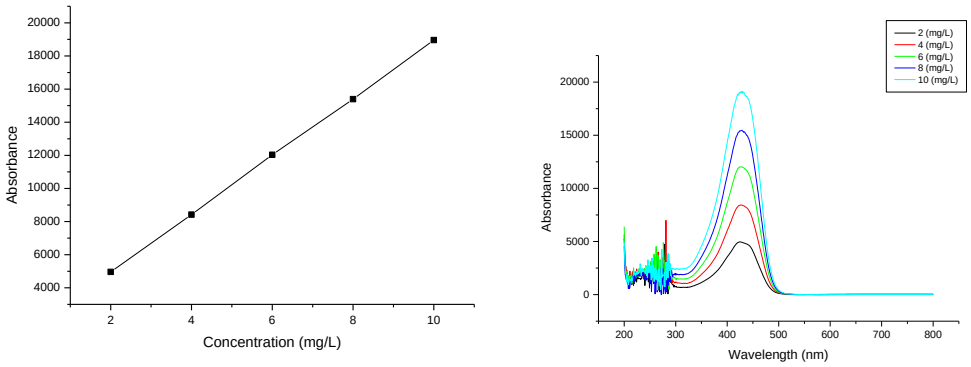

Figure 4.25: The absorbance of curcumin in ethanol as influenced by curcumin concentration and UV-VIS spectra of curcumin in ethanol as influenced by curcumin concentration

Furthermore, concentrations exceeding 10 mg/L results in the peaks broadening and flattening as seen in Figure 4.26.

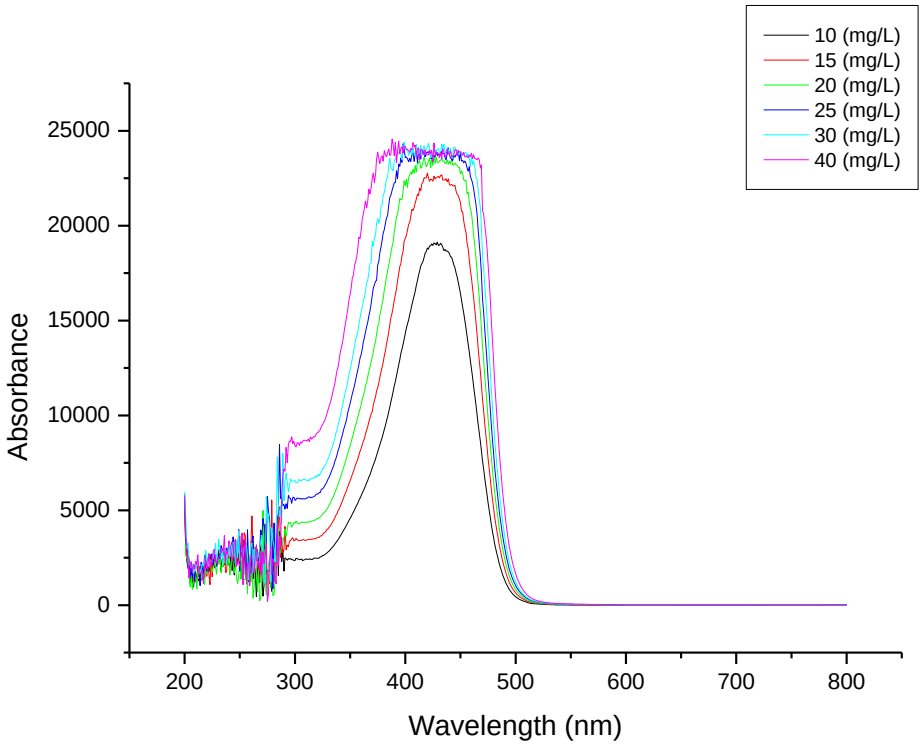

Figure 4.26: UV-VIS spectra of curcumin in ethanol as influenced by curcumin concentration

Curcumin loaded mats were placed in phosphate buffered saline (PBS) at pH 7.4 to attempt a release of the drug as determined by Sampath *et al.*[50] and Blanco-Padilla *et al.*[51] The curcumin loaded mats were generated from 15 wt% PCL polymer solutions and 15 wt% PCL/IPM emulsion (with a), the solvent system used was PA/FA (60:40). The curcumin loading was such that the curcumin concentration would be 50 mg/g in the electrospun fibres generated from the conventional and emulsion spinning solution. Table 4.14 shows the relationship between solution composition and average fibre diameter, Figure 4.27 shows the curcumin loaded nanofibre sheet.

Table 4.14: SEM image of electrospun PCL fibres and fibre diameter distribution as influenced by the presence of a dispersed phase

Sample	SEM	Fibre diameter distribution
15 wt% PCL in PA/FA (avg diameter : 134 ± 47 nm)	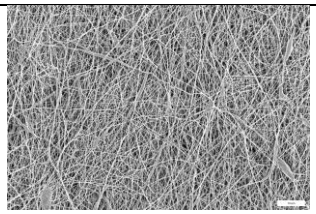	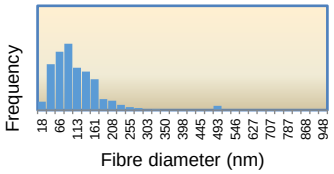
15 wt% PCL/IPM emulsion in PA/FA (avg diameter: 282 ± 90 nm)	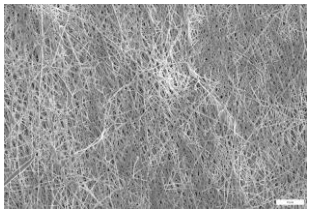	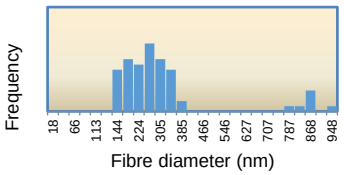

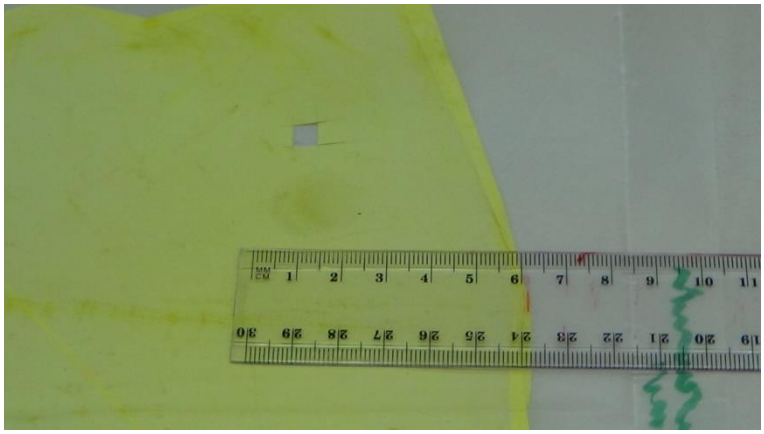

Figure 4.27: Image of curcumin-encapsulated PCL fibres generated from an emulsion with IPM as the dispersed phase

This solvent system was chosen because it was earlier shown that it yields relatively small average fibre diameter. Table 4.14 shows that emulsion electrospinning leads to thicker fibres than conventional electrospinning. This difference in average fibre diameter may influence the release study. Xu *et al.*[52] showed that thicker PEG-PLA fibres resulted in a slower release of the water-soluble drug doxorubicin. Furthermore, Figure 4.27 shows that the curcumin was successfully incorporated into the fibres, pressure was applied onto the mat above the ruler in the picture. This applied pressure led to an imprint that suggests that the oil is still present in the fibres.

The samples were incubated at 37 ^{o}C (to emulate human body temperature) for 7 days. Aliquots of 10 millilitres from the samples were drawn daily (and replaced with an equivalent volume of release media), the phosphate buffered saline (PBS) was evaporated with the curcumin reconstituted in 5 millilitres of

ethanol. The loaded concentration of the curcumin in the conventional and emulsion (curcumin loaded in the oil) polymer solutions was such that the material composition in the fibres would be 50 mg of curcumin per gram of fibre. The electrospun material analysed for release a 200 mg, such that the concentration in the vial was 10 mg/L.

There was no observed release of the curcumin after 7 days from fibres generated from conventional and emulsion electrospinning. The fibres generated from conventional electrospinning only wetted after 4 days in the release media, with the fibres derived from emulsion electrospinning samples partially wet after 7 days. The difficulty in wetting of the fibres could be influenced by the hydrophobicity of the drug, the polymer properties and presence of oil in the emulsion electrospun fibres. In a review Mondal *et al.*[53], stated that one of the challenges in using PCL in biomedical applications, is its hydrophobic nature and poor wetting characteristics. In the same review, the intrinsic PCL surface properties were modified by physical, chemical and biological methods.

Rapid release profiles are often associated with polymer compositions with rapid degradation rates. Mollo and Corrigan[54] investigated the effect of varying lactide percentage in poly (lactide-glycolide) (PLGA) on the release of amoxicillin. They showed that release of the drug slowed with increasing lactide amounts. This result was attributed to the increasing polymer degradation times which are caused by the increased lactide amount. The degradation rates are influenced by the ability of the polymer to incorporate aqueous media that promotes hydrolytic degradation.[55] The incorporation of aqueous media is also influenced by the presence of crystal domains in the polymer.[55] This is because polymers that possess crystal domains undergo a multi-step degradation process.

Dias *et al.*[56] suggested that the incorporation of the aqueous media occurs first in electrospun PLLA fibres. The initial step is the incorporation of aqueous media into the amorphous domains and subsequent hydrolytic degradation of the polymer chains. The second step is the degradation of the crystals domains. PCL exhibits a higher amount of crystallinity compared to the other aliphatic (hydroxy) polyesters and this fact deters rapid aqueous media incorporation and increases the degradation rate of the polymer.[26,55] PCL has a reported bulk degradation time of 2 years, which might explain the lack of burst release.[56]

Additionally, the presence of the oil in the emulsion electrospun fibres may enhance hydrophobicity of the PCL. This enhanced hydrophobicity is evidenced by the longer wetting times of the fibres, and it might increase the overall degradation time of the PCL. This enhanced hydrophobicity is supported by the results shown by Olewnik-Kruszkowsha *et al.*[57] The authors showed that the addition of the additive, montmorillonite slows the degradation rate of PLA. They attributed the slower degradation rate to reduced water-uptake brought on by the presence of montmorillonite. Interestingly, Nelson *et al.*[58] showed that increasing the gelatin amount in PCL/gelatin fibres led to a faster degradation rate. The increase in the degradation rate is attributed to increased hydrophilicity of the fibres, brought on by the presence of gelatin in the polymer matrix. The above-mentioned factors may have hindered the desired sustained release of the curcumin observed in the current study.

An attempt to increase the release rate of CUR from the electrospun fibres was explored. A surfactant (Polysorbate 80) was added to both emulsion and conventional spinning solutions, such that it will act as a solubilizer for the curcumin in the release media.[59] Additionally, the surfactant could potentially modify the surface properties of the electrospun nanofibres by rendering them hydrophilic as observed by Hu *et al.*[60]

Table 4.15 shows the relationship between solution composition and average fibre diameter.

Sample	SEM	Fibre diameter distribution
15 wt% PCL in PA/FA (avg diameter : 111 ± 52 nm)	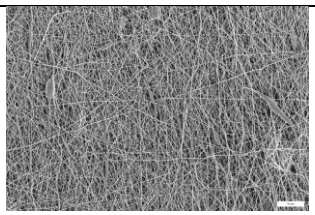	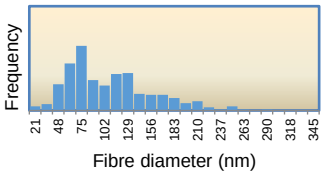
15 wt% PCL emulsion in PA/FA (Avg diameter: 149 ± 77 nm)	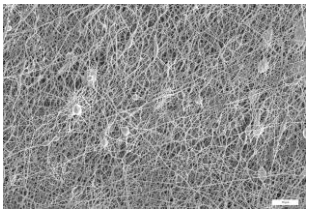	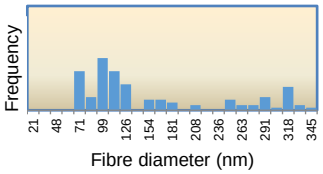

Table 4.15 shows that the addition of the surfactant led to thinner fibres forming, as expected.[21] The surfactant added contributed 2.5% of the total solids in both the conventional and emulsion spinning solutions. Given the difficulty in obtaining curcumin release from the initial test, the concentration of the curcumin in the conventional and emulsion electrospun fibres placed in the vials was increased 50 mg/g. The surfactant-loaded fibres were hydrophilic in nature. This hydrophilic nature led to a burst release of curcumin which was observed within an hour of the release study. Figure 4.28 shows the relationship between absorbance and curcumin released in the media.

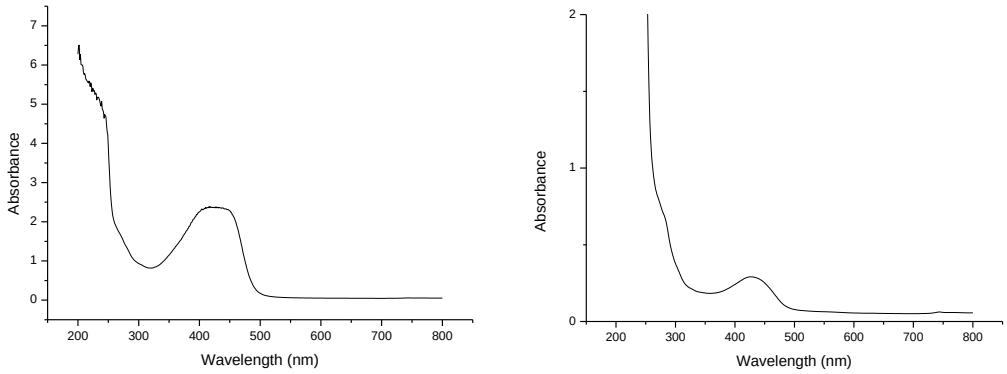

Figure 4.28: Curcumin peaks obtained electrospun PCL fibres generated from (a) conventional, (b) emulsion

The amount of curcumin released was less than 2 mg/L, which is less than 4% of the total curcumin loaded. After this burst release, no curcumin was released after 2 months. This observation could be caused by the fact that when the first aliquot is removed, the solubilizer is potentially removed. This hypothesis is based on the assumption that hydrophilic nature of the fibres, increases the swelling ability of the fibres, which causes the surfactant to “seep” from the polymer matrix.

A further attempt was explored to obtain a steady release of curcumin from the electrospun fibres. The spinning solution was aged for 4 days prior to conventional electrospinning, and emulsion formation and spinning. Table 4.16 shows the relationship between solution age and average fibre diameter.

Table 4.16: Electrospun PCL fibres generated from a conventional solution and an emulsion solution as influenced by the presence of a surfactant

Sample	SEM (1000X)	Fibre diameter distribution
15 wt% PCL in PA/FA (avg diameter : 121 ± 88 nm)	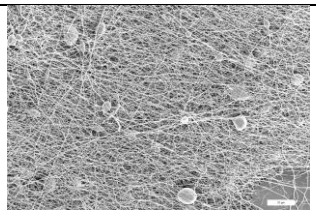	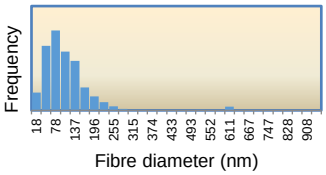
15 wt% PCL/IPM emulsion in PA/FA (Avg diameter: 333 ± 196 nm)	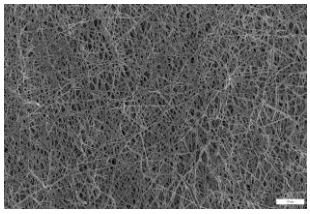	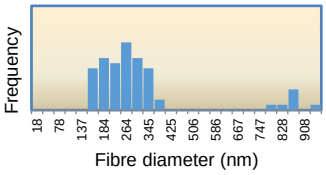

The surfactant was added on the day of spinning, in order to minimise the chance of flocculation.[34] Furthermore, emulsions were formed on the day of spinning. Table 4.3 shows that the solution aging decreases the average fibre diameter and increases the variation in fibre diameter. As mentioned above, thicker fibres are expected to exhibit slower drug release rates than thinner fibres. A similar result was observed with the fibres electrospun from the aged solution. A burst release was observed within the first hour, with no additional release of curcumin after 3 weeks. The concentration of curcumin released was less than 2 mg/L, 50 mg/L was loaded onto the sample vial.

To conclude this section of the study, sustained release of curcumin from emulsion electrospun PCL fibres was not obtained. The challenge in obtaining sustained release of curcumin from the emulsion electrospun fibres appears to lie with the difficulty in wetting the electrospun fibres and the enhanced hydrophobicity brought on by oils used to encapsulate curcumin. Modification of the surface properties of the electrospun fibres was investigated with the addition of a surfactant to the spinning solutions. The presence of the surfactant on the electrospun fibres led to immediate wetting of the fibres. This fact suggests that the electrospun fibres became hydrophilic. The hydrophilicity of the electrospun fibres led to a burst release of curcumin. However, sustained release of the curcumin was not observed, suggesting that the surfactant may be acting as a solubilizer for the curcumin. Lastly, the observations suggest that solution age, and subsequently molecular weight of PCL does not influence the release of curcumin in aqueous media. This observation may be useful in biomedical applications of curcumin and other poorly soluble drugs. An example would be in the long-term implantation of PCL, as used in the regeneration of the meniscus. The curcumin could be used to aid healing once a specific healing stage is reached, such as granulation of the surrounding tissue.

4.9 References

(1) Van der Schueren, L.; De Schoenmaker, B.; Kalaoglu, Ö. I.; De Clerck, K. *Eur. Polym. J.* **2011**, *47*, 1256–1263.

(2) DeRuiter, J. *Princ. Drug Action* **2005**, *1*, 1–11.

(3) Bhardwaj, N.; Kundu, S. C. *Biotechnol. Adv.* **2010**, *28*, 325–347.

(4) Antheunis, H.; Meer, J. Van Der; Geus, M. De; Heise, A. *Biomacromolecules* **2010**, *11*, 1118–1124.

(5) Niu, H.; Lin, T. *J. Nanomater.* **2012**, *2012*, 1–13.

(6) Yalcinkaya, F.; Yalcinkaya, B.; Jirsak, O. *J. Nanomater.* **2015**, *2015*.

(7) Ferreira, J. L.; Gomes, S.; Henriques, C.; Borges, J. P.; Silva, J. C. *J. Appl. Polym. Sci.* **2014**, *41068*, 37–39.

(8) Luo, C. J.; Stride, E.; Edirisinghe, M. *Macromolecules* **2012**, *45*, 4669–4680.

(9) Yang, G.; Li, H.; Yang, J.; Wan, J.; Yu, D. *Nanoscale Res. Lett.* **2017**, *12*.

(10) S. De Vrieze, T. Van Camp, A. N. *J. Mater. Sci.* **2009**, *44*, 1357–1362.

(11) Zhou, F. *Aerosol Sci. Technol.* **2016**, *50* (11), 1201–1215.

(12) Lavielle, N.; Popa, A. M.; De Geus, M.; Hébraud, A.; Schlatter, G.; Thöny-Meyer, L.; Rossi, R. M. *Eur. Polym. J.* **2013**, *49*, 1331–1336.

(13) Gholipour Kanani, A.; Bahrami, S. H. B. *J. Nanomater.* **2011**, *2011*, 1–10.

(14) Brenner, E. K.; Schiffman, J. D.; Thompson, E. a.; Toth, L. J.; Schauer, C. L. *Carbohydr. Polym.* **2012**, *87*, 926–929.

(15) Cui, S.; Yao, B.; Sun, X.; Hu, J.; Zhou, Y.; Liu, Y. *Mater. Sci. Eng. C* **2016**, *59*, 885–893.

(16) Huang, C.; Niu, H.; Wu, J.; Ke, Q.; Mo, X.; Lin, T. *J. Nanomater.* **2012**, *2012*.

(17) Lukas, D.; Sarkar, A.; Pokorny, P. *J. Appl. Phys.* **2008**, *103*, 1–8.

(18) Zhou, F. L.; Gong, R. H.; Porat, I. *Polym. Int.* **2009**, *58*, 331–342.

(19) Jiang, G.; Zhang, S.; Wang, Y.; Qin, X. *Mater. Lett.* **2015**, *144*, 22–25.

(20) Ogulata, R. T.; Icoglu, H. I. *J. Text. Inst.* **2015**, *106*, 57–66.

(21) Hu, J.; Prabhakaran, M. P.; Ding, X.; Ramakrishna, S. *J. Biomater. Sci. Polym. Ed.* **2015**, *26*, 57–75.

(22) McKee, M. G.; Wilkes, G. L.; Colby, R. H.; Long, T. E. *Macromolecules* **2004**, *37*, 1760–1767.

(23) Wang, C.; Wang, Y.; Hashimoto, T. *Macromolecules* **2016**, *49*, 7985–7996.

(24) Shenoy, S. L.; Bates, W. D.; Frisch, H. L.; Wnek, G. E. *Polymer.* **2005**, *46*, 3372–3384.

(25) Koski, A.; Yim, K.; Shivkumar, S. *Mater. Lett.* **2004**, *58*, 493–497.

(26) Antheunis, H.; Van Meer, J. C. Der; De Geus, M.; Kingma, W.; Koning, C. E. *Macromolecules* **2009**, *42*, 2462–2471.

(27) Sinha, V. R.; Bansal, K.; Kaushik, R.; Kumria, R.; Trehan, A. *Int. J. Pharm.* **2004**, *278*, 1–23.

(28) Yu, H.; Huang, N.; Wang, C.; Tang, Z. *J. Appl. Polym. Sci.* **2003**, *88*, 2557–2562.

(29) Chang, H. M.; Prasannan, A.; Tsai, H. C.; Jhu, J. J. *Appl. Surf. Sci.* **2014**, *313*, 828–833.

(30) Jenkins, M.J., Harrison, K. L. *Polym. Adv. Technol.* **2008**, *19*, 1901–1906.

(31) Zhang, J.; Liu, H.; Ding, J.-X.; Zhuang, X.-L.; Chen, X.-S.; Li, Z.-M. *RSC Adv.* **2015**, *5*, 32604–32608.

(32) Enayati, M. S.; Behzad, T.; Sajkiewicz, P.; Bagheri, R.; Ghasemi-Mobarakeh, L.; Łojkowski, W.; Pahlevanneshan, Z.; Ahmadi, M. *Iran. Polym. J.* **2016**, *25*, 647–659.

(33) Jenkins, M.J., Harrison, K. L. *Polym. Adv. Technol.* **2006**, *17*, 474–487.

(34) Kong, Y.; Nikolov, A.; Wasan, D. *Ind. Eng. Chem. Res.* **2010**, *49*, 5299–5303.

(35) Kanouni, M.; Rosano, H. L.; Naouli, N. *Adv. Colloid Interface Sci.* **2002**, *99* (3), 229–254.

(36) Luo, C. J.; Nangrejo, M.; Edirisinghe, M. *Polymer.* **2010**, *51*, 1654–1662.

(37) Badawi, M. A.; El-khordagui, L. K. *Eur. J. Pharm. Sci.* **2014**, *58*, 44–54.

(38) Yan, S.; Xiaoqiang, L.; Shuiping, L.; Xiumei, M.; Ramakrishna, S. *Colloids Surfaces B Biointerfaces* **2009**, *73*, 376–381.

(39) Zhang, H.; Zhao, C.; Zhao, Y.; Tang, G.; Yuan, X. *Sci. China Chem.* **2010**, *53*, 1246–1254.

(40) Forward, K. M.; Flores, A.; Rutledge, G. C. *Chem. Eng. Sci.* **2013**, *104*, 250–259.

(41) Wooster, T. J.; Golding, M.; Sanguansri, P. *Langmuir* **2008**, *24*, 12758–12765.

(42) Liu, R.; Cai, N.; Yang, W.; Chen, W.; Liu, H. *J. Appl. Phys.* **2010**, *116*, 1313–1321.

(43) Qi, H.; Hu, P.; Xu, J.; Wang, A. *Biomacromolecules* **2006**, *7*, 2327–2330.

(44) Wang, C.; Ma, C.; Wu, Z.; Liang, H.; Yan, P.; Song, J.; Ma, N.; Zhao, Q. *Nanoscale Res. Lett.* **2015**, *10*, 439.

(45) Erez, Y.; Simkovitch, R.; Shomer, S.; Gepshtein, R.; Huppert, D. *J. Phys. Chem. A* **2014**, *118*, 872–884.

(46) Reisch, A.; Klymchenko, A. S. *Small* **2016**, *12*, 1968–1992.

(47) Jiang, G.; Qin, X. *Mater. Lett.* **2014**, *128*, 259–262.

(48) Paaver, U.; Laidmäe, I.; Santos, H. A.; Yliruusi, J.; Aruväli, J.; Kogermann, K.; Heinämäki, J. *Asian J. Pharm. Sci.* **2016**, *11*, 500–506.

(49) Priyadarsini, K. *Molecules* **2014**, *19*, 20091–20112.

(50) Sampath, M.; Lakra, R.; Korrapati, P.; Sengottuvelan, B. *Colloids Surfaces B Biointerfaces* **2014**, *117*, 128–134.

(51) Blanco-Padilla, A.; López-Rubio, A.; Loarca-Piña, G.; Gómez-Mascaraque, L. G.; Mendoza, S. *LWT - Food Sci. Technol.* **2015**, *63*, 1137–1144.

(52) Xu, X.; Chen, X.; Wang, Z.; Jing, X. *Eur. J. Pharm. Biopharm.* **2009**, *72*, 18–25.

(53) Mondal, D.; Griffith, M.; Venkatraman, S. S. *Int. J. Polym. Mater. Polym. Biomater.* **2016**, *65*, 255–265.

(54) Mollo, A. R.; Corrigan, O. I. *Int. J. Pharm.* **2003**, *268*, 71–79.

(55) Fabra, M. J.; Lopez-Rubio, A.; Lagaron, J. M. *Food Hydrocoll.* **2013**, *32*, 106–114.

(56) Dias, J. C.; Ribeiro, C.; Sencadas, V.; Botelho, G.; Ribelles, J. L. G.; Lanceros-Mendez, S. *Polym. Test.* **2012**, *31*, 770–776.

(57) Olewnik-Kruszkowska, E.; Kasperska, P.; Koter, I. *React. Funct. Polym.* **2016**, *103*, 99–107.

(58) Nelson, M. T.; Johnson, J.; Lannutti, J. *J. Mater. Sci. Mater. Med.* **2014**, *25*, 297–309.

(59) Das, R. K.; Kasoju, N.; Bora, U. *Nanomedicine Nanotechnology, Biol. Med.* **2010**, *6*, 153–160.

(60) Hu, J.; Prabhakaran, M. P.; Tian, L.; Ding, X.; Ramakrishna, S. *RSC Adv.* **2015**, *5*, 100256–100267.

Chapter 5: Conclusions and recommendations

5.1 Conclusion

The main objective of this study was to incorporate poorly soluble active pharmaceutical ingredients (API) into medical devices. Electrospun fibres were the desirable device format to deliver the APIs as they have been shown to possess bio-mimicking properties. Furthermore, electrospun fibres can be implanted in the target area, providing direct access to the API. Emulsions were chosen as the method to incorporate the poorly soluble drugs into the electrospinning solutions. The study also focused on utilizing a free surface electrospinning method to electrospin multicomponent solutions. More specifically, the patented ball electrospinning methodology (SNC *BEST*™) was investigated for its ability to form complex nanofibre morphologies.

The first objective of the study focused on utilizing carboxylic acids as alternative electrospinning solvents for aliphatic polyesters. Carboxylic acids were chosen as they are classified as lower risk solvents by the FDA for use in medical devices. Formic acid, acetic acid, propionic acid and butyric acid successfully dissolved polycaprolactone to varying degrees. It was shown that the pKa influenced the dissolution time of PCL in carboxylic acids, with a larger pKa leading to longer dissolution times. Fibres were generated by electrospinning from formic acid and acetic acid derived solutions, while an additive (salt) was required to generate fibres from the propionic acid and butyric acid derived solutions. It was evident from the conductivity measurements that the conductivity influenced the formation of fibres, with highly conductive solutions showing good electrospinnability. Furthermore, it was shown that highly conductive solutions lead to thinner fibres. This is attributed to the enhanced bending and whipping of the polymer jet as it moves toward the collector.

The study also included an investigation of the effect solution age on the solution properties, and subsequent electrospinnability. It was shown that the surface tension and conductivity remained relatively unchanged as the solution age increased. However, the viscosity decreased with an increase in solution age. The decrease in viscosity coincided with a decrease in average fibre diameter, and the emergence of a film as one of the electrospinning products. This confirmed that solution viscosity can be related to average fibre diameter in carboxylic acid derived polycaprolactone solutions, more specifically, a higher viscosity value leads to a higher average fibre diameter. Furthermore, SEC analysis showed that a higher viscosity and higher fibre diameter is associated with a high average molecular weight of the polymer. It was additionally shown that the dispersity index increases with solution age, confirming that the polymer chains in formic acid undergo random chain scission. DSC analysis of electrospun fibres showed that the electrospinning process leads to an inconsistence crystal size distribution.

Stable (oil-in-acid) emulsions were successfully formed with PCL dissolved in the acid. It was shown that the dispersed phase type influenced the need for a stabiliser, suggesting that the compatibility of the oil with the acid dictates emulsion stability. The emulsions could be electrospun with both needle and ball electrospinning, confirming that the spinneret configuration does not influence the ability to

electrospin emulsions. More specifically, oil globules can readily flow into the electrospinning jets and free surface electrospinning does not lead to phase separation of the emulsion components. The presence of a dispersed phase led to an increase in average fibre diameter, suggesting that the dispersed phase may impact the mass flow into the electrospinning jet, or diminish the bending and whipping instabilities. STEM analysis showed that the internal fibre morphology was an islands-at-sea morphology. The internal fibre morphology may be influenced by the electrospinnability of the components of the dispersed phase.

Curcumin was successfully incorporated into the nanofibres by electrospinning emulsions. It was shown that the dispersed phase type influences the morphology of the electrospun fibres, this can be attributed the ability of the dispersed phase to fully diffuse into the continuous phase during electrospinning. Fluorescence analysis showed that the curcumin remained chemically active after electrospinning, which suggests that emulsion electrospinning is a safe method of encapsulating APIs into nanofibres. Rapid release of curcumin into aqueous media proved unsuccessful. However, a surfactant added to the spinning solutions led to a burst release within the first half an hour with no additional release after that. This observation is attributed to the fact that the surfactant acted as solubilizer for the curcumin, and was removed along with the first aliquot, and thus no additional release was observed.

5.2 Recommendations for future work prospects

Polymeric fibres have gained popularity in the biomedical industry due to their ability to form tissue engineering scaffolds and drug device combination products. As mentioned in the study, this wide range of applications in the biomedical industry requires processing multicomponent solutions and forming fibres with complex morphologies utilizing different solvents. The current study focused on utilizing safer solvent systems on PCL, and how parameters such as solution age, solvent type and conductivity can alter the electrospinning results that may include fibre size, fibre morphology and polymer crystallinity. Further studies should focus on whether the results shown here are applicable to other commercially available biocompatible polymers. That would allow for greater flexibility in designing medical devices as important fibre characteristics such as degradation can be controlled by changing multiple parameters (solvent type or polymer or device format). Furthermore, the influence of the salt additives on the physical properties of the fibres would be useful, more specifically whether complexes form in solution that may alter wettability. The crystallinity of PCL fibres influences the degradation rate of the polymer in biological media, it would be useful to study whether carboxylic acids can alter the crystallinity and subsequently hasten polymer degradation. Additionally, polymer degradation can be related to the release of APIs encapsulated in medical devices, a study on how degradation of aliphatic polyesters influences the release of poorly soluble drugs. Lastly, the electrospinning of multi-polymer solutions (comprising of aliphatic polyesters and hydrophilic polymers) may be studied to see whether the resulting fibres offer sustained release of poorly soluble drugs.

Appendix A

Table A1: Surface tension of PCL (15 wt %) polymer solutions

Sample	Surface tension (mN/m)
FA	50.83
AA	32.67
PA	34.27
BA	32.53
PA, 4 wt% $NaCH_3COO$	32.67
PA, 4 wt% TEB	32.40
BA, 6 wt% $NaCH_3COO$	30.33
BA, 6 wt% TEB	32.10

Table A2: Viscosity of PCL (15 wt %) polymer solutions

Sample	Viscosity (cP)
FA	1183
AA	3651
PA	2788
BA	3200
PA, 4 wt% $NaCH_3COO$	3996
PA, 4 wt% TEB	6222
BA, 6 wt% $NaCH_3COO$	2822
BA, 6 wt% TEB	3568

Table A3: Conductivity of PCL (15 wt %) polymer solutions

Sample	Conductivity (ms/cm)
FA	92.88
AA	0.25
PA	0.00
BA	0.00
PA, 4 wt% $NaCH_3COO$	0.62
PA, 4 wt% TEB	92.75
BA, 6 wt% $NaCH_3COO$	0.40
BA, 6 wt% TEB	32.67

Table A4: Needle electrospinning observations for various PCL polymer solutions

Polymer Solution Composition	Observations
10 wt%, FA	Smooth bead-free fibres
15 wt%, FA	Smooth bead-free fibres
10 wt%, AA	Beaded fibres
15 wt%, AA	Smooth bead-free fibres
10 wt%, PA	Film observed
15 wt%, PA	Film observed
10 wt%, BA	Electrospray observed
15 wt%, BA	Electrospray observed
15 wt%, PA, 4 wt% SA	Smooth bead-free fibres
15 wt%, PA, 4 wt% TEB	Smooth bead-free fibres
15 wt%, BA, 6 wt% SA	Smooth bead-free fibres
15 wt%, BA, 6 wt% TEB	Smooth bead-free fibres